4-8-2008

Heat Fluxes in Tampa Bay, Florida

Kristin L. Sopkin
University of South Florida

Heat Fluxes in Tampa Bay, Florida

by

Kristin L. Sopkin

A thesis submitted in partial fulfillment
of the requirements for the degree of
Master of Science
College of Marine Science
University of South Florida

Major Professor: Mark E. Luther, Ph.D.
Steven D. Meyers, Ph.D.
Robert H. Weisberg, Ph.D.

Date of Approval:
April 8, 2008

Keywords: turbulent heat flux, bulk algorithm, heat budget, radiative heat flux, BRACE

Table of Contents

List of Tables

List of Figures

Heat Fluxes in Tampa Bay, Florida

Kristin L. Sopkin

ABSTRACT

The Meyers et al. (2007) Tampa Bay model produces water level and three-dimensional current and salinity fields for Tampa Bay. It is capable of computing temperature but is presently run without active thermodynamics. Variations in water temperature are driven by heat exchange at the water-atmosphere boundary and advective heat flux at the mouth of the bay. The net heat exchange surface boundary condition is required for computations of three-dimensional temperature fields. Components of the surface heat budget were measured or derived at an observational tower in Middle Tampa Bay. Net heat exchange at the surface of Tampa Bay was computed from June 2002 to May 2005. Total heat energy gained or lost at the bay-atmosphere interface includes turbulent and radiative heat fluxes.

An initial examination of turbulent heat exchange, the portion of total surface heat flux driven by atmospheric turbulence, demonstrated the skill of a bulk flux algorithm (TOGA COARE v. 3.0) in predicting measured sensible heat flux over Tampa Bay (R^2 = 0.80 and RMSE of 11.02 W/m^2 from June through November of 2002). Insolation was measured directly at the observational tower. Solar radiation is reflected in proportion to sea surface albedo, computed following Payne (1972). Based upon Secchi depth readings, Tampa Bay was classified as a water body type 7. The amount of penetrating insolation reflected from the bottom was computed for this type 7 estuary. Upwelling longwave radiation is emitted in proportion to the water temperature according to the Stefan-Boltzmann law. Eleven bulk formulas for computing downwelling longwave radiation were assessed for skill in reproducing observations made at buoys moored on the West Florida Shelf. Berliand and Berliand (1952) best represented downwelling longwave heat flux measurements at the buoys and is appropriate for application over Tampa Bay.

Surface heat flux dominates cooling in fall and warming in spring while advective heat exchange becomes important during the summer. Extreme events, including tropical cyclones and extratropical fronts, dramatically impact surface heat exchange, driving rapid cooling. The methods applied in computation of heat flux components are amenable to real-time modeling exercises.

Chapter One

Introduction

Study Objectives

Many chemical, physical and biological parameters in marine systems are influenced by water temperature including gas solubility, chemical kinetics and speciation, phytoplankton growth and nutrient uptake rates, and water density and stratification. The ability to accurately model water quality, biological processes, and current fields is therefore dependent upon knowledge of the three-dimensional temperature structure within a model domain. This study focuses on changes in water temperature within Tampa Bay, Florida.

Temperature variations within the bay are driven by heat transfer at the air-sea interface and at the boundary between the waters of the Gulf of Mexico and the Tampa Bay estuary. Prior to this study, a systematic investigation into the processes of heat exchange at the ocean-atmosphere boundary has not been completed, yet is central to understanding changes in estuarine heat storage.

Net heat exchange at the water surface is the summation of the radiative and the turbulent heat fluxes. The radiative fluxes include incoming shortwave ("solar") radiation, a portion of which is reflected from the ocean surface as outgoing shortwave radiation, incoming longwave ("atmospheric") radiation, and outgoing longwave radiation emitted at the sea surface. Turbulent heat transfer is partitioned into a sensible heat exchange and a latent heat flux component. Sensible heat flux occurs by conduction in response to a temperature gradient between the ocean surface and an overlying air mass or contacting precipitation. The latent heat flux component represents heat transfer into or out of the bay as water molecules condense or evaporate at the water surface. The rate of change of heat energy stored within the Tampa Bay estuary must equal the sum of the net heat exchange at the air-sea interface and the advective heat exchange at the mouth of the bay. This balance of energy exchange is termed the "heat budget" of the bay.

In addition, accurate parameterization of the salinity budget is crucial to modeling estuarine density distribution and circulation patterns. The amount of freshwater lost at the sea surface due to evaporation is highly variable, fluctuating with changes in humidity, wind speed, and air and water temperatures. Rates of evaporation over the estuary are not currently directly measured. For modeling purposes, over-water evaporation rates are assumed equivalent to averaged daily rates obtained from an evaporation pan located near McKay Bay. Pans cannot account for physical processes that occur within a large body of water, such as the downward mixing and storage of heat. As one component of this study, a more realistic description of the over-water

evaporation rate is produced in computations of the calculated latent heat flux component of the heat budget.

Study objectives include (1) utilizing data from a meteorological tower located in Middle Tampa Bay to quantify net surface heat transfer over Tampa Bay and assess the contribution of individual components of this net surface flux to the total heat exchanged at the air-sea boundary, (2) estimating advective heat exchange at the mouth of the estuary and constructing a closed heat budget for the estuary, and (3) determining the relative importance of freshwater loss through evaporation to the freshwater budget of the bay.

Study Area

Situated on the west central Florida Gulf coast between 27.5º N and 28.1º N and 82.3º W and 82.8º W, encompassing an area of 398 square miles at high tide, Tampa Bay is Florida's largest estuary and is home to the largest and busiest of the State's ports (see Figure 1-1 for location of the Bay on Florida's west coast). More than two million people reside within the Bay's watershed region. Estuarine water quality is heavily impacted by human activity through freshwater withdrawal from rivers feeding the estuary, chemical and oil spills into the bay, injection of hypersaline and heated waste waters from desalination facilities and coal-fired power plants and, during heavy rainfall events, overflow of human sewage and of highly acidic process water from abandoned phosphate mines into the bay. Numerical models of bay circulation, temperature structure and water quality are useful tools for guiding governing bodies in making informed decisions by predicting the impacts of estuarine and surface water resource management policy to the bay.

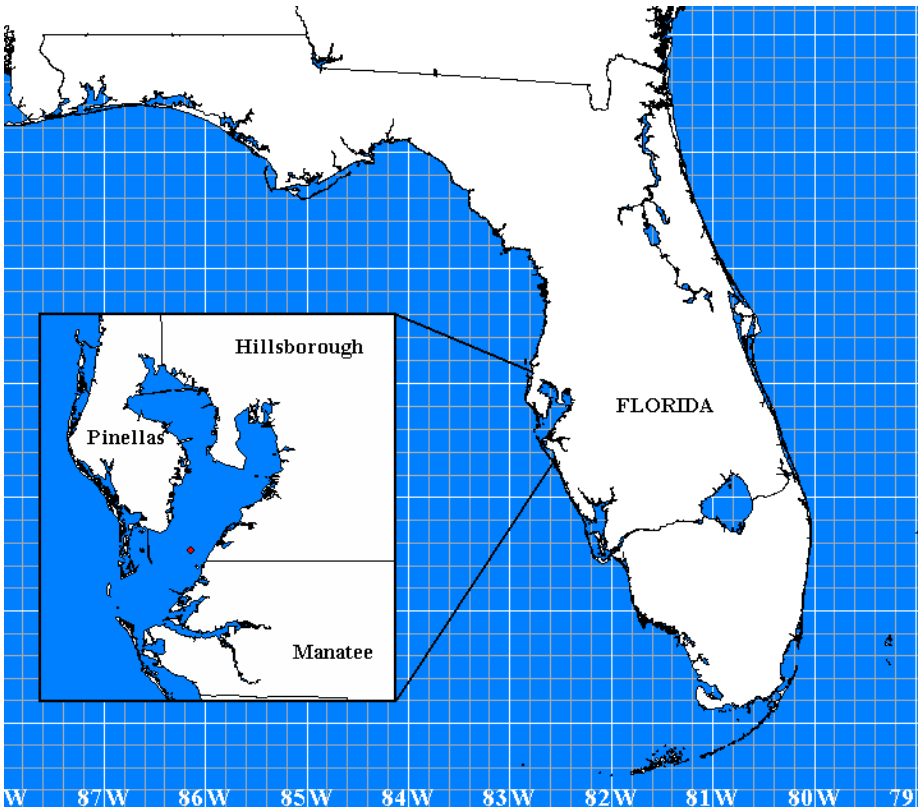

Figure 1-1: The location of Tampa Bay on Florida's west coast. The red marker indicates the position of the BRACE tower within Tampa Bay.

The Port of Tampa is Florida's largest port. More than fifty million tons of cargo pass through the Port annually carrying commodities ranging from chemicals (including phosphate, anhydrous ammonia, and sulfuric acid in support of Florida's phosphate and fertilizer industry) to coal and building materials. In addition, the Port of Tampa is home port to several cruise lines that collectively transported in excess of 900,000 passengers in the year 2006 (Tampa Port Authority; http://www.tampaport.com/).

Tampa Bay is characterized as a broad and shallow estuary with a mean depth of only about 12 ft. To facilitate the passage of large vessels, narrow shipping channels were dredged and are maintained at 43 ft deep. The main channel extends 40 miles up the center of the bay connecting the Port to the Gulf of Mexico. The largest of the cruise vessels are over 950 ft. long and must navigate through lanes that take multiple turns and are as narrow as 200ft in places (Tampa Bay Soundings, Winter 2003). When this passage is turned treacherous by weather or poor visibility, there is increased danger of ship collisions, groundings, and cargo spills with potentially catastrophic results. Model nowcasts and forecasts of water level and current speed and direction can aid in the safe navigation of large commercial vessels in and out of the Port of Tampa. Tides in Tampa Bay can vary significantly from astronomical tide level predictions under forcing by strong winds in the West Florida Shelf region. Accurate, model-produced water level

predictions provide warning of storm surge dangers to residents in the low-lying regions surrounding Tampa Bay.

As the bay area population continues to grow and Port operations expand, improved hydrodynamic and coupled models of biological, physical and chemical processes within the Bay are expected to play an increasingly important role in the safe navigation and stewardship of the Tampa Bay estuary.

Earliest efforts in modeling Tampa Bay hydrodynamics neglected baroclinic circulation under the assumption that density driven circulation is unimportant in a shallow and vertically well-mixed estuary like Tampa Bay. C. R. Goodwin (1980, 1987) of the USGS utilized such a vertically-integrated, two-dimensional, finite-difference numerical model to examine the impacts of dredge and fill operations on circulation patterns and flushing in Tampa Bay. With a subsequent implementation of the first three-dimensional numerical model in Tampa Bay, a relative of the Princeton Ocean Model called ECOM-3D, Galperin et al. (1991) demonstrated that the strong horizontal gradient in salinity from Hillsborough Bay (where the bulk of freshwater runoff is received) to the mouth of the estuary results in a two-layer estuarine circulation pattern that is unresolved by two-dimensional models. Vincent (2001) redeployed the ECOM-3D model in Tampa Bay with a higher resolution grid and with the ability to ingest real-time observations as part of an automated nowcast-forecast system of Tampa Bay hydrodynamics. Sheng et al. (2003) modeled Tampa Bay using their CH3D-IMS, a modeling system that integrates models of water quality and biological processes with a three-dimensional, finite difference numerical model of hydrodynamics. Recent modeling of Tampa Bay by Weisberg and Zheng (2006a,b) utilized an implementation of FVCOM, a three-dimensional, time-dependent finite volume model. Weisberg and Zheng (2006a) used their model to analyze the residual circulation of the bay and Weisberg and Zheng (2006b) assessed the storm surge threat in the bay.

The Tampa Bay model utilized by Meyers et al. (2007), a component of the Tampa Bay Coastal Prediction System (TBCPS), is a three-dimensional, time-dependent, nowcast-forecast implementation of the ECOM 3D finite-difference model based upon the earlier work of Vincent et al. (2000), Vincent (2001), and Galperin et al. (1991). At present, this model predicts salinity, water level, and currents with proven accuracy at 2,244 grid points in a domain that extends from the head of tides southward to the mouth of the estuary and resolves depth with 11 layers in the vertical. See Vincent (2001) and Meyers et al. (2007) for descriptions of model verification studies.

In order to calculate current velocities, the Meyers et al. model requires specification of freshwater sources, including precipitation, river discharge and underground seepage, and freshwater loss through evaporation at the surface. Currently, the model algorithm utilizes daily averaged evaporation rates as measured by a Southwest Florida Water Management District (SWFWMD) maintained evaporation pan located near McKay Bay in hindcast studies. When observed evaporation rates are not available, this parameter is assigned a constant value in model computations. Preliminary bulk formula estimates of evaporation rate performed by Vincent (2001) indicated that annual freshwater volume loss via evaporation is of similar magnitude, but opposite sign, as the annual precipitation rate.

Model prediction of water temperature throughout the bay requires accurate parameterization of the net heat flux at the air-sea interface of the estuary. Consequently,

the capacity of the Meyers et al. Tampa Bay model to project temperature at each grid point within the bay is currently unexploited; water temperature is assigned a constant value of 25 ºC. On average, the presence of a strong horizontal salinity gradient is the main force driving large-scale estuarine circulation, however, water temperature may play a role in governing circulation in localized areas such as points of freshwater inflow, or in areas of large gradients in bathymetry leading to lateral temperature gradients during periods of strong surface heat flux.

Vincent (2001) highlighted the need for improved understanding of the surface heat fluxes and the freshwater budget of the Bay for specification of model boundary conditions. The present research is expected to allow model prediction of bay temperature, supporting future coupling of biological and water quality models to the hydrodynamic model.

Data Collection

In May of 2002, a tower located near Port Manatee Turn in Middle Tampa Bay (27º 39.708'N, 82º 35.669'W) was instrumented with meteorological and oceanographic sensors as one component of the Bay Regional Atmospheric Chemistry Experiment (BRACE). Figure 1-1 illustrates the location of the BRACE tower within Tampa Bay. Developed in response to the Tampa Bay Atmospheric Deposition Study (TBADS) finding of the importance of direct atmospheric loading of pollutants to bay waters, the stated mission of BRACE is to estimate the rate of atmospheric deposition of nitrogen species to Tampa Bay (Poor 2000). The BRACE tower sensor array has been continuously maintained since May of 2002, providing data required for estimation of nitrogen deposition velocity and quantification of air-water heat exchange. The time period of data collection encompasses three complete seasonal cycles, including periods of above and below average temperatures and rainfall. This time frame also includes extreme weather events, such as during the 2004 hurricane season in which four major hurricanes made landfall in the state of Florida, within the three-year study period. Events occurring over short time scales, such as the passage of tropical storms and extratropical fronts, have a marked impact on the individual components of the heat budget. Therefore, this study also demonstrates the need for frequent in situ measurements and coastal observing systems in order to adequately resolve variability in individual heat budget components.

Data acquired from this tower include air temperature, humidity and horizontal wind velocity measured via R. M. Young sensors at two heights (5 meters and 10 meters above mean sea level), insolation determined by LI-COR LI-200SZ pyranometer, and precipitation and barometric pressure measured by R. M. Young meteorological instruments. A SeaGauge sensor, mounted at a depth of 2.5 meters below mean sea level, monitors water temperature, salinity, and water level. Additionally, a CSI CSAT3 sonic anemometer mounted at 6.9 meters above mean sea level measures the three-dimensional wind speed and the turbulent flux of sensible heat. A photograph of the BRACE tower is provided in Figure 1-2. Meteorological data is gathered at 5 meters above mean sea level in addition to the standard 10-meter measurement height in order to generate a more complete data set. The additional data allows for estimation of the vertical gradients of

temperature and moisture in the surface layer and computation of energy budget components via several methods.

Figure 1-2: Photo of the BRACE observational tower.

Meteorological data are collected at the BRACE tower at six-minute intervals. CSI sonic anemometer flux data are sampled at a frequency of 10 Hz and compiled into half hourly averages. Above water data are telemetered by line-of-sight radio to the Ocean Modeling and Prediction Lab (OMPL) located on the University of South Florida St. Petersburg campus. Data are uploaded in real-time to the OMPL website (http://comps1.marine.usf.edu/BRACE) and a complete set of the data in raw form is continually appended with the most recent data and made available to the public on the OMPL ftp site (ftp://comps.marine.usf.eud/pub/BRACE). SeaGauge data are stored on the instrument and are collected when the sensor is recovered for cleaning and recalibration. Records of instrument deployment and recovery, as well as certificates of calibration, are available on the OMPL ftp site.

Organization of Thesis

This thesis constitutes the first in-depth heat budget study completed within Tampa Bay. Results are presented here as three independent analyses: a six-month examination of bulk sensible and latent heat flux estimations produced by the TOGA COARE 3.0 algorithm and the NOAA Buoy Model (see Chapter Three for descriptions of these algorithms), a three-year investigation of the total heat budget of Tampa Bay, and an 18-month analysis of the freshwater budget of the Bay.

Chapter Two provides a detailed description of each component of the heat and freshwater budgets and outlines study methods. The parameterization of each freshwater budget component supplied to the Meyers et al. Tampa Bay model is described.

Chapter Three compares two bulk flux algorithms, TOGA COARE v. 3.0 and the NOAA Buoy Model, and explores the utility of each model in predicting several observed flux parameters and in estimating the atmospheric deposition of nitrogen in a coastal region. The NOAA Buoy Model has been the preferred algorithm for modeling turbulent heat flux during the BRACE direct deposition studies (Mizak et al. 2007, Poor et al. 2001, Evans et al. 2004, Poor et al. 2004), while the TOGA COARE algorithm is more commonly utilized within the greater scientific community. This six-month BRACE turbulent heat flux study is an adaptation of an article recently published in *Atmospheric Environment:* Sopkin, K, C. Mizak, S. Gilbert, V. Subramanian, M. Luther, and N. Poor, 2007: Modeling Air/Sea Flux Parameters in a Coastal Area: A Comparative Study of Results from the TOGA COARE Model and the NOAA Buoy Model.

Expanding on the BRACE turbulent heat flux study, Chapter Four includes parameterizations of the radiative heat flux components and extends the study to a three-year period. Particular emphasis is placed on analysis of extreme event impacts on net heat exchange at the surface.

Chapter Five compares evaporation rates produced in latent heat flux computations presented in Chapter Four to pan-measured evaporation rates supplied to the Meyers et al. Tampa Bay model and investigates fluctuations in the relative importance of evaporation to the freshwater budget of the bay.

Chapter Six summarizes the findings of this research. Improved understanding of the heat balance in Tampa Bay is expected to permit water temperature prediction by the Meyers et al. model throughout the bay. Additionally, verification of NOAA Buoy Model results supports previous estimates of atmospheric nitrogen deposition rates over the estuary under BRACE.

Chapter Two

Methods

Turbulent Heat Fluxes

The planetary boundary layer is the lower portion of the atmosphere that responds to surface-atmosphere interactions on a time scale of hours. This atmospheric layer extends approximately 10 km above the earth's surface and is characterized by turbulent flow. Turbulent eddies are generated by convective instabilities and by vertical velocity shears resulting from mean winds encountering surface friction and roughness elements. These atmospheric eddies, with length scales ranging from millimeters to thousands of meters, act to transport heat and pollutants near the surface. The fraction of ocean-atmosphere heat exchange that is driven by turbulent transfer includes the sensible and latent heat fluxes.

Sensible Heat Exchange

The vertical flux of sensible heat, Q_S, is defined as:

$$Q_S = \rho c_p \overline{w'T'} \qquad (1)$$

where ρ is the density of air, c_p is the heat capacity of air, w is vertical wind velocity and T is air temperature (Arya 2001). The quantity $\overline{w'T'}$ is the averaged product of measured temperature and vertical wind velocity fluctuations away from the mean that occur in response to the passage of turbulent eddies (Fleagle and Businger 1980). This averaged vertical turbulent heat flux can differ considerably from zero, resulting in a net transport of heat to or from the estuarine surface (Stull 1984). The direction of transport depends upon the shape of the surface boundary layer temperature profile.

Heat exchange resulting from contacting precipitation typically represents a heat loss from the ocean. The temperature of a falling droplet of rain is expected to be close to the wet bulb temperature and thus cooler than the ambient air and sea surface temperatures in tropical regions (Gosnell et al. 1995, Anderson, Hinton and Weller 1998). On long-term average, the sensible heat flux due to rain accounts for only a small portion of the total heat energy lost at the surface, but sensible heat exchange due to precipitation can account for up to 60% of the net heat flux at the surface during individual rainfall events (Anderson, Hinton and Weller 1997).

Sensible heat exchange was determined via three methods in this study, including 1) direct measurement of the eddy covariance of temperature and the vertical component of wind velocity, 2) bulk aerodynamic representation, and 3) gradient approximation. The sensible heat loss due to precipitation is computed by bulk method.

Latent Heat Exchange

Latent heat exchange at the air-sea interface results from the mean vertical turbulent transport of moisture near surface. Analogously to the sensible heat flux, this turbulent transport is represented as the averaged product of the turbulent fluctuations of the vertical wind component and the specific humidity, $\overline{w'q'}$, where q is the specific humidity (defined as kilograms of water per kilogram of air). The latent heat flux is then given by:

$$Q_L = \rho L_e \overline{w'q'} \qquad (2)$$

where L_e is the latent heat of vaporization. Latent heat exchange almost always constitutes a heat loss from the ocean and is typically of much greater magnitude than the sensible heat exchange. High winds and low humidity accelerate evaporation from the sea surface and thus heat energy loss from the sea due to latent heat exchange. The magnitude of latent heat transfer will be derived from 1) bulk aerodynamic formula and 2) gradient approximation.

Quantification of Turbulent Fluxes

Eddy Covariance Method –

The eddy covariance method is utilized for direct measurement of the sensible heat flux component of turbulent heat exchange. In order to calculate Q_S, turbulent fluctuations of vertical wind and air temperature are measured by a CSI CSAT3 3-D sonic anemometer and FW05 fine wire thermocouple that are mounted at the BRACE tower. The sonic anemometer measures the transit time of ultrasonic pulses between transducers mounted on three non-orthogonal axes. Wind speeds along these axes are derived from the time of flight of the ultrasonic signals and are commuted to the orthogonal wind speed components. Both averaged wind properties and turbulent wind fluctuations are produced. The CSAT3 is mounted according to manufacturer specification at a height of 6.9 meters and is oriented into the predominately easterly sea breeze in order to minimize flow distortion around the arms of the anemometer. Samples are acquired at the rate of 10 Hz, and sensible heat flux is computed half-hourly using equation 1. Fast response measurements of humidity are not available from BRACE tower instrumentation, and therefore, it is not possible to determine latent heat exchange via this technique.

Bulk Aerodynamic Formulas –

Bulk formulas are useful for calculating both sensible and latent heat fluxes. This approach to determining turbulent heat transfer takes advantage of the Monin-Obukhov Similarity Theory (MOST). MOST makes the assumption that within the lower approximately 10% of the planetary boundary layer, termed the surface layer, turbulent fluxes of heat are constant with height. Additionally, MOST assumes that turbulent transfer is the dominant mechanism driving vertical heat exchange within the surface layer. In the bulk sensible heat transfer formula, the eddy covariance of vertical wind and

temperature is approximated as the difference between measured temperature at a pre-defined height within the well-mixed surface layer (T_a) and at the surface (T_s) multiplied by the horizontal wind speed (U). Bulk estimations of latent heat flux (Q_L) make similar use of measured humidity at a pre-defined height (q_a) and the surface (q_s). Sensible and latent heat flux components may therefore be written as:

$$Q_S=\rho c_p U C_H(T_s-T_a) \quad (3)$$

$$Q_L=\rho L_e U C_E(q_s-q_a) \quad (4)$$

where C_H and C_E are the dimensionless heat and moisture transfer coefficients, respectively. Two bulk transfer algorithms (described in detail in Chapter Three) will be used to estimate sensible and latent heat exchange, including the Tropical Ocean Global Atmosphere Coupled Ocean-Atmosphere Response Experiment (TOGA COARE) version 3.0 algorithm and the NOAA Buoy model.

The TOGA COARE v3.0 algorithm utilizes rainfall rates observed at the BRACE tower and the Gosnell et al. (1995) representation of heat transfer at the ocean's surface due to precipitation to compute the sensible heat flux due to precipitation.

Gradient Method –

Both sensible and latent heat fluxes may be computed with the gradient method. According to this method, turbulent fluxes may be inferred from gradients of wind, temperature and humidity between measurements taken at two different heights (z_1 and z_2) above the influence of surface roughness elements. Arya (2001) notes that this is in contrast to the bulk aerodynamic method, which requires standard meteorological data from a single height as well as some parameterization of the wind-dependent surface roughness. In applying this method, it is assumed that the wind, temperature and humidity profiles between measurement heights are either logarithmic or linear in form and the actual gradient in the scalar values is approximated in simple finite difference form:

i. linear approximation

$$\left(\frac{\partial M}{\partial z}\right)_{z_a} \approx \frac{\Delta M}{\Delta z} = \frac{M_2 - M_1}{z_2 - z_1} \quad (5)$$

where $z_a = (z_1+z_2)/2$ is the arithmetic mean height, or

ii. logarithmic approximation

$$\left(\frac{\partial M}{\partial z}\right)_{z_m} \approx \frac{M_2 - M_1}{z_m \ln(z_2 / z_1)} \quad (6)$$

where $z_m = (z_1 z_2)^{1/2}$ is the geometric mean height and M represents scalar wind speed, temperature or humidity values (Arya 2001).

Arya (1991) demonstrated that the logarithmic gradient profile approximation is preferred in near-neutral to unstable surface layer conditions while a linear approximation performs as well or more accurately when approximating gradient profiles in a stable atmosphere. The author recommends the logarithmic approximation for general application and notes that, for a reasonable ratio of measurement heights, error is expected to be less than 2% for the logarithmic gradient approximation and twice this error for resulting flux estimates. In contrast, the linear approximation may produce error

as large as 8% and twice this amount for fluxes computed following this method. Sensible and latent heat fluxes are computed assuming a logarithmic temperature and moisture gradient profile.

From these gradient approximations, the gradient Richardson number (a dimensionless ratio of buoyant forces to shear-driven turbulence), the Monin-Obukhov scaling parameters u_* (the friction velocity, a velocity scale), T_* and q_* (temperature and humidity scales, respectively), and the Monin-Obukhov stability parameter may be determined. The stability and scaling parameters allow computation of the turbulent fluxes of latent and sensible heat. Unlike the bulk transfer algorithms, the gradient method requires no specific information about the surface such as surface roughness parameterization or sea surface temperature. The BRACE tower configuration satisfies Arya's recommendation that the ratio of measurement heights does not exceed 2 in order to minimize error in profile approximations.

Radiative Heat Fluxes

Sources of radiative heat flux at the surface may be partitioned, according to wavelength, into longwave (emitted predominately in the range of 3-100 μm) and shortwave (primarily spanning 0.15-4.0 μm) radiation (Arya 2001). The intensity of downwelling solar (shortwave) energy arriving at the surface is dependent upon factors such as latitude, time of day and year, and absorptivity of the atmosphere. A fraction of insolation is reflected back from the ocean surface according to surface albedo. The albedo, or reflectivity, of the ocean varies between about 0.05 and 1 (indicating complete reflection of incident shortwave radiation) in response to sea state and the angle of the sun above the horizon (Stull 1988). Water most effectively absorbs incident radiation in the infrared spectrum; the majority of irradiance in wavelengths greater than visible light is absorbed within the upper meter of the ocean (Jerlov 1976). Energy of shorter wavelengths may penetrate far more deeply into the water column depending upon the characteristics of the particular water body (turbidity, ocean color, and amount of particulate matter) and the quantity of shortwave irradiance passing through the water surface. In water that is sufficiently clear (and shallow) some amount of the shortwave radiation penetrating the ocean surface may reach the bottom and reflect upwards to re-emerge at the water surface. The portion of downwelling shortwave radiation that is reflected at the ocean surface, or that reflects from the bed and re-emerges at the surface, is unavailable for heating of estuarine waters. Net shortwave radiation represents a heat gain by the ocean during daytime hours.

Upwelling longwave radiation represents a loss of heat from water as energy is emitted from the ocean surface according to sea surface temperature. The atmosphere absorbs much of this outgoing longwave radiation in addition to a considerable portion of solar radiation. A percentage of the energy absorbed by the atmosphere is re-emitted in the form of downwelling longwave radiation and acts to warm surface waters. The magnitude of atmospheric radiation is strongly dependent upon conditions such as amount, height, and type of cloud cover. Gill (1982) notes that the sum of upwelling and downwelling longwave radiation components typically acts to cool the ocean and the high heat capacity of water results in this parameter remaining fairly constant from day to night.

Incoming Shortwave Radiation

Insolation at the BRACE observational tower is measured by a LI-COR LI200SZ Silicon Pyranometer mounted at 5.8 m above mean sea level. The pyranometer responds to wavelengths ranging from 0.4 μm to 1.1 μm, with the manufacturer reporting a typical error of ± 3% when the instrument is operating under natural daylight conditions. Measurements of downwelling shortwave radiation are acquired at six-minute intervals.

Surface Reflected Shortwave Radiation

Upwelling shortwave radiation is computed from measured insolation, $Q_{SW\downarrow}$:

$$Q_{SW\uparrow} = -\alpha Q_{SW\downarrow} \qquad (7)$$

given some parameterization of the sea surface albedo, α. Payne (1972) presented a method for determination of surface albedo based upon two factors: the atmospheric transmittance and the solar altitude. The atmospheric transmittance, T, is a measure of attenuation of solar radiation by atmospheric scattering and absorption and is written as:

$$T = Q_{SW\downarrow} / (S\sin\theta/\gamma^2) \qquad (8)$$

where the denominator represents the no-sky radiation. The transmittance ranges from 0 (for extremely overcast conditions) to 1 (indicating complete transmittance of solar radiation in the absence of an atmosphere). Solar altitude and estimates of no-sky solar radiation are produced by the freely available Sea-Mat Air-Sea Toolbox functions for Matlab (http://woodshole.er.usgs.gov/operations/sea-mat/). Payne (1972) provides, in table format, values of sea surface albedo as a function of the calculated atmospheric transmittance and sun altitude.

Bottom Reflected Shortwave Radiation

The percentage of surface penetrating insolation that remains at depth in a water column depends upon factors that vary widely between water masses such as turbidity, plankton concentrations, quantity of suspended particulate material, and the presence or absence of colored dissolved organic matter. Jerlov (1968) developed a scheme of categorizing water masses according to their transparency to radiative heat flux, allowing prediction of light levels at various depths for each of 10 defined classes: five oceanic types ranging from clear, low-nutrient regions (type I) to areas of upwelling (type III) and five coastal water types, reflecting the selective absorption of shorter wavelengths by yellow colored substances and particulate matter in near-shore regions, in order of decreasing clarity from type 1 to type 9.

A single coastal body of water may shift between classes as optical characteristics vary with seasonal or greater frequency. Low precipitation and freshwater runoff associated with unusually dry periods can lead to water that is more transparent than normal, while increased rains and surface water flow are linked with a sharp increase in concentrations of nutrients (leading to enhanced phytoplankton growth) and colored organic matter that are injected into near-shore waters. Schmidt et al. (2001) demonstrated that precipitation rates over the Tampa Bay watershed and river discharge volumes into the Bay are strongly modulated by El Niño – Southern Oscillation events. Under the influence of El Niño winters, the south central area of Florida encompassing

the Tampa Bay watershed region experiences increased rainfall and stormwater runoff into the Bay, while La Niña periods typically bring drier conditions. Events occurring over much shorter time scales also impact Tampa Bay such as hurricanes and tropical storms that carry large volumes of rain and bring high winds, increasing water turbidity.

Paulson and Simpson (1977) note that, for most cases, observed Secchi depth is nearly equivalent to the level at which the irradiance penetrating the water column falls to a tenth of the surface radiative flux value. This relationship between Secchi depth reading and percent radiant energy remaining is useful for classification of Tampa Bay waters where observations of irradiance at depth are unavailable. As part of their mission to monitor and regulate the quality of Hillsborough County resources, the Environmental Resources Management division of the Hillsborough County Environmental Protection Commission (EPCHC) analyzes chemical, biological, and physical parameters, including Secchi depth readings, at monthly intervals at stations located throughout Tampa Bay. These data have been collected since 1972 and are published for public usage on the EPCHC website (http://www.epchc.org/). Monthly EPCHC observations from January 2002 through December 2004 were utilized in this study for the purpose of categorizing the coastal water types found in Tampa Bay.

Two EPCHC sampling stations are situated near to, and straddling, the BRACE tower in water depths comparable to MSL at the tower of 4.61 m (see Figure 2-1 for location of these stations relative to the meteorological tower). EPCHC station number 21 is located just east-northeast of the tower (27.663 N, 82.564 W), in mean water depth of 5.1 m as observed by the EPCHC for the three year period, and station number 90 is positioned slightly south-southwest of the tower in water averaging 4.5 m deep (27.626 N, 82.592 W). Monthly observations of Secchi disk visibility were very similar between these EPCHC stations and were averaged to produce monthly estimated Secchi depth values in the region of the BRACE tower.

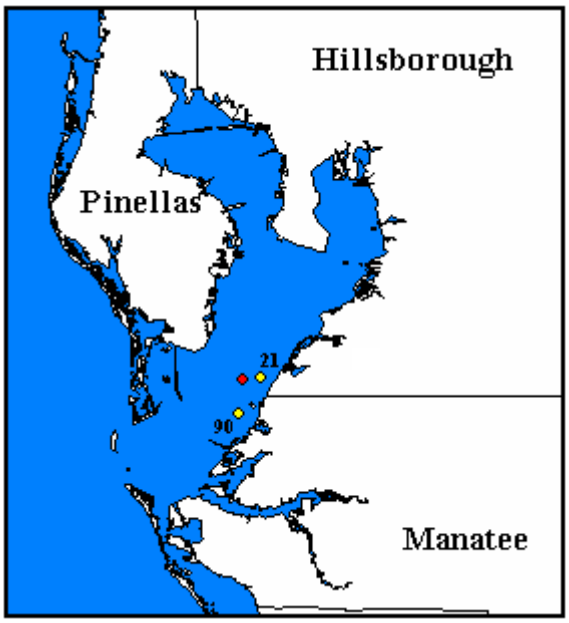

Figure 2-1: Locations of EPCHC Stations 21 and 90 relative to the BRACE observational tower (red marker) in Tampa Bay.

Jerlov (1968) presented percentages of light remaining versus increasing depth for each of the five coastal water types (see Table 2-1 for an adaptation of Jerlov's table XXI). For the period spanning 2002 through 2004, the averaged Secchi depth readings were compared with Jerlov's percent irradiance remaining values for each coastal type and the estuarine waters were categorized according to Jerlov's scheme, assuming that observed Secchi depth is equivalent to the level of 10% radiant energy remaining. Tampa Bay may be variously classified as coastal water type 3 during exceptionally clear periods (8.3% of the monthly observations) to coastal type 9 (or even more opaque than a water mass described by this type) at its murkiest (27.8% of observations). Fifty percent of the thirty-six monthly Secchi depth measurements, as well as the mean Secchi depths observed at EPCHC stations 21 and 90 (2.68 m and 2.65 m, respectively), are consistent with Jerlov's type 7 coastal waters. For the purpose of this heat budget study, the mean case of water type 7 is applied to all calculations of bottom-reflected radiation.

Table 2-1: Adaptation of Jerlov's (1968) Table XXI. Percent light remaining versus depth for coastal water types.

Depth	Type 1	Type 3	Type 5	Type 7	Type 9
0	100	100	100	100	100
1	36.9	33.0	27.8	22.6	17.6
2	27.1	22.5	16.4	11.3	7.5
5	14.2	9.3	4.6	2.1	1.0
10	5.9	2.7	0.69	0.17	0.052

Assuming the bed reflects the incident radiation completely, emergent radiation is represented by the amount of penetrating irradiance remaining after passing downward through the water column and reflecting from the bottom to re-emerge at the surface (a distance of 9.22 m, twice the mean sea level at the tower). Percent irradiance present at this depth can be derived from Jerlov's tabulated values if it is assumed there is exponential decay of radiant energy between 5 and 10 m. An estimated 0.25% of surface penetrating radiation remains after the attenuation of radiant energy over a depth twice that of the water column at the BRACE tower. Inclusion of this component of the heat budget as a means of more completely representing penetrating radiation in shallow coastal regions was recommended by Virmani (2005) and Virmani and Weisberg (2003).

Tampa Bay waters are typically very turbid with visibility decreasing northward up the bay, away from the influence of tidal flushing by Gulf waters. Nutrients and suspended particles carried by riverine and stormwater runoff and sediment resuspended by maintenance dredging of the shipping channels contribute to poor water clarity. In Lower Tampa Bay, visibility reaches a maximum depth on average annually of 2.5 m as recorded by Secchi disk readings (State of the Bay, TBEP; http://www.tbep.org/). Estuarine waters are expected to fall into the clearest case (type 3) infrequently, during periods of unusually low rainfall and streamflow. On clear sky days for brief periods of maximum insolation (1000 W/m^2 incoming shortwave radiation), assuming complete reflectance of penetrating solar radiation from the bottom of the Bay, emergent radiation for maximally transparent, case 3 waters is an estimated 32.7 W/m^2 at the tower. This quantity falls to 0.8 W/m^2 or less reflecting from the sea floor to re-emerge at the surface when Tampa Bay corresponds to murky case 9 coastal waters. The deviation of these values from the quantity of emergent radiation computed for the case 7 classification assumed here (an estimated 2.5 W/m^2 reflecting from the bottom and lost at the surface) represents the maximum error incurred by applying coastal case 7 to all computations of emergent radiation at the BRACE tower. EPCHC data indicates the bay would be classifiable as a Type 3 coastal water body only seldom with peak errors corresponding to brief periods of clear skies and maximum sun. Much of Tampa Bay is significantly shallower than the MSL at the tower and a higher fraction of penetrating shortwave radiation is expected to be reflected from the bottom of the bay and lost, particularly under conditions of low surface runoff and reduced nutrient input, in these very shallow regions. The error associated with the computation of penetrating radiation by the above method is expected to be small and to average out in the long term. A more dense set of measurements of irradiance at depth is required to capture all of the variability in bottom-reflected radiation at the BRACE tower as well as the spatial variability in bottom-reflected shortwave radiation from the shoals to the shipping channels of Tampa Bay.

Incoming Longwave Radiation

Downwelling longwave radiative heat flux is not directly measured at the BRACE tower and must therefore be estimated by bulk parameterization. As previously noted, atmospheric radiation is heavily dependent upon cloud conditions. The presence of a cloud layer can affect the intensity of downwelling longwave radiative heat flux to a varying degree, depending on such properties as cloud base height, cloud type, water droplet size and other characteristics which are seldom measured. Most bulk

parameterizations of downwelling longwave radiation require some estimate of cloud cover, introducing uncertainty into approximations of atmospheric radiation. Reed (1977) compared methods of estimating insolation based upon observed cloud distribution and recommended the following empirical formula instead:

$$Q_{SW\downarrow} / Q_0 = 1 - 0.062C + 0.0019a \qquad (10)$$

where the left hand side is the ratio of measured insolation at the surface to the no-atmosphere radiation (Q_0), C is the observed cloud cover, and a is the noon solar altitude. Rearrangement of this relation gives:

$$C = (1 + 0.0019a - Q_{SW\downarrow} / Q_0) / 0.62 \qquad (11)$$

permitting estimation of cloud cover from measured downwelling shortwave radiation and computed no-sky radiation. Downwelling and net longwave radiation were determined using this approximated cloud cover in the absence of observations of cloudiness over the bay during this study.

Fung et al. (1984) examined the performance of eight bulk net longwave transfer equations under clear sky settings in climates spanning from tropical to subarctic during mean and perturbed temperature and precipitation conditions. The authors give preference to the Berliand and Berliand (1952) formulation both for its skill in replicating radiative transfer equation results and the incorporation of a nonlinear dependence on vapor pressure and air temperature. More currently, Josey et al. (2003) reviewed two empirical formulas for approximating atmospheric radiation recently applied in climatological research studies. Josey et al. (2003) determined that neither formula reliably reproduced measured downwelling longwave radiation and presented a new formulation for estimating atmospheric radiation. The bulk longwave radiative heat flux parameterizations considered in these studies were evaluated in their skill at predicting incoming longwave radiation observed on the West Central Florida Shelf.

The Coastal Ocean Monitoring and Prediction System (COMPS) is a network of offshore and nearshore instrumentation maintained along the West Florida Shelf that provides real-time meteorological and oceanographic data. The array is coupled with computer prediction models producing nowcasts/forecasts of current speed and direction and sea levels over the entire West Florida Shelf from the Florida Keys northward to the Mississippi Delta region (http://comps.marine.usf.edu/). The Tampa Bay PORTS and TBCPS are two components of this comprehensive coastal monitoring system. As part of the COMPS assemblage of offshore buoys, the C10 buoy is moored approximately 27 nm southwest of the mouth of Tampa Bay (27.169 N, 82.926 W) in waters 24.7 m deep. A second COMPS station, the C14 buoy, is positioned roughly 57 nm northwest of the estuary entrance (28.306 N, 83.398 W) in a water depth of 21 m (see Figure 2-2 for locations of COMPS moorings relative to Tampa Bay). Both moorings are instrumented with pyrgeometers as well as an array of meteorological sensors supplying real-time observations at twenty-minute intervals. Data available from these stations include air and sea surface temperatures, relative humidity, barometric pressure and incoming shortwave radiation in addition to measured downwelling longwave radiation. C10 and C14 buoy instrumentation permits application of bulk longwave formulae to measured meteorological parameters and comparison of the results produced by these formulations to observed downwelling longwave radiation at each site.

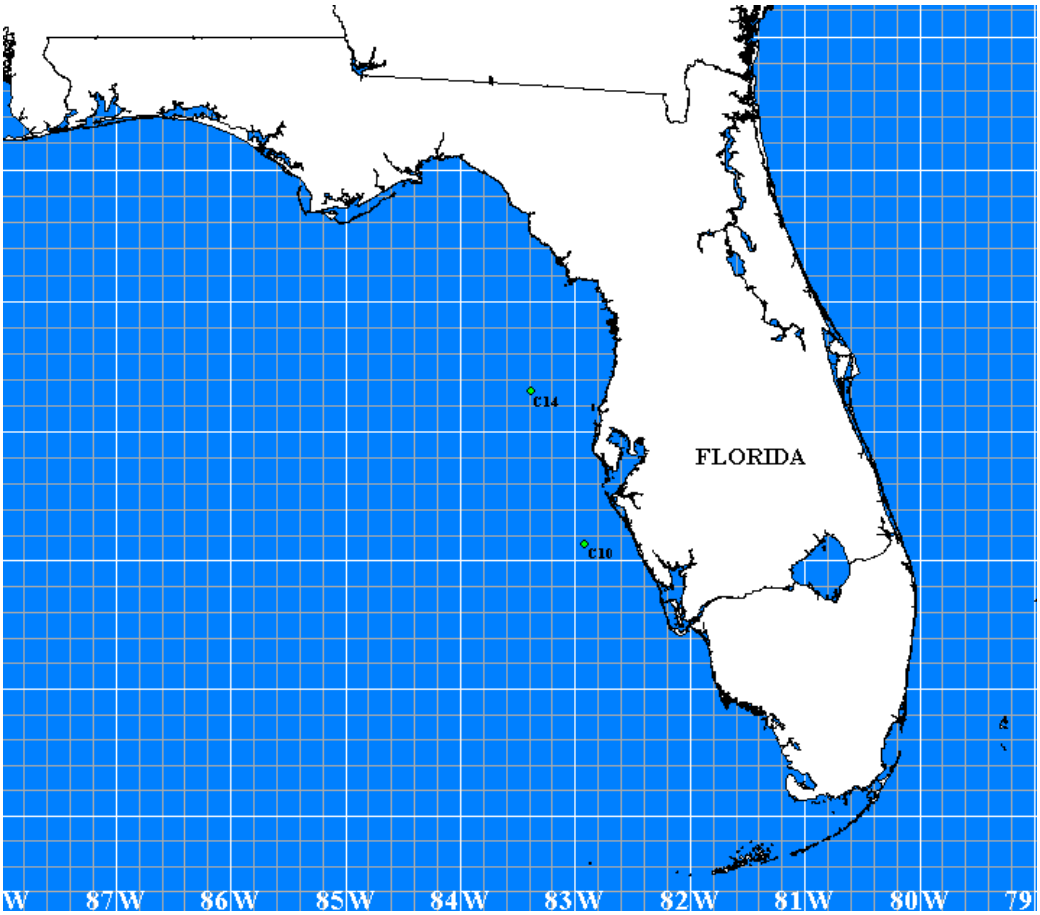

Figure 2-2: Positions of buoys C10 and C14 on the WFS relative to Tampa Bay.

Josey et al. (2003) suggest that air water vapor content is an important factor contributing to incoming longwave radiative flux intensity within the latitudinal band (20°-35° N/S) encompassing Tampa Bay and the COMPS buoy network, a supposition that is substantiated by the present research. Data returned from the C10 and C14 sensor arrays were analyzed for the covariance of the observed flux of longwave radiation with each of the meteorological variables required as input to the bulk formulae, including air temperature, relative humidity, and cloudiness represented by the ratio of measured insolation to the no-sky radiation. The highest correlation is found between relative humidity and measured downwelling longwave radiation. No clear relationship exists between incoming longwave radiation and approximated cloud cover. This close association with relative humidity, a quantity that is directly measured at the COMPS buoys and the BRACE tower, increases confidence in the use of bulk formulae to parameterize the downwelling longwave radiation over the Tampa Bay region.

Assessment of the reviewed formulas resulted in the finding that the Berliand and Berliand (1952) formulation, recommended by Fung et al (1984), best represents downwelling longwave heat flux measurements made at the C10 and C14 buoys. Incoming longwave heat flux measured and modeled (Berliand and Berliand, 1952)

twenty-minutely at the C10 mooring, from day of year 156 through end of year 2003 (n = 13246), were closely correlated ($r^2 = 0.82$) with a RMS difference of 17.0 W/m^2 (Figure 2-3). A similar comparison at buoy C14, from yearday 267 through 365 (n = 4855) results in an RMS difference between modeled and observed downwelling longwave heat flux of 18.4 W/m^2 with an r^2 value of 0.77 (Figure 2-4).

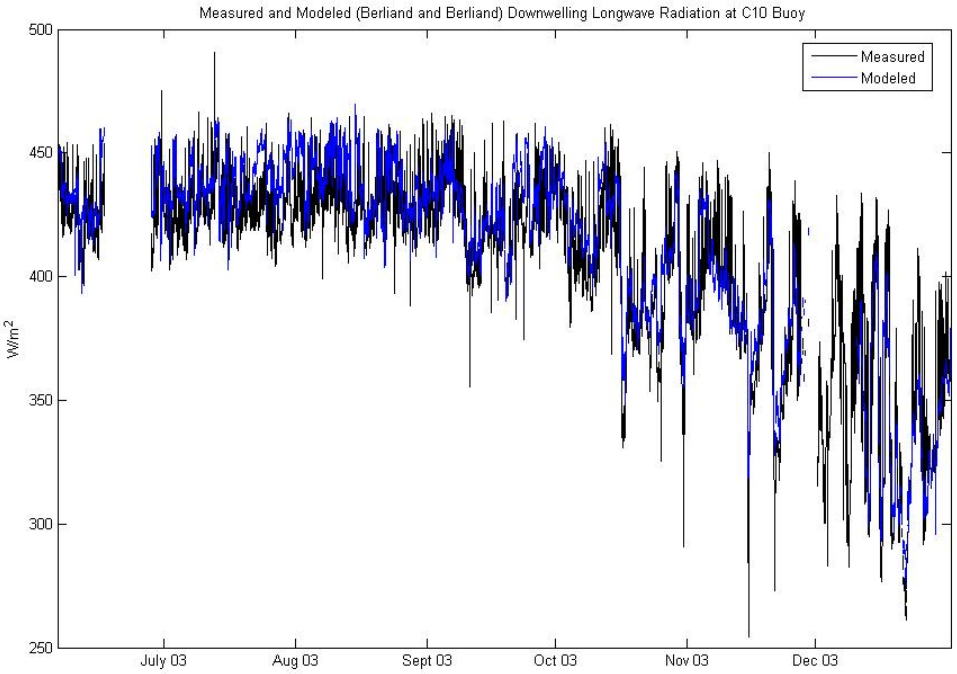

Figure 2-3: Observed and modeled (Berliand and Berliand, 1952) downwelling longwave radiation at the C10 Buoy from yearday 156 through end of year of 2003.

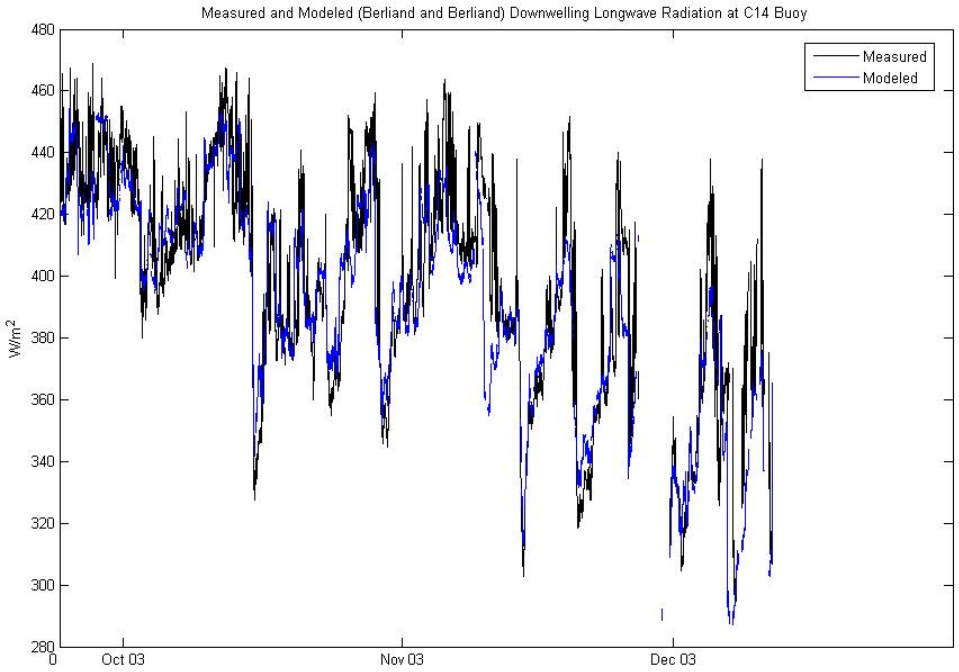

Figure 2-4: Observed and modeled (Berliand and Berliand, 1952) downwelling longwave radiation at the C14 Buoy from yearday 267 through end of year of 2003.

According to Berliand and Berliand (1952), the net longwave radiation, $Q_{LW\uparrow\downarrow}$, may be written as:

$$Q_{LW\uparrow\downarrow} = \varepsilon\sigma T_a^4 [0.39 - 0.05(e_a)^{1/2}] F(C) + 4\varepsilon\sigma T_a^3 (T_s - T_a) \qquad (12)$$

where ε is the emissivity of the ocean surface, σ is the Stefan-Boltzmann constant, T_a is measured air temperature in degrees Kelvin, T_s is the sea surface temperature in Kelvins, e_a is the near surface vapor pressure, and $F(C)$ is a cloud correction factor which is a function of cloud cover. Cloud conditions estimated following Reed (1977), as described above, provide the necessary cloud cover estimates. Fung et al. (1984) present three expressions for the cloud correction factor. That of Clark et al. (1974) is preferred for application to latitudes less than 50˚ N/S and is utilized in this study. The Clark et al. (1974) correction factor is given by:

$$F(C) = 1 - bC^2 \qquad (13)$$

where b is an empirical constant that varies with latitude, increasing with increasing latitude in effort to parameterize the cloud types that are typical for each climate regime, and C is approximated cloud cover.

Outgoing Longwave Radiation

Thermal radiation from the sea surface is most commonly approximated by the Stefan-Boltzmann law:

$$Q_{LW\uparrow} = \varepsilon\sigma T^4 \qquad (14)$$

where ε is the emissivity of the ocean surface, σ is the Stefan-Boltzmann constant, and T is the temperature of the sea surface in Kelvin. Estimations of the emissivity of a body of water range from 0.95 to 0.98 though Kantha (2000) notes that 0.97 is typically used.

Closing the Heat Budget

Net heat energy transfer to or from the bay at the air-sea interface is written as the sum of the net radiative and turbulent heat fluxes:

$$Q_{net} = Q_S + Q_p + Q_L + Q_{SW\uparrow\downarrow} + Q_{LW\uparrow\downarrow} + Q_{pen} \qquad (15)$$

where Q_p is the sensible heat flux due to rainfall as computed by the COARE algorithm. The net surface heat flux, $Q(t)$, is also determined by examination of the rate of heat storage within the bay (the change in depth-averaged water temperature, T, through time), assuming there is no horizontal advection, following Morey and O'Brien (2002):

$$\frac{dT}{dt} = \frac{Q(t)}{\rho c_p H} \qquad (16)$$

where H is the depth of the water column.

Variation in the heat content of the estuary is the result of ocean-atmosphere heat exchange and advective heat flux between Tampa Bay and the Gulf of Mexico. The difference between the net heat transfer at the surface, Q_{net}, and the total heat flux, $Q(t)$, derived from the observed change in heat content in the estuary, $\frac{dT}{dt}$, represents the error incurred by neglecting advective heat exchange at the mouth of the bay and an error term resulting from uncertainties in the measurement and computation of heat budget components.

Tampa Bay is characteristically well mixed in the vertical and bulk sea temperature measured mid-depth at the BRACE tower is representative of the depth-averaged temperature. Examination of water temperature measured monthly near-surface, mid-depth and near-bottom at EPCHC stations 21 and 90, in close proximity to the BRACE observational tower (see Figure 2-1), over 2004 confirms this assumption. At station 21, an average temperature gradient of only 0.14 ºC with a maximum gradient of 0.51 ºC was found and, at station 90, a mean temperature gradient over the water column of 0.18 ºC with a maximum gradient of 0.74 ºC.

The EPCHC water quality monitoring protocol dictates that each station within Tampa Bay is sampled monthly. However, approximately one-third of the stations are visited over the course of a single day. Complete coverage of Tampa Bay occurs over three days of sampling, unevenly spaced throughout the month. Thus, in illustration, stations located throughout Old Tampa Bay (the northwest arm of the bay) were sampled on the 6th of January 2004, Hillsborough Bay stations (northeastern portion of the bay) and several Middle Tampa Bay stations were visited on the 21st, while sampling of the remainder of Middle Tampa Bay stations and Lower Tampa Bay stations was completed on the 28th of January 2004. On a single day, sampling typically begins around 8:30 AM local time with the final sample gathered around 3:30 PM. Individual stations are sampled at random hours throughout the year. Despite the asynoptic nature of the EPCHC dataset, assessment of mid-depth water temperatures over 2004 reveals little horizontal variation in water temperature. Sampling occurred over 72 days (three days

per month) in the year 2004. Stations sampled on a given day were divided in two groups: stations visited in the morning hours and those stations sampled in the afternoon. The range of mid-depth water temperature measurements attained over the course of a morning or afternoon was, on average, 0.86 ºC for those stations in water depth of 3 ft. or greater (n = 364). Bulk sea temperature measurements acquired at the BRACE tower, thus rates of surface heat exchange derived at the observational tower, may be considered representative of Tampa Bay.

Evaporation Rate and Freshwater Budget Analysis

The latent heat of vaporization of water (L_e; J/kg) is the amount of energy required to convert one kilogram of water from liquid to gas phase and is a function of the temperature of the bulk liquid. Latent heat of vaporization at the BRACE tower is approximated according to measured bulk water temperature (T_s) following Stull (1988):

$$L_e = (2.501 - 0.00237T_s)\, 10^6 \qquad (17).$$

Given a computed rate of heat loss from the Bay which incorporates computations of evaporation rate (the latent heat flux; $J/s \cdot m^2$) and an estimate of the amount of heat contained within each kilogram of water vapor formed (J/kg), the over-water rate of evaporation (E) is given:

$$E = Q_L / L_e \qquad (18).$$

Daily averaged evaporation rates inferred from over-water latent heat exchange at the BRACE meteorological tower were compared to rates acquired via evaporation pan technique at a SWFWMD site located near McKay Bay. The relative importance of this parameter to the freshwater budget of the bay is established by comparison with freshwater source parameterizations (precipitation rates, underground seepage, and surface runoff) supplied as boundary conditions to the Meyers et al. Tampa Bay model.

A Meyers et al. model hindcast analysis of the response of bay residual circulation to intervals of above and below average freshwater inflow was completed for the period of 2001 through 2003 (Meyers et al. 2007). During this period, precipitation rates supplied to the model were gathered from four stations located around the bay: the Sarasota/Bradenton Airport (call sign SRQ), the St. Petersburg Albert Whitted Airport (SPG), the St. Petersburg/Clearwater International Airport (PIE), and Tampa International Airport (TPA). Hourly rainfall data from these stations were averaged to daily values for model input.

There are more than one hundred surface sources supplying freshwater to Tampa Bay (TBEP; http://www.tbep.org). USGS daily averaged streamflow data provides surface freshwater runoff rates where point runoff sources are gauged. Streams that are not gauged are scaled from gauges located upstream or are assigned flow rates according to gauges located in basins that are nearby and similar in size and land cover. Groundwater seepage is parameterized as an approximate 8% augmentation of the mean flow from each surface water source following Brooks (1993). These boundary conditions, combined with evaporation rates produced in computations of latent heat exchange at the BRACE Tower for the time interval of June 2002 through December 2003 of this hindcast study, were used in construction of a freshwater budget for Tampa Bay.

Chapter Three

BRACE Six-Month Turbulent Heat Flux Study

Introduction

Estuaries and coastal regions are particularly susceptible to nutrient over-enrichment due to their close proximity to source-rich regions (National Research Council, 2000). The impact of these nutrients poses a significant threat to sensitive ecosystems by accelerating the rate of eutrophication and leading to toxic algal blooms, which can affect human health and are often responsible for causing massive fish kills and aquatic species morbidity and mortality (National Research Council, 2000). As a corollary to the increase in reliance on fossil fuels and inorganic fertilizers, excess inputs of nitrogen and phosphorus to coastal estuaries are also expected to occur. As witnessed in the Tampa Bay Estuary, this will likely result in a continual decline in ecosystem quality unless direct actions are taken to reduce the influx of nutrients from agricultural runoff, industrial discharges, and the atmospheric deposition of nutrients released from fossil fuel combustion. The BRACE study was created to focus on these issues by assessing the impacts of local sources of atmospheric nitrogen on the health of the estuary and improving nitrogen deposition estimates over Tampa Bay. The focus of this research is on atmospheric deposition, which is a relatively new research concept that was once considered irrelevant by the scientific community (TBEP, 1996). Recently, Hicks et al. (2000) have shown that in some locations dry atmospheric deposition may be responsible for up to 40% of the nitrogen entering coastal water bodies.

To effectively manage an ecosystem such as the Tampa Bay Estuary, a comprehensive understanding of the nutrient input pathways is necessary. In comparison to industrial discharges that are routinely monitored by state and local officials, it is much more challenging to monitor and estimate the atmospheric deposition of nutrients to an ecosystem, due to the spatial and temporal variability associated with this input, as well as the inherent difficulty is determining transfer rates over the entire estuary. Although models have been developed to estimate air/sea transfer rates over open oceans, relatively few are specific to coastal areas, which experience unique meteorological processes because they are located adjacent to land masses. Nevertheless, many of these models are based on the bulk exchange method and parameterized according to the Monin-Obukhov Similarity Theory (MOST) for heat, moisture, and momentum transfer governing the deposition process (Arya, 1988; Hicks, 1975; Hicks and Liss, 1976; and Liu and Schwab, 1987). Based on this process, air/sea mass transfer rates can be approximated as the product of the modeled heat transfer coefficient (D_H) and measured wind speed (u_z) (Valigura, 1995).

The present research had two objectives: 1) to critically assess and validate the TOGA COARE (Fairall et al., 1996) and the NOAA Buoy (Valigura, 1995) models, by

comparing direct measurements of sensible heat and friction velocity with modeled estimates and 2) to compare and contrast several important modeled flux parameters. This study was conducted to summarize model differences and to guide potential users through these differences so that nitrogen air/sea transfer rates determined during the BRACE study can more accurately be estimated over Tampa Bay.

Model Theory

TOGA COARE

The Tropical Ocean Global Atmosphere (TOGA) Coupled Ocean-Atmosphere Response Experiment (COARE) bulk flux algorithm was initially developed by the NOAA Environmental Technology Laboratory (Fairall et al., 1996). Model development began in recognition of an inability to predict or diagnose tropical ocean/atmosphere interactions, which are widely known to play an essential role in global climate variability.

Development of the bulk flux algorithm began on preliminary COARE cruises in 1990 as an integral part of the "interface component" of TOGA COARE. Of primary importance during the COARE project were balancing the surface radiative and turbulent heat fluxes of the tropical western Pacific region to within stringent limits of accuracy, and the formulation and validation of improved flux parameterizations. Since the inception of the program, the COARE bulk flux algorithm has undergone continuous revisions and has been released for community use at several stages of model construction. Although originally formulated under the COARE Pacific Warm Pool Study and verified with data from the COARE domain centered in equatorial Pacific, the model authors note that development of the algorithm incorporated measurements from mid-latitude regions and therefore expect the COARE code to be relevant at these higher latitudes (Lukas and Webster, 1992; Fairall et al., 1996).

Among other refinements, the most recent release of the COARE algorithm used in this study (version 3.0) is tuned to an expanded data set (including observations made in North Atlantic and North Pacific regions) and introduces a variable representation of the Charnock parameter to improve model performance at higher wind speeds, extending the applicability of the model from the Tropics to high latitudes (Fairall et al., 2003). The COARE algorithm, though developed for open ocean studies, has been applied to shallow water and coastal regimes prior to the present study (Sun et al., 2003; Beardsley et al., 1998). For a complete description of the COARE bulk algorithm version 3.0 and an explanation of model verification results, please see Fairall et al. (2003).

The model requires input measurements of wind speed, air and bulk water temperature, relative humidity, downward solar flux (insolation), air pressure, and downward longwave radiation (estimated following method described in Chapter 2). Model outputs include sensible and latent heat fluxes, friction velocity, and the dimensionless heat transfer coefficient (D_H) allowing for comparison of the COARE 3.0 estimation of these parameters with the NOAA Buoy model results and permitting the external calculation of air/sea transfer rates of soluble gases.

NOAA Buoy Model

The NOAA Buoy model code was produced by a BRACE scientist (Bhethanabotla 2002) from research conducted by Valigura (1995) of the NOAA Air Resources Laboratory. It is used as a tool for estimating air/sea transfer rates of nitric acid over coastal water bodies (Valigura, 1995). Although model application was originally intended for a highly soluble compound, its applicability has been extended to calculate the deposition of other nitrogen species to Tampa Bay, Florida (Bhethanabotla, 2002; Evans et al., 2004; Poor et al., 2001). The model was formulated based on the works of Hicks (1975), Hicks and Liss (1976), and Liu and Schwab (1987) and includes both the bulk exchange method and the flux-gradient relationships for heat, moisture and momentum. Model development included the use of near-surface, over-water coastal meteorological data obtained from a network of buoys to simulate existing small-scale coastal conditions. Given that the model was developed for nitric acid, which is highly soluble in alkaline seawater, transfer was considered unidirectional. Additional assumptions were that surface and quasi-laminar resistances are negligible compared to aerodynamic resistance, and therefore were not considered during model synthesis (Valigura, 1995). Finally, a major assumption in the model is that nitric acid gas and sensible heat are similarly regulated by aerodynamic resistance (Hicks and Liss, 1976). As shown in Valigura (1995), sensible heat flux is dependent, according to the bulk transfer theory, on the dimensionless heat transfer coefficient (D_H). The D_H is also used to calculate the air/sea gas exchange rates, which are calculated as the product of D_H and measured wind speed at each time step.

Inputs to the model include hourly wind speed, air and bulk water temperature, and relative humidity. The model begins iteration with an initial approximation of the transfer coefficients until the modeled temperature and wind gradients match the measured wind speed and temperature differentials (Valigura, 1995). Model outputs include sensible and latent heat flux, friction velocity, dimensionless heat transfer coefficient and gas transfer rate.

Model Differences

Specific Humidity

The bulk aerodynamic formula for latent heat exchange at the air/sea interface requires specification of the specific humidity difference between a reference height and the surface. This specific humidity gradient is derived from vapor pressure computed from observed relative humidity at height and saturated air (assuming a 2% humidity reduction to account for salinity) at the surface.

The TOGA COARE algorithm adopts Tetens' (1930) equation for vapor pressure, incorporating an enhancement factor to compensate for application of the formula to moist air as opposed to pure water vapor, in the form recommended by Buck (1981) for typical use. Alternatively, the NOAA Buoy model employs Bögel's (1979) accuracy improved adaptation of Tetens' formula but does not include an enhancement factor. Provided the same meteorological inputs, however, these distinct vapor pressure formulations produce perfectly correlated results with a maximum separation of less than

1% of the range of computed hourly vapor pressure for the six month period of this study, indicating choice of equation form does not explain modeled specific humidity differences.

Tetens' equation within the TOGA COARE code is supplied ambient air and bulk water temperatures and returns saturated air and sea surface vapor pressures. Multiplication by observed relative humidity at height and an assumed 98% saturation humidity at the surface converts the respective saturation vapor pressures to vapor pressures. In contrast, the NOAA Buoy model derives dewpoint temperatures at the sea surface from ambient air temperature and salinity corrected saturated humidity, and at height from ambient air temperature and measured relative humidity, computing surface vapor pressure directly from these dewpoint temperatures.

Cool Skin

Over the ocean, turbulent fluxes are typically directed from ocean to atmosphere, acting in conjunction with the net longwave radiative flux to cool the surface waters. The upward exchange of heat at the air/sea interface generates a millimeter-scale surface film usually several tenths of a degree cooler than the bulk water temperature. It is this skin temperature that is required for input to the bulk aerodynamic formulas. Where the interfacial temperature is not measured, the bulk water temperature must be corrected for this cool skin anomaly.

Fairall et al. (1996) represent the total heat loss at the surface as the sum of sensible and latent heat fluxes and the net longwave radiative flux. A fraction of incident shortwave radiation is absorbed in the cool skin layer, increasing the skin temperature. The TOGA COARE algorithm applies the effective surface cooling, adjusted for net shortwave radiative warming, to subsequent computations of cool skin layer thickness, δ, and temperature correction, ΔT_c. The expressions for δ and ΔT_c in both shear and buoyancy driven turbulence regimes, as described by Paulson and Simpson (1981), are merged for incorporation in the TOGA COARE code.

Within the NOAA Buoy model the surface boundary heat loss is equal to the total of the sensible and latent heat fluxes and the outgoing longwave radiation. No adjustment is made for the absorption of shortwave radiation within the surface film and heating contributed by atmospheric longwave radiation is neglected. The cool skin temperature correction equation does not differ between shear and convective settings.

Warm Layer

The COARE 3.0 code includes a separate algorithm as a correction for the influence of a diurnal warm layer on the bulk water temperature. Formulated for application to coastal regimes, the NOAA Buoy model incorporates an adjustment to bulk temperature that accounts for the thermal skin but does not correct for warm layer development. To directly compare COARE 3.0 model results with the NOAA Buoy model output, the warm layer option within the COARE 3.0 model was disabled. Because Tampa Bay is characterized as a shallow and vertically well-mixed estuary, the warm layer correction is seldom likely to be necessary; a warm layer would evolve only during times of very still winds and strong solar heating.

Wind Speed/ Gustiness/ Slip

Both models incorporate mechanisms to deal with non-zero flux values in a low wind speed environment because theoretically, low wind speeds should not yield zero flux. The COARE model includes a gustiness parameter in all computations using the wind speed to overcome this issue (Godfrey and Beljaars, 1991). This parameter is strictly a function of a constant convective parameter and the convective scaling velocity and is used in all subsequent computations of sensible and latent heat fluxes, friction velocity, velocity roughness length, Obukhov length scale (and therefore is used in stability function computation) and transfer coefficients. The NOAA Buoy model eliminates conditions caused by extremely low wind speeds by ignoring all time steps where the wind speed falls below 0.7 m/s (in the six month dataset, ~1% of wind measurements). In remaining cases, the wind speed includes a "slip correction" that is used in further calculations of fluxes, friction velocity and the Obukhov length scale. This computation takes into account the wind-induced skin velocity of the water, e.g. if the skin is slipping along in the direction of the wind, being driven by the wind, then the effective wind speed available for driving surface fluxes is reduced. The TOGA COARE authors specify that wind speed model input should be the wind speed relative to the sea surface. Surface current speed and direction, however, are not available from the BRACE tower array and therefore observed rather than effective wind speeds are passed to the TOGA COARE model, neglecting correction for wind driven surface slip.

Sea Surface Roughness

Charnock's (1955) relation describes sea surface roughness dependence upon wind stress and includes a constant that is tunable to local conditions. This parameter is assigned a large range of values (typically from 0.01 to 0.03) in the literature, but is particular to the study site, increasing in value from open ocean to fetch-limited and near-shore regimes (Lange and Højstrup, 2000). Evidence of a dependence of the Charnock "constant" upon wind speed led the authors of the TOGA COARE code to incorporate a variable "constant" in the latest version (Fairall et al. 2003). The "constant" is fixed at a value of 0.011, which is generally applied to open ocean settings, during low wind speed intervals. However, at moderate to high speeds between 10 and 18 m/s, the "constant" varies linearly, increasing with increasing wind speed. The resulting increase in estimates of surface roughness has the effect of predicting greater near-surface turbulence and fluxes. Above 18 m/s the parameter is again a fixed number at 0.018. Alternatively, within the NOAA Buoy model, this number is an invariable constant set equal to 0.016. At the BRACE study site, it was discovered that less than 2% of hourly winds during the time frame of data collection from June through November of 2002 were greater than 10 m/s and most were observed in the month of November. Therefore, the higher value chosen by Valigura (1995) for the Charnock constant is likely more appropriate for flux studies in a coastal environment.

Atmospheric Stability

The MOST assumes that, within the surface layer, turbulent transfer is the dominant mechanism driving vertical heat exchange and that the turbulent fluxes of heat are constant with height. Wind, temperature and specific humidity gradients within this layer can be characterized as universal (Ψ) functions of a non-dimensional atmospheric stability parameter: the ratio of measurement height, z, to the Monin-Obukhov length scale, L. The structure of the universal (Ψ) functions is not specified and several schemes have been derived.

The NOAA Buoy model assumes that the form of the universal functions is as previously applied to the study of atmospheric deposition of SO_2 (Hicks and Liss 1976), namely: under neutral to stable conditions ($z/L \geq 0$), the NOAA Buoy model follows the recommendations of Webb (1970) for the structure of Panofsky's (1963) universal functions and for unstable settings ($z/L < 0$) the formulations suggested by Dyer and Hicks (1970) are adopted. Valigura (1995) notes that MOST is considered applicable over a limited atmospheric stability parameter range ($-1 \leq z/L \leq 1$), outside of which either buoyancy driven turbulence dominates and friction velocity becomes an inappropriate scaling parameter (in the limit of extreme instability) or turbulent vertical mixing is suppressed in a stably stratified atmosphere.

The TOGA COARE code parameterizes a stable surface layer following the Beljaars and Holtslag (1991) universal function equations. These expressions have been effectively applied to conditions of extreme stability ($z/L \approx 10$) and perform in near-neutral stability regimes like the Webb (1970) functions adopted by the NOAA Buoy model. For unstable environments, the TOGA COARE algorithm blends the universal (Ψ) functions appearing in the NOAA Buoy model code with a form applicable to highly unstable, convective settings.

Experimental Methods

Study Area and Modeling Period

Tampa Bay is the largest open water estuary in Florida covering approximately 645 square kilometers with an average depth of about 4 meters and a maximum depth of about 10 meters at the various shipping channels. Hourly meteorological, sensible heat, and friction velocity measurements were made from June through November, 2002 at the Port Manatee Turn Tower, which is located in Middle Tampa Bay and is one of the Tampa Bay Physical Oceanographic Real-Time System sites (see http://ompl.marine.usf.edu/PORTS/gt03010.html). The tower was funded in part by the Bay Regional Atmospheric Chemistry Experiment (BRACE) and is located at latitude 27N 39' 50", longitude 82W 34' 50", approximately 7 nautical miles southeast of St. Petersburg, FL, and 4 nautical miles west-northwest of Port Manatee, FL. The tower is in water approximately 5 meters deep and extends above the water surface by 10 meters. Please visit the OMPL website (http://comps.marine.usf.edu/BRACE) for a complete description, photograph, and diagram of the research tower.

Meteorological Data Collection

Hourly measurements of sensible heat flux and friction velocity were made at a height of 6.9 meters above mean sea level (MSL) with a Campbell Scientific CSAT3, 3-dimensional sonic anemometer. Hourly air temperature and relative humidity were measured at a height of 5.0 meters above MSL and wind speed and wind direction were measured at a height of 10.0 meters above MSL using R.M. Young Company meteorological sensors. Hourly measurements of the bulk water temperature were made at approximately 2.4 meters below MSL with a Sea-Bird Electronics temperature gauge. All instruments were certified calibrated by the respective manufacturers and certificates are available at the COMPS website (ftp://comps.marine.usf.edu/pub/BRACE/seagauge_data/instr/). Instruments were operated, maintained and serviced according to the manufacturers' specifications by the Ocean Modeling and Prediction Lab in the USF College of Marine Science.

Model Application

The micrometeorological data were available in real-time via the Web at http://comps.marine.usf.edu/BRACE/ and were used as inputs to the TOGA COARE and NOAA Buoy models. The modeled outputs of sensible heat and friction velocity were compared to the actual CSAT3 measurements (n = 4,028) made at the tower. In addition, the modeled outputs of sensible and latent heat, the dimensionless heat transfer coefficient, and friction velocity were used for inter-model comparisons of flux parameters (n = 4,126).

QA/ QC

Rutgersson et al. (2001) found that measured heat fluxes during extreme rain events can produce biased data. Ultrasonic anemometers are unable to measure wind during rainfall. This bias is due to small water droplets beading on the transducer's surface and interfering with signal transmittance. Based on this information, hourly measurements of recorded rainfall were paired with the observed and model predicted sensible heat flux and friction velocity data to determine if rainfall biased those measurements. If during a rain event a measurement spiked high or low compared to the remaining hourly measured data points, it was considered an outlier and that time step was deleted from the measured data. As a result of this analysis, a total of 138 hours or approximately 3.4% of the measured to modeled dataset were removed for a total of 3,890 data points.

Results

Observed and Predicted Flux Parameters

The TOGA COARE and NOAA Buoy modeled results were compared with measured sensible heat flux and friction velocity from June through November 2002 (n = 3,890). The sensible heat flux comparison is shown in both Figure 3-1 and Table 3-1, in

which the observed and predicted values indicate that both models were reasonably predictive of heat transfer at the water surface with R^2 values of 0.80 and RMS model differences of 11.02 and 12.52 W/m^2 for the TOGA COARE and NOAA Buoy models, respectively (Table 3-1). Average and standard error sensible heat values were 17.74 W/m^2 and 0.34 W/m^2 for the TOGA COARE model and 16.86 W/m^2 and 0.39 W/m^2 for the NOAA Buoy model, respectively. When the same comparison was made for friction velocity (Figure 3-2; Table 3-1), both modeled R^2 values were 0.52 and RMS differences of 0.06 m/s were found for the TOGA COARE and NOAA Buoy models. Average and standard error friction velocity values were 0.17 m/s and 0.0012 m/s for the TOGA COARE model and 0.16 m/s and 0.0013 m/s for the NOAA Buoy model, respectively. These results indicate that there was reasonable agreement for this flux parameter.

Table 3-1: Performance statistics for predicted and observed sensible heat (H, W/m^2) and friction velocity (u*, m/s) for all data and data during stable atmospheric conditions (Kara 2005).

ALL DATA (n=3,890)	TOGA COARE		NOAA BUOY	
Measure	H	u*	H	u*
Correlation Coefficient (R)	0.89	0.73	0.89	0.73
Root Mean Square Error (RMS)	11.02	0.06	12.52	0.06
Fractional Bias (FB)	0.21	0.05	0.26	0.08
Normalized Mean Square Error (NMSE)	0.15	0.11	0.19	0.11
Factor of Two Analysis (Fa2)	63%	92%	53%	88%

STABLE DATA (n=223)	TOGA COARE		NOAA BUOY	
Measure	H	u*	H	u*
Correlation Coefficient (R)	0.23	0.40	0.23	0.39
Root Mean Square Error (RMS)	9.84	0.12	12.91	0.12
Fractional Bias (FB)	-1.30	0.21	-1.49	0.27
Normalized Mean Square Error (NMSE)	4.37	0.59	5.54	0.65
Factor of Two Analysis (Fa2)	33%	85%	18%	77%

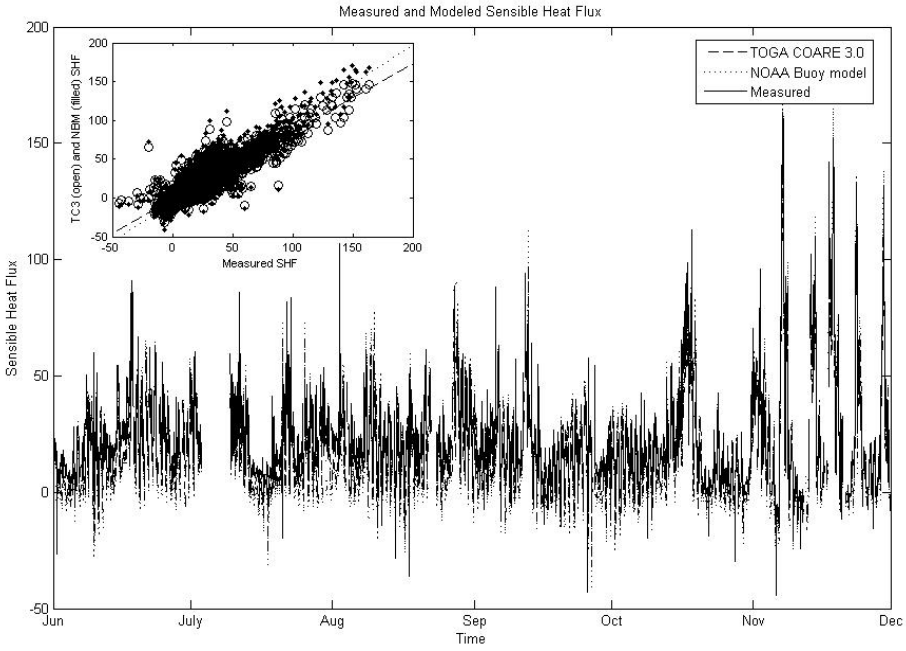

Figure 3-1: Hourly measured and modeled time series and scatterplot of sensible heat (W/m^2). The R^2 value for both modeled series with the measured was 0.80. During summer months (June – September) the R^2 value was about 0.50 for both models while the fall months (October – November) show improved agreement with an R^2 value of about 0.83.

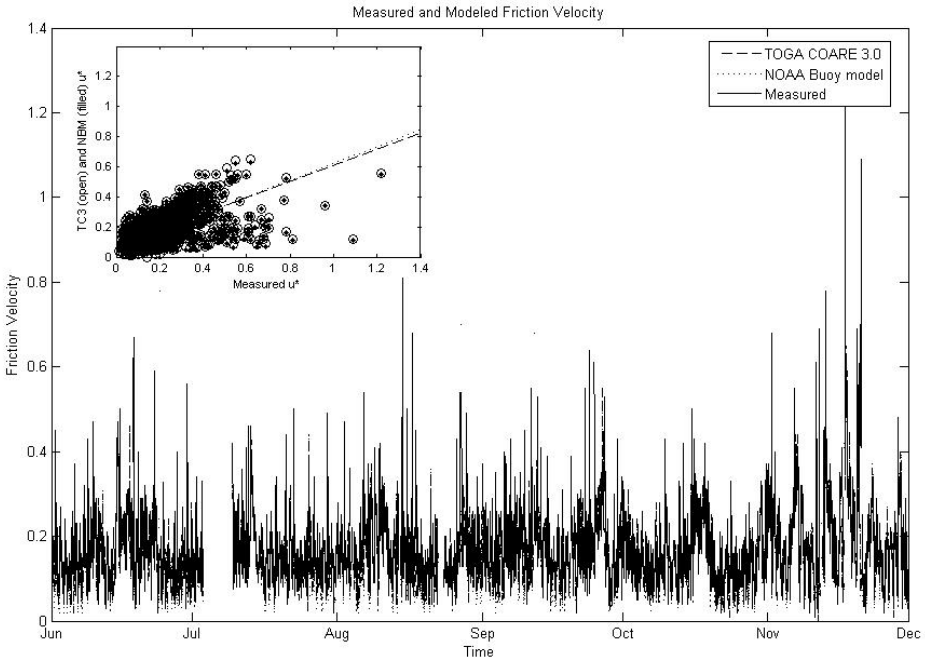

Figure 3-2: Hourly measured and modeled time series and scatterplot of friction velocity (m/s). The R^2 value for both modeled series with the measured was 0.52. During summer months (June – September) the R^2 value was about 0.44 for both models while the fall months (October – November) show improved agreement with an R^2 value of about 0.65.

Measures of model performance, as described by Ahuja and Kumar (1996), Chang and Hanna (2004), Gudivaka and Kumar (1990), Kumar et al. (1993), Kumar et al. (1999), Riswadkar and Kumar (1994) and Patel and Kumar (1998) were used to characterize the quality and reliability of the models. According to Kumar et al. (1993), model performance is acceptable if the following performance statistics are observed: $-0.5 \leq FB \leq 0.5$ and $NMSE \leq 0.5$. The results for the entire observed to predicted data set ($n = 3,890$), shown in Table 3-1, support the hypothesis that both models predict reasonably well the aforementioned flux parameters. The same analysis was also completed just for hourly data points corresponding to a stable atmosphere as described by Kara (2005), in which the air temperature exceeded the bulk sea temperature by at least 0.75 K ($n = 223$). Results indicate that for this stability class, model performance declined significantly for sensible heat. For example, both the Fractional Bias and Normalized Mean Square Error, which offer a measure of the mean error and scatter in the data set, respectively, are both within recommended acceptable limits for the entire data set, but fall outside of these limits for the stable data (Table 3-1). In addition, a Factor of Two Analysis, defined as the percentage of the predictions within a factor of two of the observed values, indicated that for sensible heat flux and friction velocity, a majority of the predicted values were within this range for the entire data set for both the TOGA COARE and NOAA Buoy models (Table 3-1). However, when the analysis was

conducted for the stable data set, a majority of the predicted values of sensible heat were outside of this range (Table 3-1). These analyses demonstrate that because the MOST is unreliable during stable conditions, the models must be used cautiously when the atmosphere is strongly stable.

Inter-Model Comparison

Sensible Heat Flux/ Dimensionless Heat Transfer Coefficient –

As shown in Figure 3-3, NOAA Buoy and TOGA COARE modeled sensible heat flux approximations are nicely correlated with a RMS model difference of 3.7 W/m^2. Specification of the dimensionless heat transfer coefficient (D_H), which is used to calculate air/sea gas exchange, is an important variable in the calculation of sensible heat exchange via bulk algorithms (see Valigura, 1995). The magnitude of D_H is governed by atmospheric stability and wind speed. As shown in Figure 3-4 as a horizontal cluster of open circles, the NOAA Buoy model designates 7.0% (n = 292) of the data set as extremely stable (z/L > 2, Monin-Obukhov Similarity Theory no longer applies). During this period, a constant value is assigned to Panofsky's Ψ_W function, resulting in fairly constant and small values for the NOAA Buoy model computed D_H. For 60% of those time steps classified as extremely stable by the NOAA Buoy model, the TOGA COARE model classifies the stability as neutral to unstable, resulting in a large range of D_H values (in contrast to NOAA Buoy modeled results). As previously noted, the TOGA COARE authors extend applicability of their model to extremely stable regimes following Beljaars and Holtslag (1991).

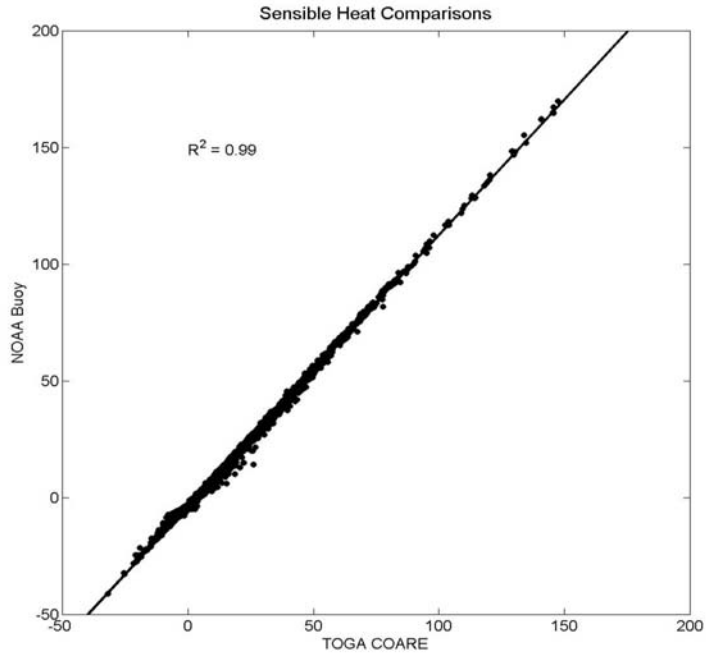

Figure 3-3: Scatterplot of modeled hourly sensible heat flux (W/m^2). Models are highly correlated with very little scatter.

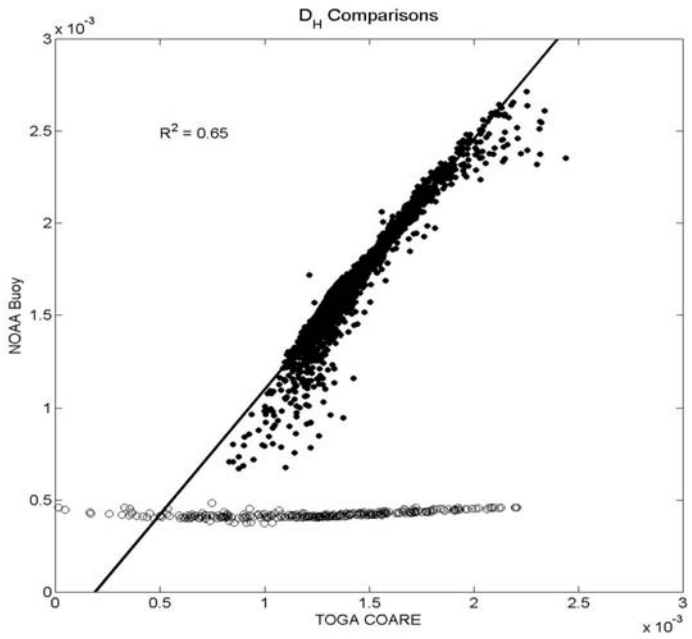

Figure 3-4. Scatterplot of modeled hourly D_H. The horizontal cluster of open circles represents, in part, model divergence of stability classification. The NOAA Buoy model estimates extremely stable conditions, but for 60% of these data points, the TOGA COARE model predicts neutral to unstable stability.

Friction Velocity –

The friction velocity is one of the fundamental MOST scaling parameters defined as the square root of kinematic wind stress. This velocity scale is a measure of the turbulent shear strength in the surface layer and is important to bulk estimations of heat, moisture and momentum flux at the air/sea boundary. Results show that the NOAA Buoy and TOGA COARE model estimated friction velocity values agree very well (R^2 value of 0.99) (Figure 3-5).

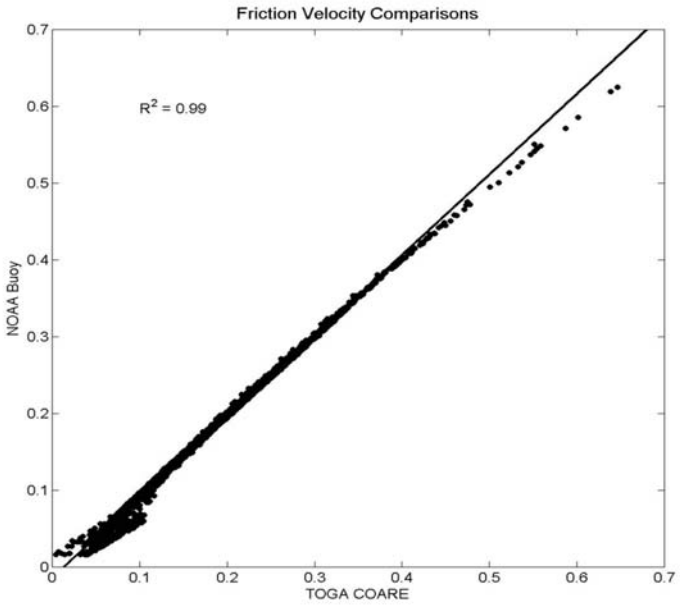

Figure 3-5: Scatterplot of modeled hourly friction velocities (m/s). Models are highly correlated with very little scatter.

Latent Heat Flux –

NOAA Buoy model and TOGA COARE model latent heat exchange estimations agreed less satisfactorily with an R^2 value of 0.47 and RMS difference of 67.90 W/m^2 (Figure 3-6). A sensitivity analysis led to a basic alteration to the section of the NOAA Buoy model code that calculates the specific humidity gradient. The vapor pressure computations were restyled to accept ambient air temperature at height and measured bulk water temperature as inputs to the expression for vapor pressure, rather than internally computed dewpoint temperatures, as described previously. The resulting air and sea surface saturation vapor pressures were then converted to vapor pressures via multiplication by the observed relative humidity at height and assumed 98% relative humidity, respectively. No modifications were made to the form of the vapor pressure expression chosen by the NOAA Buoy model author. This simple adjustment to the NOAA Buoy model algorithm improved intermodel comparisons of latent heat flux dramatically (R^2 value of 0.99 and a model difference RMS value of 39.4 W/m^2) (Figure 3-6).

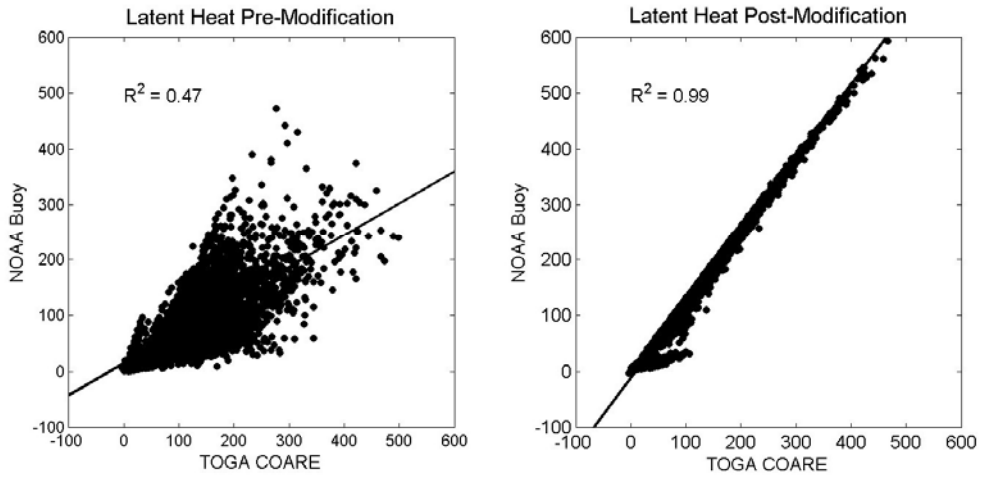

Figure 3-6: Scatterplot of modeled hourly latent heat flux (W/m^2) comparisons for pre- and post- modification of vapor pressure.

Discussion and Conclusions

Measured and modeled comparisons of sensible heat flux and friction velocity over a six-month period showed that the TOGA COARE and NOAA Buoy models were reasonably predictive of these flux parameters, although a slight under-prediction of sensible heat flux by both models was observed. As described previously, it is suspected that this propensity to under-predict sensible heat will likely correspond with an under-prediction of the dimensionless heat transfer coefficient used to calculate air/sea nitrogen gas transfer rates. An evaluation of the sensible heat flux comparisons revealed that despite this tendency, modeled results were still within recommended performance limits as described by Kumar et al. (1993), although model performance is compromised when applied to stable regimes. These results strongly caution against the use of these models during stable atmospheric conditions.

It is thought that the models are under-predicting sensible heat due to a characteristic of the MOST and bulk transfer methods for estimating heat, moisture, and momentum exchange, which are embedded in both models. Oost et al. (2000) and Rutgersson et al. (2001) showed that the predicted heat transfer coefficient gradually decreases with decreasing air/sea temperature differentials and low wind speeds, and is often smaller than expected under these conditions, resulting in a lower sensible heat flux approximation. Due to the limited fetch and relatively low wind speeds typical of a coastal estuary, it is not surprising then that this characteristic would result in lower than expected heat transfer estimates as compared to direct sonic anemometer measurements of sensible heat exchange. To test this hypothesis with results, a diurnal frequency distribution of predicted and observed sensible heat flux ratios less than 0.8 (n = 2120; ~54% of the dataset) was developed to determine if lower than expected heat flux predictions occurred more frequently during the late afternoon and evening hours. This

time frame typically contains periods of increasing stability due to low winds, very low air-sea temperature differences from the heating of the day and reduced sensible heat exchange between the atmosphere and oceans (Arya, 1988), particularly in the summer season. Results show that approximately 67% of those ratios occurred in the late afternoon and evening hours (1500 - 0200 LST) when the average measured sensible heat flux decreased from 26.12 W/m^2 during the daytime to 17.54 W/m^2 in the evening. Likewise, the same analysis conducted for friction velocity (n = 915; ~23% of the dataset) found that approximately 60% of those ratios also occurred during that time period, confirming the hypothesis that similar to results from the previously mentioned studies, sensible heat transfer is under-predicted by the bulk transfer theory during periods of decreasing air-sea temperature differentials, or when air temperature is greater than water temperature. An additional evaluation of measured and modeled momentum transfer showed that despite frequent spikes in measured friction velocity, both the TOGA COARE and NOAA Buoy models also adequately predicted this flux parameter. Based on this study and compared with previous research (Rutgersson et al., 2001; Valigura, 1995), it is believed that both models provide acceptable methods for estimating heat and gas exchange across the air/sea interface in coastal areas.

Despite differing cool skin correction schemes resulting in disparate air/sea temperature gradients computed by each model, both models produced closely corresponding sensible heat flux values, although the TOGA COARE predicted values were generally greater than those estimated with the NOAA Buoy model. For the small percentage of the data set associated with periods of extreme stability, the models disagreed in both their predictions of stability classification and the dimensionless heat transfer coefficient. Under these conditions, the universal functions included in the calculation of D_H are set to a constant by the NOAA Buoy model and consistently small values of D_H are generated. The NOAA Buoy model typically under-predicts TOGA COARE produced D_H for this case, leading to estimated sensible heat flux and air/water transfer rates of lesser magnitude. The TOGA COARE model's representation of Panofsky's universal functions addresses extremely stable or unstable atmospheric states and is likely more applicable in the very stable settings that are more prominent during the summer season. In contrast, during neutral to unstable atmospheric conditions, the modeled values of D_H closely agree.

The greatest divergence in model results appeared in estimations of latent heat exchange. Sensitivity analysis of the model algorithms led to the discovery that the majority of model differences were attributed to the vapor pressure calculation. Therefore, a simple adjustment to the NOAA Buoy model's computation of vapor pressure, following Buck (1981) by utilizing ambient air temperatures rather than dewpoint temperatures and converting resulting saturation vapor pressure to vapor pressure, improved modeled latent heat flux agreement. This standardized the vapor pressure calculation method between the models and dramatically improved latent heat comparisons.

Based on this analysis, both models are suitable for use in a coastal environment to estimate nitrogen air/sea gas exchange, although the NOAA Buoy model requires fewer meteorological inputs. However, if the purpose is to conduct more sophisticated microscale modeling of air/sea interactions, the TOGA COARE model is recommended.

Chapter Four

Three-Year Heat Budget Study

Introduction

The Tampa Bay estuary, located on the west central Florida Gulf coast, is Florida's largest open water estuary (http://www.tbep.org/). In the semi-enclosed Tampa Bay basin, water temperature is modulated primarily by ocean-atmosphere heat transfer at the bay surface and secondarily by advective heat exchange with the waters of the Gulf of Mexico at the southern mouth of the bay. Water temperature variations in this subtropical estuary govern the abundance and distribution of organisms and influence circulation dynamics.

A numerical model of Tampa Bay hydrodynamics is established (Vincent 2001, Meyers et al. 2007) and has been utilized in assessing the potential impacts to estuarine circulation and water quality of bay management policy concerning withdrawal of freshwater from source rivers, construction of a desalination facility on Tampa Bay, and injection into the bay of process waste water from the Piney Point phosphate mine. This Meyers et al. model is one component of the Tampa Bay Coastal Prediction System and is a three-dimensional, time-dependent implementation of the ECOM-3D model predicting current speed and direction, water level, and salinity with proven accuracy. The reader is referred to Vincent (2001) and Meyers et al. (2007) for complete descriptions of model specifics and verification study results. The model is fully capable of predicting water temperature throughout the bay. However, exploitation of the thermodynamic capabilities of the model requires specification of a previously undefined net surface heat flux boundary condition. Quantification of heat exchange rates at the bay surface boundary will permit initiation of the active thermodynamic component of the Meyers et al. Tampa Bay model and support future coupling of biological and water quality models to the hydrodynamic model.

Recently, investigations into the non-tidal circulation of the Tampa Bay emphasized the sensitivity of the residual circulation to changeable boundary conditions; alterations to freshwater inflow, wind stress, and wind direction modify the time-averaged circulation (Meyers et al. 2007, Wilson et al. 2006). While modeled and measured parameters (water level, salinity, and current velocity) are typically in good agreement, it is suggested that isolated inconsistencies between modeled and observed variables likely result from error in boundary condition characterization, including heat transfer at the surface boundary, implying a potential intermittent and localized sensitivity to a lack of active thermodynamics as well.

Vincent (2001) also highlighted the need for improved understanding of the surface heat fluxes for specification of model boundary conditions. Inclusion of real-time net surface heat exchange computations in model forcing will enable calculation of water

temperature everywhere in the bay. The primary objective of the present research is therefore quantification of the net surface heat transfer over Tampa Bay and assessment of the contribution of individual components of this net surface flux to the total heat exchanged at the air-sea boundary.

Several recent studies conducted on the West Florida Shelf (WFS) identified trends in sea temperature response to atmospheric forcing and ocean dynamics in the eastern Gulf of Mexico (He and Weisberg, 2002, 2003, Virmani and Wesiberg 2003). The spring transitional period, characterized by ocean warming and strengthening stratification, and the episodic cooling and destratification associated with the fall transition are both dominated by ocean-atmospheric heat exchange; advective heat flux on the WFS overall plays a secondary, and oftentimes opposing, role to cooling or heating driven by the net surface flux. Conversely, ocean circulation dominates the WFS heat budget during the summer months. Superimposed on these seasonal variations are interannual variations and the impacts of shorter time-scale weather events (see Virmani and Weisberg 2003).

Closer to the West Florida coastline (at a station located in 15 m of water), He and Weisberg (2003) demonstrated a shift in the relative importance of advective and surface heat flux even more dramatically in favor of atmospheric control for the spring and fall seasons. Virmani and Weisberg (2003) note that the shallower, near-shore regions of the Gulf of Mexico are more responsive to surface heat flux. This variable response to atmospheric forcing of Gulf waters shoreward implies that the impacts on ocean heat content of surface fluxes measured and derived over the Gulf at comparable latitude are likely an incomplete characterization of the rapid response of water temperature to heat fluxes over Tampa Bay, a shallow and vertically well-mixed estuary with a mean depth of only about 4 m. To date a systematic investigation into the processes of heat exchange at the bay-atmosphere boundary has not been completed. A second objective to analyze the response of Tampa Bay to short time-scale events, such as the passing of extratropical fronts during fall transition, episodes of spring transitional warming, and the approach of tropical storms and hurricanes, follows. Finally, advective heat transfer at the mouth of the bay is estimated and the shifting relative importance of heat flux due to mixing of Gulf and Bay waters to the total change in heat content is examined.

Methods

In May of 2002, a research tower located near Port Manatee Turn in Middle Tampa Bay (latitude 27N 39’ 50”, longitude 82W 34’ 50; see Figure 1-1 for location of the tower within the Bay), in water approximately 5 m deep, was equipped with an array of sensors as one component of the Bay Regional Atmospheric Chemistry Experiment (BRACE). The tower has been continuously maintained to the present, gathering meteorological and oceanographic data at six-minute intervals. Data acquired from this tower include air temperature, relative humidity, and horizontal wind velocity measured at standard anemometric height (10 meters), insolation, precipitation, and barometric pressure. Additionally, a SeaGauge sensor mounted 2.5 meters below mean sea level records bulk water temperature and salinity. Port Manatee Turn BRACE Tower data are publicly available on the Ocean Modeling and Prediction Laboratory (OMPL) ftp site (ftp://comps.marine.usf.edu/pub/BRACE/) along with certificates of instrument

calibration and records of sensor deployment, maintenance and recovery. The BRACE tower sensor array provides measurements required for complete description of surface heat fluxes in Tampa Bay.

This study encompasses the three-year period spanning June of 2002 through May of 2005. An extended interruption occurs in the bulk water temperature data record during the three-year study period from December of 2002 through June of 2003. This information is required for estimation of several heat flux components, resulting in a gap in the heat budget analysis. During the 2004 hurricane season, the near approach of Hurricane Jeanne damaged the research tower atmospheric pressure sensor, necessitating the substitution of barometric pressure over Tampa Bay as provided by NOAA CO-OPS (St. Petersburg Station 8726520; http://co-ops.nos.noaa.gov) for the period of September through October of 2004.

The Environmental Protection Commission of Hillsborough County (EPCHC) manages a program monitoring a variety of water quality parameters, including water temperature and salinity measurements made at the surface, mid-depth, and bottom, at 56 stations throughout the Tampa Bay estuary (http://www.epchc.org/). An analysis of monthly water temperature measurements made over the year 2004 confirms that there is little horizontal thermal gradient; sea temperatures obtained at the BRACE tower are typical, on average, of temperatures throughout the bay except for brief periods during short time-scale events such as the sweeping of fronts through the bay area. Rates of ocean-atmosphere heat exchange computed at the tower are, therefore, considered representative of heat fluxes over the entire bay. In addition, water temperatures recorded monthly for the three year period spanning 2002 to 2004 at two EPCHC sampling stations located near to, and straddling, the BRACE research tower and in comparable water depth (station 21 in water 5.1 m deep and station 90 in approximately 4.5 m of water) reveal little stratification (typically, order less than 0.5 º top to bottom) confirming that Tampa Bay is characteristically well mixed in the vertical. Therefore, observed temperature supplied by the SeaGauge sensor, mounted at the BRACE tower, approximates the depth averaged bulk water temperature.

Net heat exchange at the surface boundary, Q_{net}, is the summation of the turbulent and radiative heat fluxes. The fraction of surface heat exchange occurring in response to the passage of turbulent eddies is comprised of the sensible and latent heat fluxes. Sensible heat flux is the conductive transfer of heat energy down a temperature gradient between the ocean and the overlying air mass or contacting droplets of rain. Latent heat exchange is the energy flux that occurs as a result of phase shift of water at the ocean-atmosphere interface. The net radiative heat flux is the sum of atmospheric and solar radiation arriving at the air-sea interface less portions of the incoming energy reflected or emitted at the bay surface. The total energy gained or lost at the water surface and at the mouth of the bay due to mixing of Gulf and estuarine waters must equal the change in temperature, the total heat stored within the bay. This balance between the combined rate of heat transfer at the sea surface and the mouth of the estuary and the rate of change of heat storage in the bay constitutes the “heat budget” of Tampa Bay.

Radiative Fluxes

Radiative heat energy arriving at the ocean surface is apportioned, according to wavelength, into longwave (emitted predominately in the range of 3-100 μm) and shortwave (spanning 0.15-4.0 μm) radiation.

Shortwave Radiation –

The downwelling shortwave heat flux (insolation) component of the heat budget, $Q_{SW\downarrow}$, is measured directly at the BRACE observational tower by a LI-COR LI200SZ Silicon Pyranometer mounted at 5.8 m above mean sea level. Though a slight linearly decreasing trend appears in the insolation data record, it was determined that this trend is small relative to the overall variability and is therefore negligible.

A fraction of the direct solar radiation is reflected from the ocean surface in proportion to the intensity of incident insolation and the albedo, or reflectivity, of the sea surface. Freely available Sea-Mat Air-Sea Toolbox functions for Matlab (http://woodshole.er.usgs.gov/operations/sea-mat/) provide the calculations of atmospheric transmittance and solar altitude necessary to compute surface albedo, a, after Payne (1972). Surface reflected shortwave radiative heat flux, $Q_{SW\uparrow}$, follows as:

$$Q_{SW\uparrow} = -\alpha Q_{SW\downarrow}. \qquad (19)$$

Water most effectively absorbs solar radiation in the wavelengths longer than the visible light spectrum. How deeply the energy of shorter wavelengths penetrates into the water column depends upon the amount of shortwave irradiance passing through the ocean surface and characteristics of the water body such as turbidity, color, and quantity of particulate matter present. In water sufficiently shallow and clear, a percentage of surface penetrating insolation may pass through the column, reflect from the bottom and reemerge at the surface, effectively reducing the quantity of direct solar energy that is available to warm the ocean.

Secchi disc readings recorded monthly at EPCHC sampling stations 21 and 90 as part of the EPCHC Tampa Bay water quality monitoring program were used to approximate light penetration at the BRACE tower. Jerlov (1968) proposed a scheme of classifying water masses according to their transparency to radiative flux, allowing prediction of light levels at various depths for each of ten water type categories, including five classes of coastal water types. For the years 2002 through 2004, Secchi depth readings were compared with Jerlov's values for percent irradiance remaining at depth for each coastal type and the estuarine waters were categorized according to Jerlov's scheme, assuming that observed Secchi depth is approximately equivalent to the level of 10% radiant energy remaining (Paulson and Simpson 1977). Tampa Bay varies between Jerlov's coastal water type 3 during exceptionally clear periods to coastal type 9 (or even more turbid than a water mass described by this class) at its murkiest. Both the majority and the average of Secchi depth readings at stations 21 and 90 for this three-year period identify Tampa Bay as a coastal type 7. For the purpose of this study, the mean case of water type 7 is applied to all calculations of bottom-reflected radiation, Q_{pen}. Approximately 0.25% of surface penetrating radiation remains after the attenuation of radiant energy over a depth twice that of the water column at the BRACE tower to be

reemitted at the surface. The error associated with approximating bottom-reflected radiation by the above method is therefore expected to be small, and to average out in the long term, with greatest error occurring during brief periods of clear skies and maximum sun.

Longwave Radiation –

Thermal energy is radiated from the sea surface in proportion to the temperature of the water. This upwelling longwave radiative heat flux component, $Q_{LW\uparrow}$, is typically approximated by the Stefan-Boltzmann law:

$$Q_{LW\uparrow} = \varepsilon\sigma T^4 \qquad (20)$$

where ε represents the emissivity of the ocean surface, σ is the Stefan-Boltzmann constant, and T is the temperature of the sea surface in Kelvin. Kantha (2000) notes that 0.97 is the value typically assigned to the emissivity of a body of water and this is the value chosen for this study. The atmosphere absorbs a portion of this upwelling longwave radiation, in addition to a large fraction of the incoming solar radiation, and reradiates some of this trapped heat energy as downwelling longwave radiation, $Q_{LW\downarrow}$, warming surface waters. This component is not directly measured at the BRACE observational tower and must be estimated by bulk parameterization.

The Coastal Ocean Monitoring and Prediction System (COMPS) is a network of offshore and nearshore instrumentation maintained along the West Florida Shelf that provides real-time meteorological and oceanographic observations. As part of the COMPS assemblage of offshore buoys, the C10 buoy is moored approximately 27 nm southwest of the mouth of Tampa Bay and the C14 buoy, roughly 57 nm northwest of the estuary entrance (please see the COMPS website for the location of the buoys relative to Tampa Bay; http://comps.marine.usf.edu/). An assessment of the skill of eleven bulk net longwave transfer equations (reviewed in Fung et al. 1984, Josey et al. 2003) in reproducing incoming longwave radiation observations made from June through December of 2003 at the C10 and C14 buoys resulted in the conclusion that the Berliand and Berliand (1952) formulation, recommended by Fung et al (1984), accurately represents downwelling longwave heat flux at both buoys, and is appropriate for application over the Tampa Bay region.

According to Berliand and Berliand (1952), the net longwave radiation, $Q_{LW\uparrow\downarrow}$, may be written as:

$$Q_{LW\uparrow\downarrow} = \varepsilon\sigma\, T_a^4\, [0.39 - 0.05(e_a)^{1/2}]\, F(C) + 4\varepsilon\sigma\, T_a^3\, (T_s - T_a) \qquad (21)$$

where ε is the emissivity of the ocean surface, σ is the Stefan-Boltzmann constant, T_a is measured air temperature in degrees Kelvin, T_s is the sea surface temperature in Kelvin, e_a is the near surface vapor pressure, and $F(C)$ is a cloud correction factor which is a function of cloud cover. Observations of cloud cover over the bay were unavailable and therefore estimated, following Reed (1977), using the Sea-Mat Air-Sea Toolbox functions. The Clark et al. (1974) cloud correction factor is preferred for application to latitudes less than 50˚ N/S and is the form utilized in this study.

Turbulent Fluxes

The turbulent vertical fluxes of heat (Q_S) and moisture (Q_L) at the surface are defined as

$$Q_S = \rho c_p \overline{w'T'} \qquad (22)$$

$$Q_L = \rho L_e \overline{w'q'} \qquad (23)$$

where ρ is the density of air, c_p is the heat capacity of air, L_e is the latent heat of vaporization and w is the vertical wind velocity. The quantities $\overline{w'T'}$ and $\overline{w'q'}$ are the averaged products of vertical wind velocity and measured temperature or specific humidity fluctuations away from longer term mean values. These instantaneous variations of a measured quantity from the mean, w', T', and q', occur in response to the presence of turbulent eddies in the surface layer. Where $\overline{w'T'}$ and $\overline{w'q'}$ are not directly measured, these quantities, and therefore the sensible (Q_S) and latent (Q_L) heat exchange rates, can be approximated by bulk transfer formulas:

$$Q_S=\rho c_p U C_H(T_s-T_a) \qquad (24)$$

$$Q_L=\rho L_e U C_E(q_s-q_a) \qquad (25)$$

where C_H and C_E are the dimensionless heat and moisture transfer coefficients, respectively, U is the horizontal wind speed, and the subscript $_s$ denotes surface observations while subscript $_a$ indicates measurements made at some pre-defined height.

The Tropical Ocean Global Atmosphere Coupled Ocean-Atmosphere Response Experiment (TOGA COARE) bulk transfer algorithm was initially developed in support of the COARE project objectives of better understanding of tropical air/sea interactions, improved heat flux parameterizations and the development of a balanced surface heat budget for the western tropical Pacific region. It is the tool most widely employed in turbulent heat flux studies and several iterations of the algorithm have been released for public use over the course of model development. Though originally developed for application to the open ocean of the western central Pacific zone, the most recent incarnation of the algorithm (version 3.0; ftp://ftp.etl.noaa.gov/user/cfairall/wcrp_wgsf/computer_programs/) has been validated with data from wind regimes ranging from calm to greater than 20 m/s, in open ocean and coastal regions, across latitudes spanning from equatorial to greater than 50º N, and under atmospheric conditions ranging from unstable to extremely stable (Fairall et al., 1996, 2003; Edson et al. 2006). It is this latest version of the COARE turbulent heat flux algorithm that was chosen for derivation of latent and sensible heat exchange rates over Tampa Bay.

An initial six-month study of flux parameters in the Tampa Bay Estuary demonstrated the skill of the COARE 3.0 bulk algorithm in reproducing sensible heat flux and friction velocity (a velocity scale; this parameter quantifies shear stress near surface) observations made half hourly by a CSAT3 sonic anemometer mounted at the BRACE tower (Sopkin et al. 2007). Fast response measurements of humidity, and therefore the latent heat flux, are not available from the sonic anemometer. The COARE 3.0 algorithm produces bulk estimates of latent and sensible heat exchange rates as well as heat flux due to precipitation. Surface current velocity is not monitored at the Port Manatee Turn observational tower and therefore only the 10 m winds, rather than the true

wind speeds relative to the sea surface, are supplied to the algorithm. Due to the limited fetch over Tampa Bay, this omission is not expected to incur significant error.

Closing the Heat Budget

The total surface heat budget is given by the sum of the flux terms described above:

$$Q_{net} = Q_S + Q_{pen} + Q_L + Q_{SW\uparrow\downarrow} + Q_{LW\uparrow\downarrow}. \qquad (26)$$

In the case of zero advective heat transport into or out of the bay, the net surface heat flux, $Q(t)$, may also be computed, following Morey and O'Brien (2002), as:

$$\frac{dT}{dt} = \frac{Q(t)}{\rho c_p H} \qquad (27)$$

where $\frac{dT}{dt}$ is the change in the depth averaged, bulk water temperature with time and H is the water column height. In the presence of advective flow, the remainder between the total surface heat flux, Q_{net}, and the rate of change in estuarine heat storage, $Q(t)$, is the result of advective heat exchange between the Gulf of Mexico and Tampa Bay plus error due to uncertainty in the measurement or estimation of the surface heat flux components.

Results and Discussion

Summer – June through August

Light winds, warm water temperatures, and strong insolation persist over summertime, a season typified by reduced variability in heat exchange at the bay surface (Figures 4-1 through 4-3). The radiative surface heat flux components all reach peak magnitude over the summer months, with incoming shortwave radiation nearing 1000 W/m^2 at midday. Net longwave radiation results in a heat loss, on average, of 30.6 W/m^2 from the bay over summertime. Reduced air/water temperature gradients and low wind speeds result in typically small sensible heat loss. Sensible heat flux due to precipitation represents, on average, much less than 1 W/m^2 cooling of the bay. However, convective thunderstorms in middle July of 2002 caused several peaks in the hourly mean of this component of the surface heat budget of nearly –65.0 W/m^2. Net surface heat exchange over the summer of 2002, a complete three-month time series, produced warming of the bay at a mean rate of 30.5 W/m^2. The residual, representing advective cooling plus error, over this same period was, on average, 21.7 W/m^2.

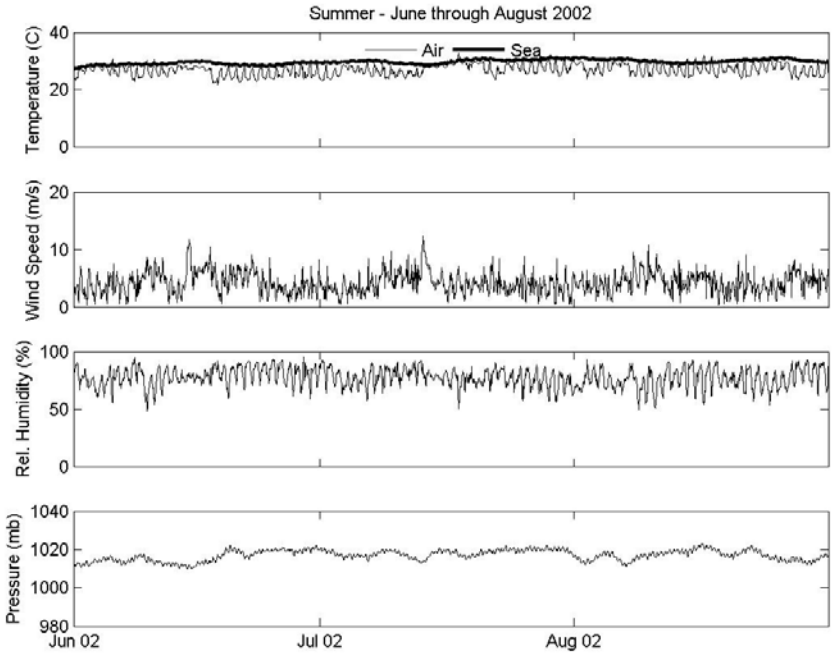

Figure 4-1a: Summer 2002 meteorological data.

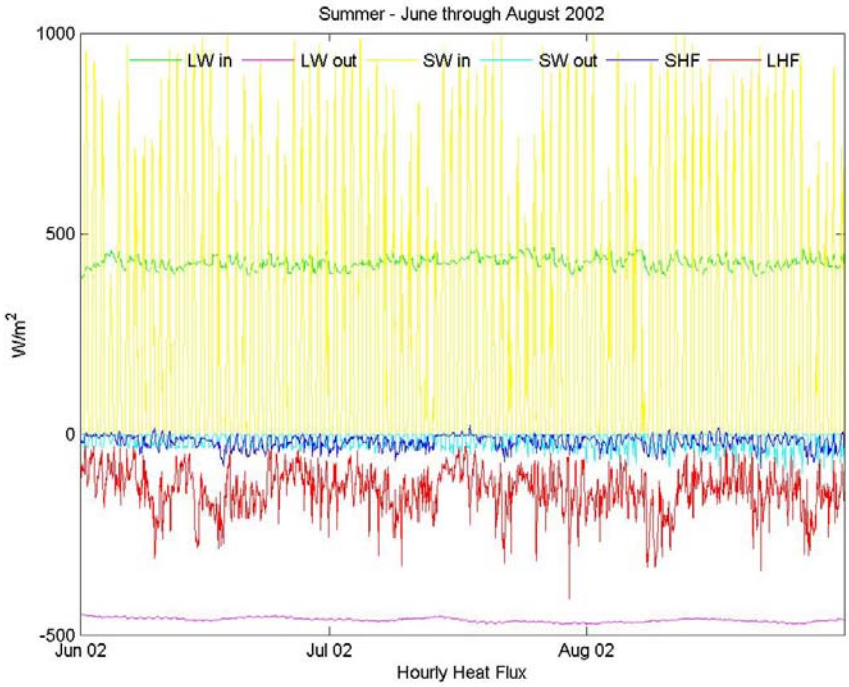

Figure 4-1b: Summer 2002 surface fluxes.

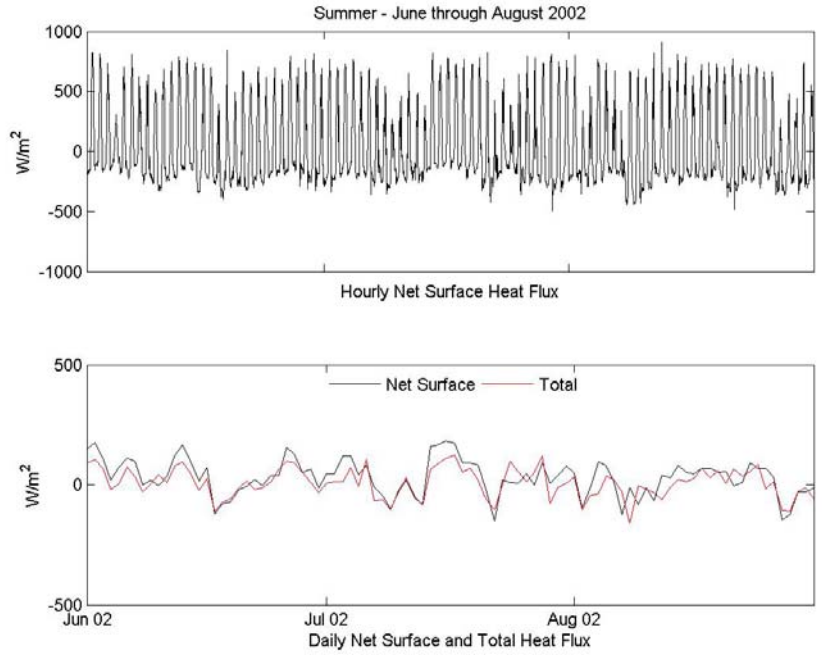

Figure 4-1c: Summer 2002 net surface and advective flux.

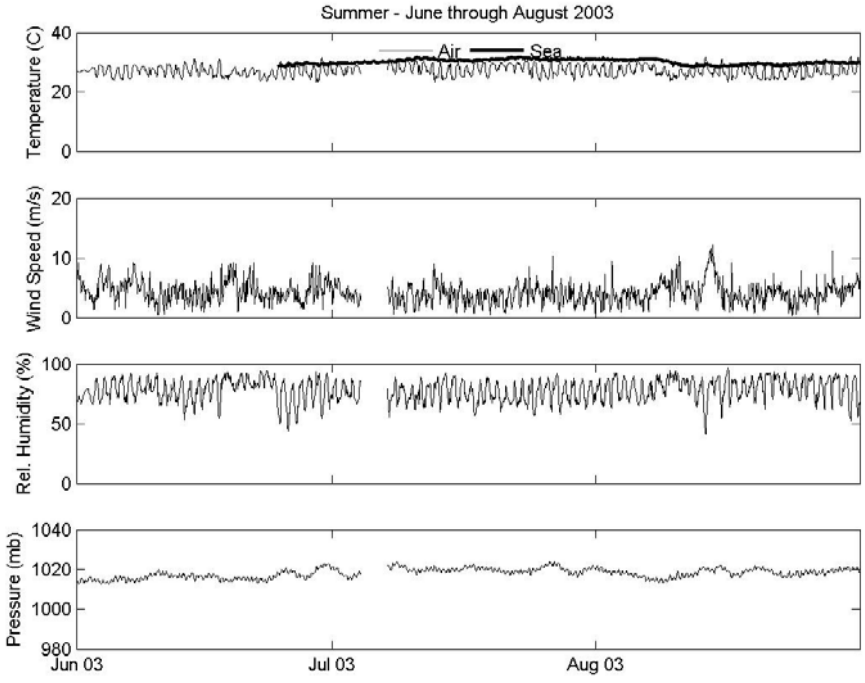

Figure 4-2a: Summer 2003 meteorological data.

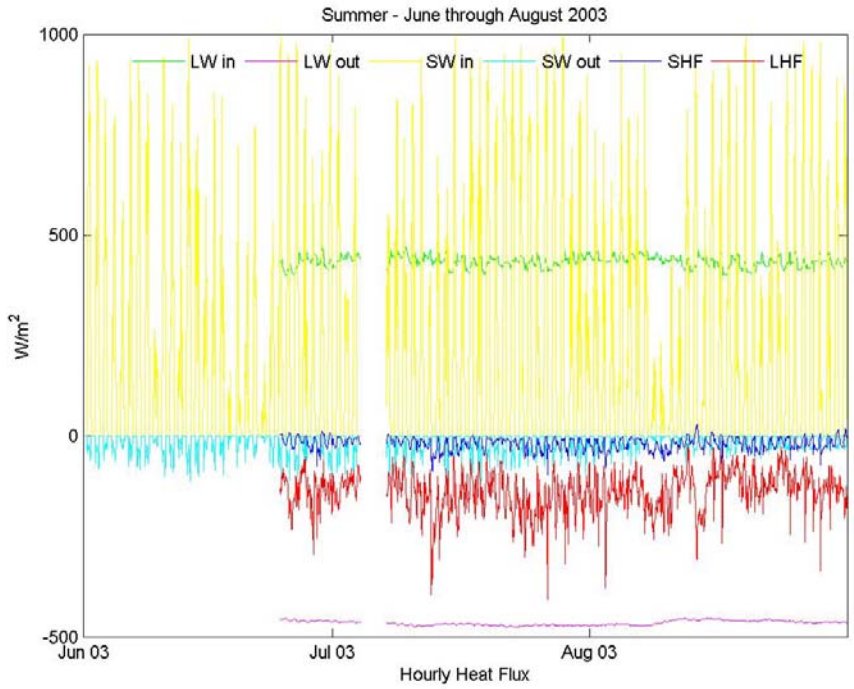

Figure 4-2b: Summer 2003 surface fluxes.

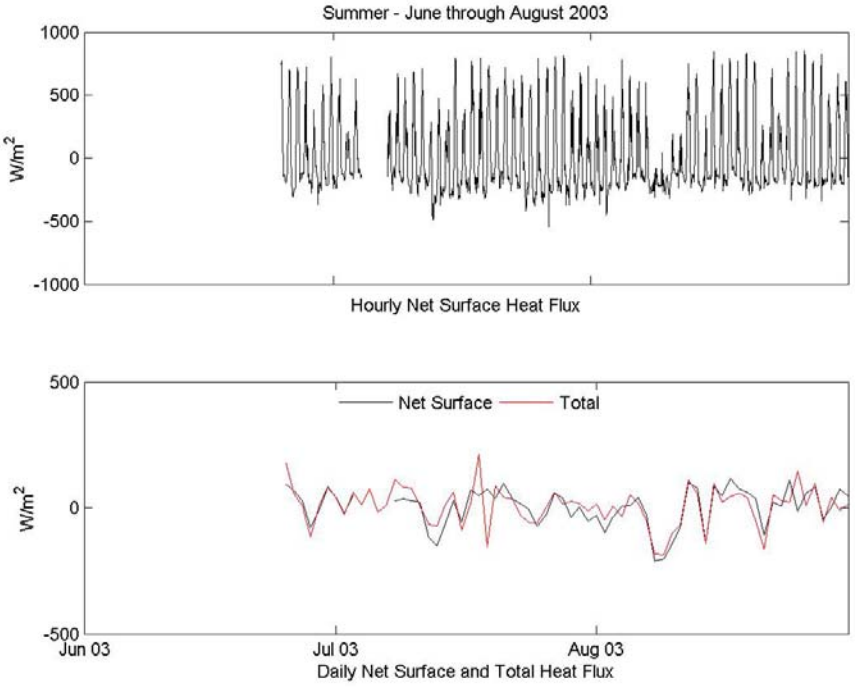

Figure 4-2c: Summer 2003 net surface and advective flux.

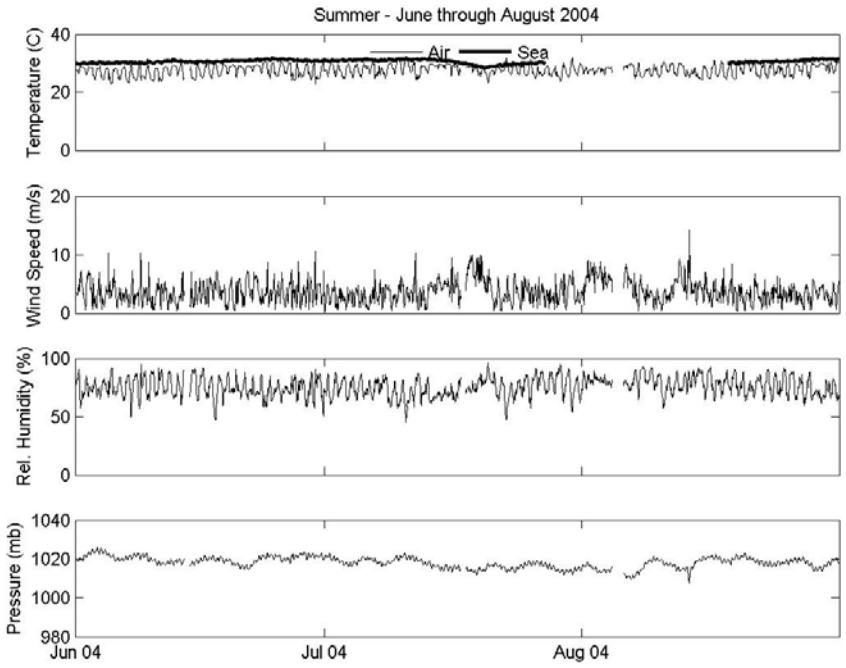

Figure 4-3a: Summer 2004 meteorological data.

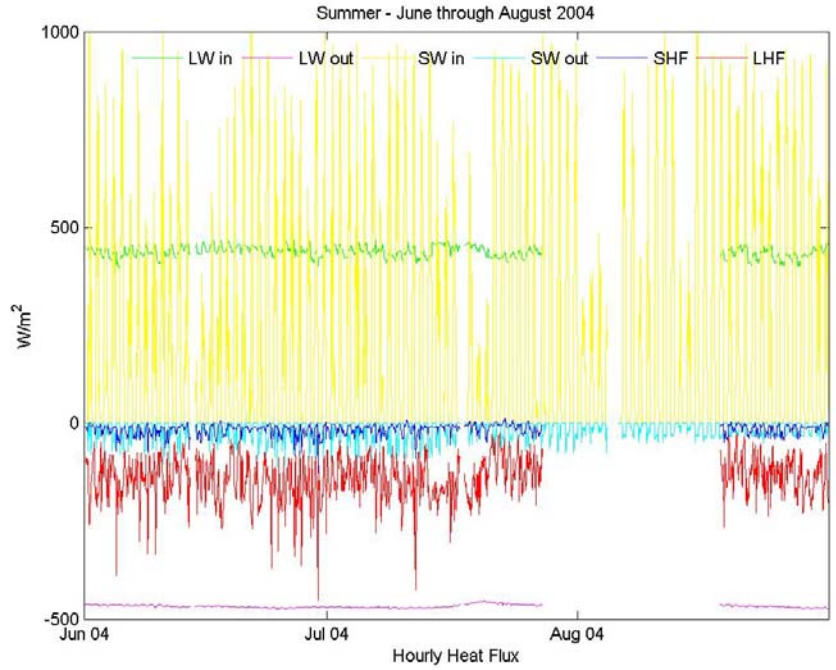

Figure 4-3b: Summer 2004 surface fluxes.

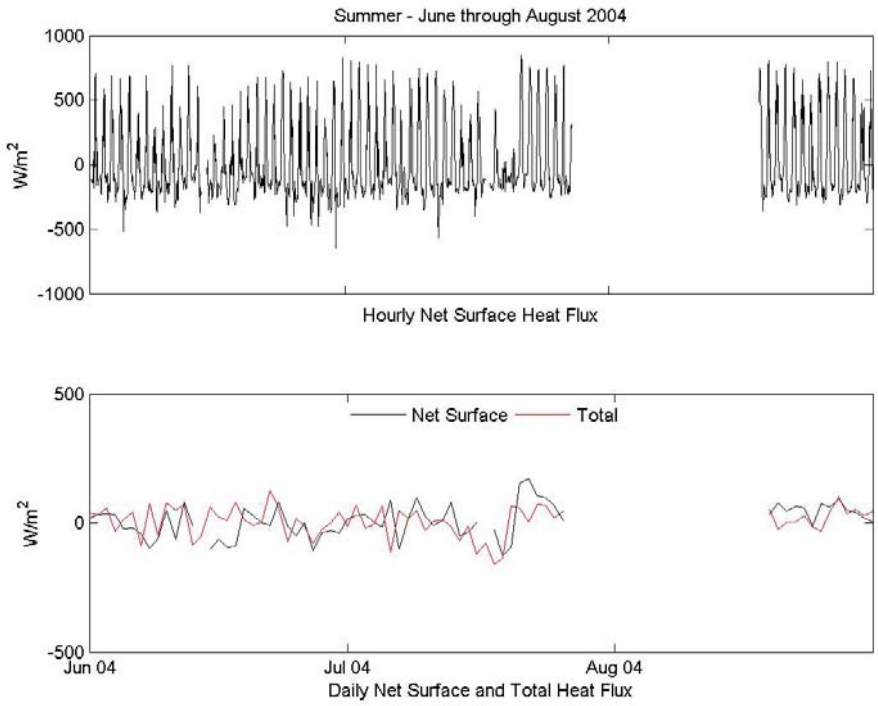

Figure 4-3c: Summer 2004 net surface and advective flux.

Fall – September through November

Weakening solar warming and sporadic high winds associated with transient tropical and extratropical systems mark the fall season (Figures 4-5, 4-6 and 4-7, a and b). Autumnal cooling of bay waters begins in September of each year, oftentimes associated with the near-approach of tropical weather systems. September is the peak of the Atlantic hurricane season. Over the three-year study period, the average seasonal decline in bay water temperature, from the beginning of September through November of each year, reached –10.8 ºC. Net surface heat flux out of the bay is, on average, remarkably similar from year to year with a mean seasonal rate of heat loss of –20.4 W/m^2. Though less significant than surface heat exchange, advective heat exchange (as the residual heat flux) contributed to fall cooling each year at a mean rate of –6.4 W/m^2 (Figures 4-5, 4-6 and 4-7, c). A straightforward look at the impact of a net surface heat loss of 20.4W/m^2 on bay temperature, assuming constant density and given a simplistic representation of the bay as a volume 4 m deep with a surface area of 1030 km^2, reveals that a steady heat flux of 20.4W/m^2 out of the bay yields a temperature change of –9.3 °C over a three month period. This is a simple check of the net surface heat budget computations presented in this study. Though advective heat exchange is not accounted for, this check demonstrates that this relatively low average net flux out of the bay is capable of producing temperature change on the order of the actual measured temperature change (-10.8 ºC) when applied over a three month period. Over the fall seasons of 2002 through 2004, averaged seasonal net shortwave and net longwave radiative fluxes were 156.0 W/m^2 and

–38.3 W/m^2, respectively while seasonally averaged sensible and latent heat loss contributed to surface cooling of bay waters at the rates of -15.2 W/m^2 and -122.3 W/m^2.

Early fall is often summer-like in character, with meteorological parameters and individual heat fluxes reduced in variability. However, expansive tropical storm systems bringing overcast skies and extreme winds to the bay area may initiate rapid cooling early in the season. Extratropical fronts pass over the bay area with increasing frequency in the latter half of the season, dramatically altering net surface heat exchange and causing a series of irregular drops in ocean temperature toward the wintertime low. On seasonal time scales, averaged individual flux components are very comparable year-to-year, while shorter time scale events drive radical fluctuations in the magnitude and direction of heat exchange of individual heat budget components. Additionally, individual events trigger large variations in the total surface heat exchange, cautioning against applying a climatological mean net surface flux in model studies. The impacts of tropical and extratropical weather systems on estuarine heat content are examined in two case studies presented below.

Hurricane Frances –

Frances came ashore near Vero Beach on Florida's East Coast as a category 2 hurricane in the early hours of September 5, 2004, the outer bands of the storm already reaching over Tampa Bay to the northwest (Figure 4-4). Near passage of the storm to the bay forced two peaks in measured wind speed (Figure 4-7a). The first exceeded 20 m/s to the S and SE around 15:00 UTC on the 5th of September. Nearest proximity of the eye of the storm to the BRACE tower appears as a strong signal in barometric pressure as observed at the NOAA CO-OPS St. Petersburg station. A minimum barometric pressure of 981.7 mb is recorded at 20:54 UTC on the 5th, concurrent with a temporary reduction in wind speed. As the eye of the storm exited the bay area, wind direction reversed abruptly, shifting to the NE, up the bay along its axis, and wind speeds observed at the BRACE tower again approached 20 m/s. This examination of the impacts of a tropical storm system on heat exchange rates in Tampa Bay spans the four-day time frame early in the fall of 2004, from the 4th through 7th of September, appearing outlined in black in Figure 7a-c.

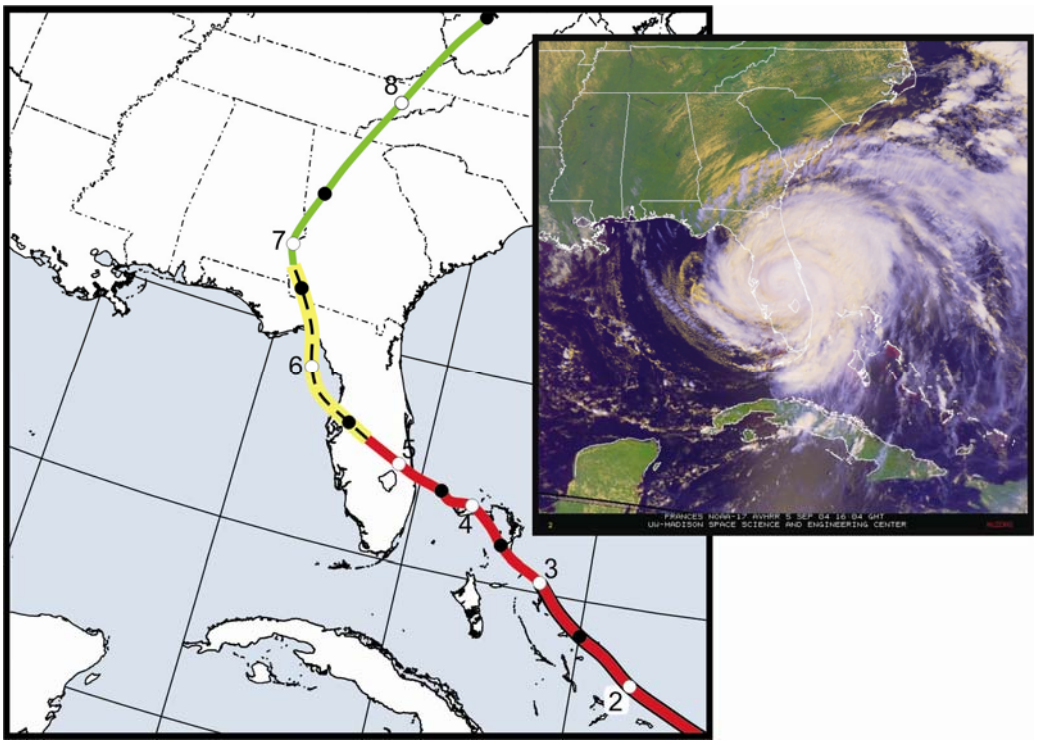

Figure 4-4: Storm track and AVHRR image of Hurricane Frances. The satellite image was captured on September 5, 2004 (NOAA). Storm track image and composite courtesy of Joan David of the National Hurricane Center, Miami.

The influence of Frances on individual components of the heat budget is apparent. High winds and cooler air temperatures drive a maximum in latent heat transfer out of the bay of -634.5 W/m^2 and peak sensible heat cooling of -154.7 W/m^2. Incoming solar radiation reduced dramatically from a mean rate of 226.0 W/m^2 over September 4th to an average daily mean of only 35.2 W/m^2 and 71.4 W/m^2 over the 5th and 6th of September, respectively (Figure 4-7b). The greatest daily average rate of surface cooling over the estuary, -460.8 W/m^2, occurred in advance of the eye on September 5th. Net surface flux continued to drive heat loss from the bay until the storm passed from the area on the 7th. Bulk water temperature was reduced by 3.3 °C over the four-day period of this case study. Virmani and Weisberg (2003) observed that the typically negative net heat flux of the fall season prevents water column temperature rise post-tropical storm. Hurricane Frances represented the first strong cooling event of this fall season and bay water temperature never recovered. A distinct signature for the passage of Hurricane Jeanne is visible as another sharp decline in the time series of barometric pressure corresponding to the 26th of September, 2004 (Figure 4-7a). The maximum-recorded wind speed at the BRACE tower for this storm reached 23.4 m/s. Jeanne induced another step-like decrease in bay water temperature from which the bay did not completely return.

While on average both surface and advective (residual) heat exchange contributed to heat loss from the bay in response to Frances (-126.4 and -66.4 W/m^2, respectively; see Figure 4-7c), it is interesting to note that as net surface heat loss reached a maximum, the

impact of surface cooling on water column temperature was lessened by a positive advective heat flux (daily mean = 116.5 W/m^2). On the other side of the storm eye advection shifted roles abruptly once more, again enhancing surface cooling (an estimated -179.9 W/m^2), with an average residual flux of -94.6 W/m^2 for September 6th. Interpretation of these findings is aided by examination of the net surface and advective heat fluxes within the context of the Wilson et al. (2006) investigation into the effects of Hurricane Frances on bay residual circulation.

The majority of freshwater input to the bay is received in the northernmost portions of the estuary resulting in a horizontal salinity gradient, from the head to the saline waters of the Gulf of Mexico at the southern mouth of the bay, that drives the overturning circulation of the bay. Typically, fresher, buoyant waters from terrestrial runoff sources flow out of the bay along the surface of the estuary while salty, dense Gulf waters flow in along the deepest portions of the bay. In the hours preceding the passage of the eye of the hurricane, peak winds to the S and SE force a set down in water level within the bay. Wilson et al. (2006) report that, as wind speed spikes, and in response to increased freshwater runoff into the bay, the Meyers et al. Tampa Bay model predicts significant outflow at the bay surface and at mid-depth. An Acoustic Doppler Current Profiler deployed near the mouth of the bay in the shipping channel at depth, measures a concurrent strong inflow in the deepest portions of the channel, in an apparent exaggeration of the general overturning circulation. While surface waters, rapidly cooled by a combination of reduced insolation and air temperatures and sharply increased wind speeds, are pushed out of the bay, enhanced return flow of warmer Gulf waters at depth and increased turbulent mixing partially mitigate surficial cooling.

As the eye transits the bay area and winds swing toward the NE, strong inflow is measured surface to bottom and setup of water level in the bay reaches a maximum of 1.2 m above mean sea level. Winds driving up the bay prevent, in large part, the outflow of cooled surface waters. Additionally, Gulf water forced into the bay at all depths likely represents a mixture of coastal waters also impacted by the storm and the return of cooler water recently driven from the bay. Advective heat flux again contributes to estuarine cooling during this phase.

Extratropical Front –

The BRACE tower recorded a dramatic shift in wind velocity at end of day on November 28th, 2003; in less than twenty minutes time, winds coming out of the southwest shifted to blow northwesterly and instantaneous wind speed increased by almost 6 m/s. Over most of the following two days, strong winds persisted out of the NW to NE over the bay, peaking on the 29th at 14.7m/s, until the front passed from the region. A detailed investigation into the effects of this event on the heat budget of Tampa Bay encompasses the final two days of November of 2003 (demarcated by thin black lines on Figure 4-6).

As cold, dry air associated with this extratropical frontal system moved into the bay area, relative humidity dropped to a minimum of 28%, remaining depressed relative to the seasonal average by a mean of 23% over the two day period. Coincident with a seasonal high barometric pressure (two-day mean: 1028.2 mb), rapidly falling air temperatures generated large gradients in air-sea temperatures with an exceptional

maximum air-sea temperature separation of 11.6 °C. For the 29th and 30th of November, a mass of air with a mean temperature of only 13.5 °C overlay bay waters of 20.6 °C on average. The net surface heat flux response to strong atmospheric forcing over this short time period is extreme: net heat loss at the bay surface reached a maximum hourly mean rate of –799.8 W/m^2 while the overall average total surface heat flux was –383.6 W/m^2. High winds coupled with dry atmospheric conditions resulted in a mean heat loss from the bay of –316.5 W/m^2 due to latent heat flux while the sudden decline in air temperature forced an average sensible heat flux of -101.8 W/m^2. Bay temperature decreased by 2.3 °C in two days. A check of the impact of constant heat loss at a rate of 383.6 W/m^2 over the simplistic box model of the bay described above results in a computed –3.8 °C temperature change over the two day period. Advective (residual) heat transfer contributed to bay warming at a mean rate of 133.6 W/m^2 over the final two days of November 2003, resulting in an actual decrease in bulk water temperature significantly less than the temperature decline predicted by the net surface heat flux alone in this simple verification.

Such considerable heat energy losses are not unusual in response to the passage of frontal systems. Another extratropical front, moving quickly through the bay area earlier in the same month, produced a peak hourly net surface flux of –879.8 W/m^2. In the 2002 fall season, a frontal system impacted the bay from November 16th through 18th, forcing a maximum hourly net surface cooling of –668.3 W/m^2. These numbers, however, are far in excess of those reported over the bay through Hurricane Frances in the fall of 2004. Though sustained high winds and reduced insolation contributed greatly to bay cooling during Frances, the maximum ocean/atmosphere temperature gradient attained was 4.2 °C while the minimum relative humidity reached was 59%. On average, relative humidity under the influence of the tropical system, at 81%, was slightly higher than the mean for the fall 2004 season (76%), somewhat limiting the impacts of the storm. Virmani and Weisberg (2003) found analogous results in a comparison of the effects of tropical and extratropical systems on the WFS heat budget during the fall (September through October) of 2000. In middle September of 2000, Hurricane Gordon forced a maximum daily net surface heat loss of nearly –300 W/m^2, yet the largest decline in water temperature over the shelf during the fall 2000 season coincided with the passage of a front in early October. Virmani and Weisberg (2003) report a maximum daily averaged surface heat flux of almost –1000 W/m^2 for this event.

For November of 2002/3, the monthly mean rates of heat exchange attributable to bay circulation dynamics were slightly in favor of warming (3.5 and 9.0 W/m^2, respectively) while mean surface heat flux dominated, driving bay-wide cooling (-76.1 W/m^2 over November 2002, under the influence of a moderate El Niño event, and –38.7 W/m^2 in November of 2003). The November 2004 data record is incomplete, preventing a similar comparison. The passage of the frontal system in the latter days of November 2003 precipitated a sharp increase in the average rate of advective warming to 133.6 W/m^2 over the 29th and 30th, exceeding average dynamical warming in advance of the eye of Frances. Analogously to the approach phase of the hurricane, prolonged elevated winds out of the North associated with this extratropical front induced a set down in tide level relative to predicted astronomical tides. As measured in middle Tampa Bay at the BRACE tower, observed water level is reduced on average 0.21 m (max. set down of

0.41 m) relative to predicted tidal elevation compared to mean set down at the tower over storm approach on September 5, 2004 of 0.12 m (max. set down of 0.31 m). Current velocity data is unavailable over the frontal system transition, however, it is likely that increased advective warming throughout this event is due to enhanced bay overturning circulation driven by a similar mechanism as during the approach of Frances; sharply cooled surface waters driven from the bay by southward winds are coupled with amplified return flow of warmer Gulf water at depth.

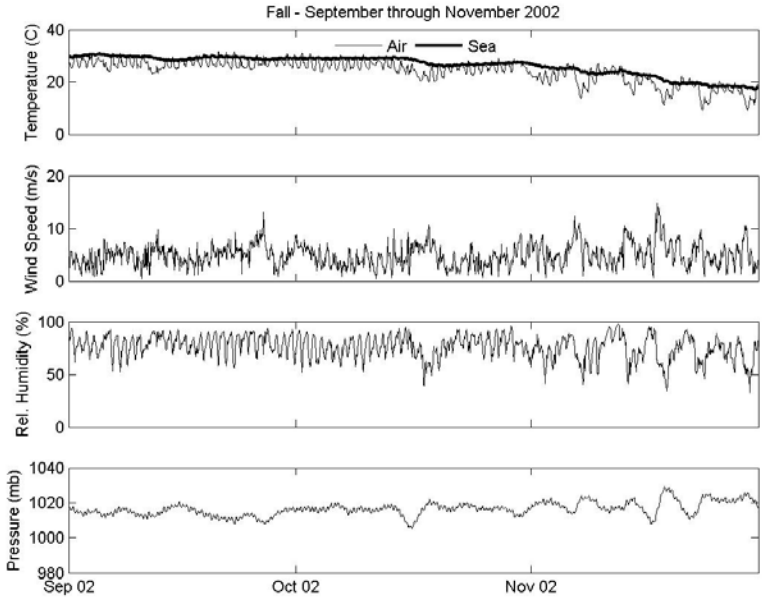

Figure 4-5a: Fall 2002 meteorological data.

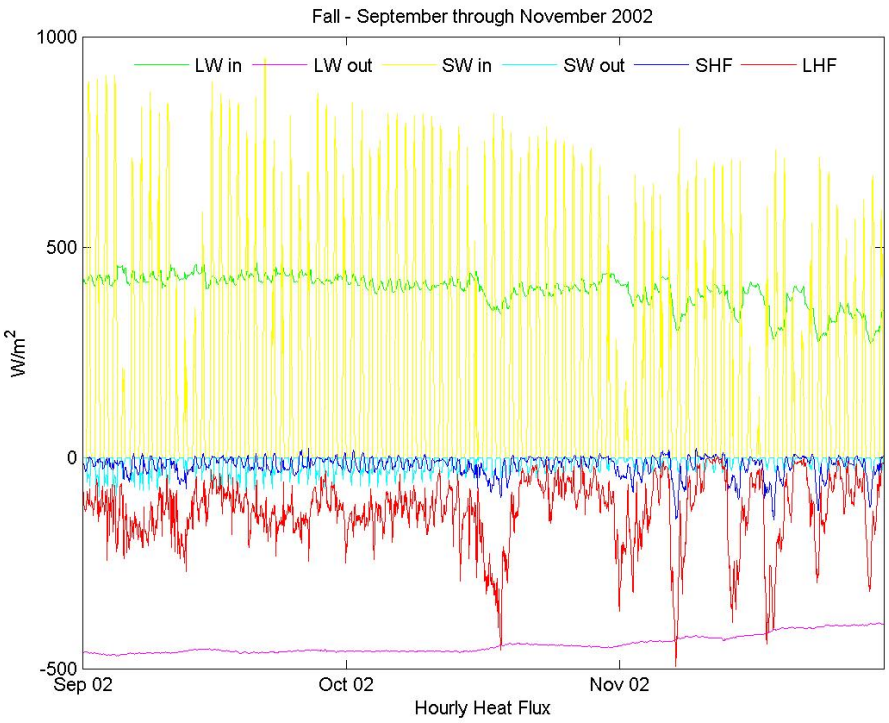

Figure 4-5b: Fall 2002 surface fluxes.

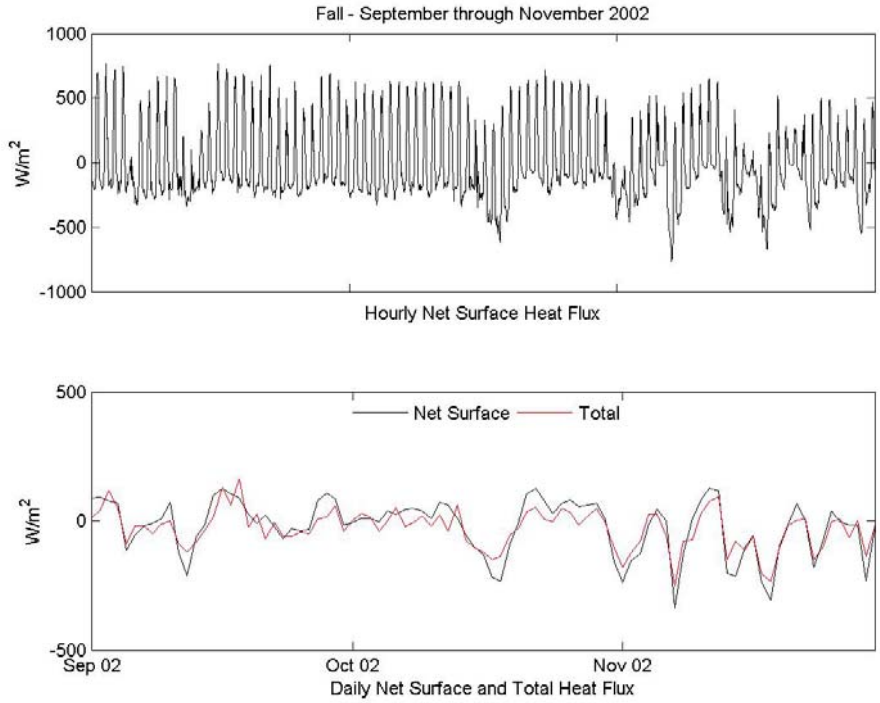

Figure 4-5c: Fall 2002 net surface and advective flux.

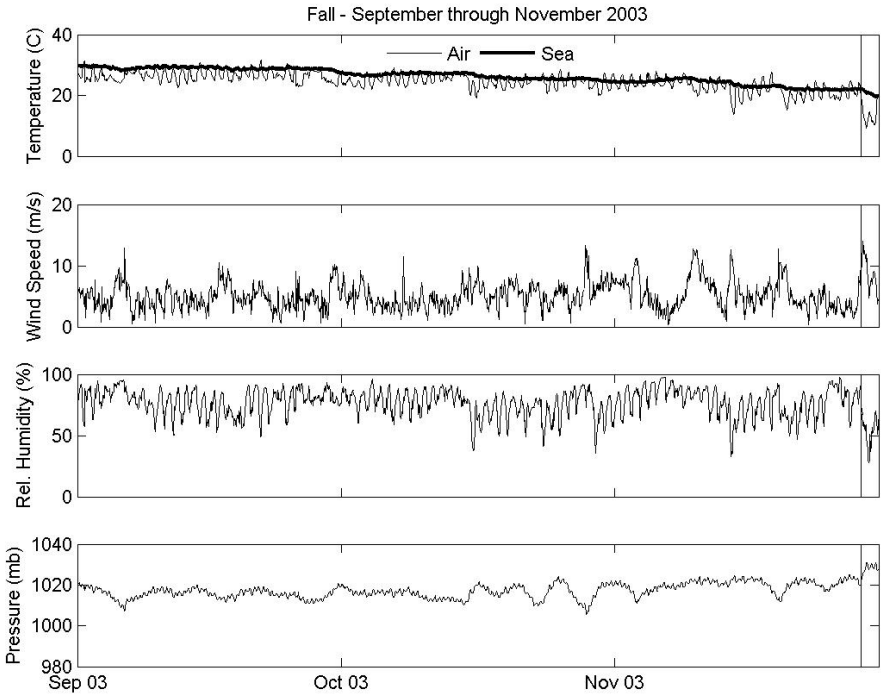

Figure 4-6a: Fall 2003 meteorological data.

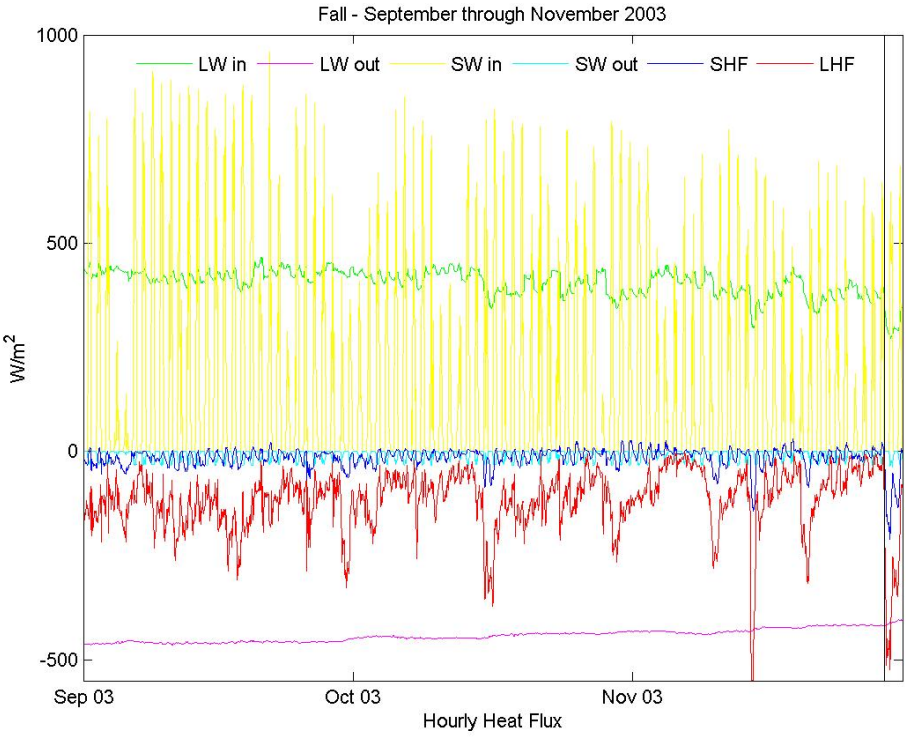

Figure 4-6b: Fall 2003 surface fluxes.

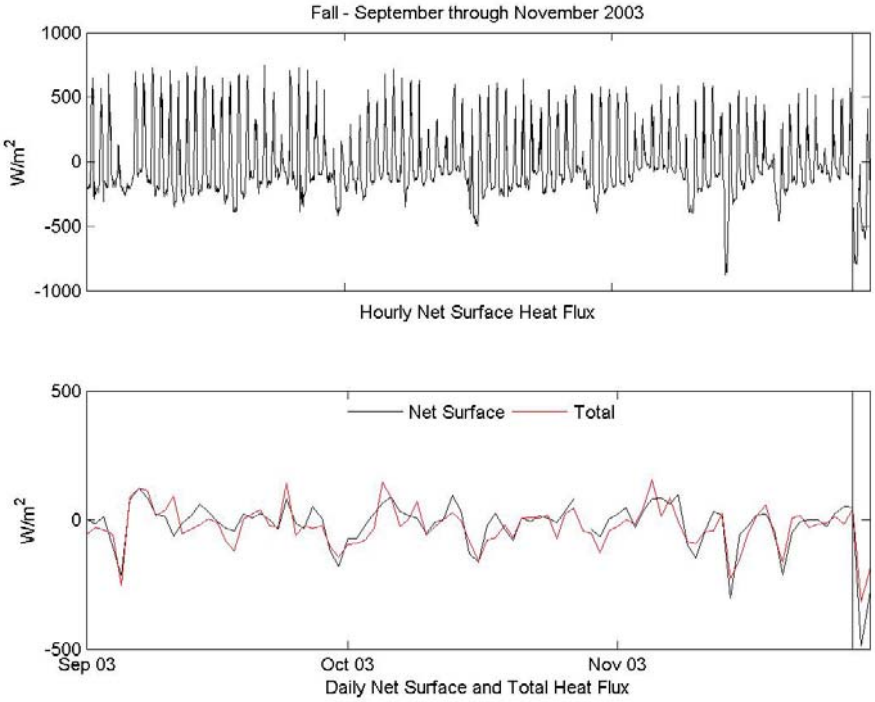

Figure 4-6c: Fall 2003 net surface and advective flux.

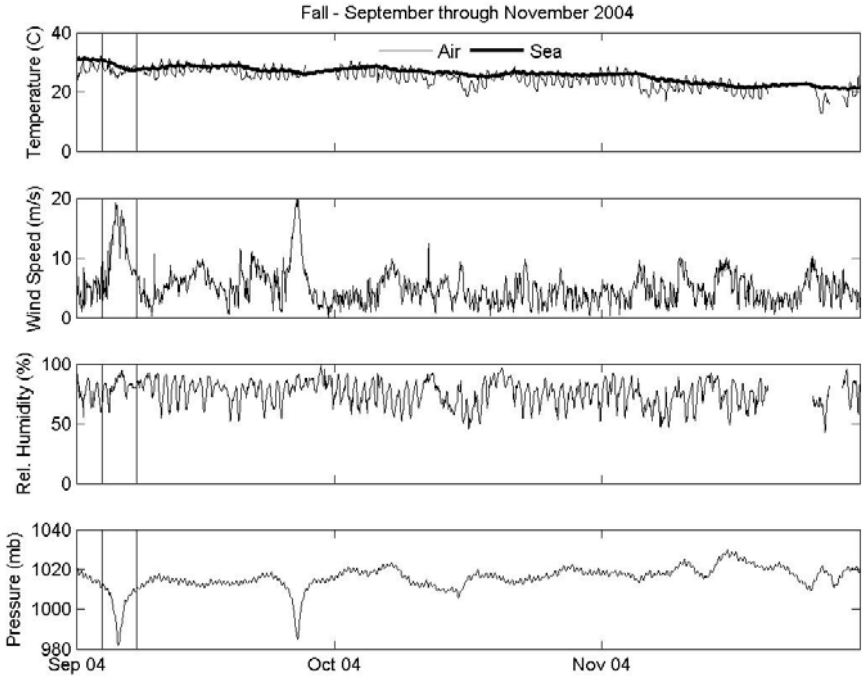

Figure 4-7a: Fall 2004 meteorological data.

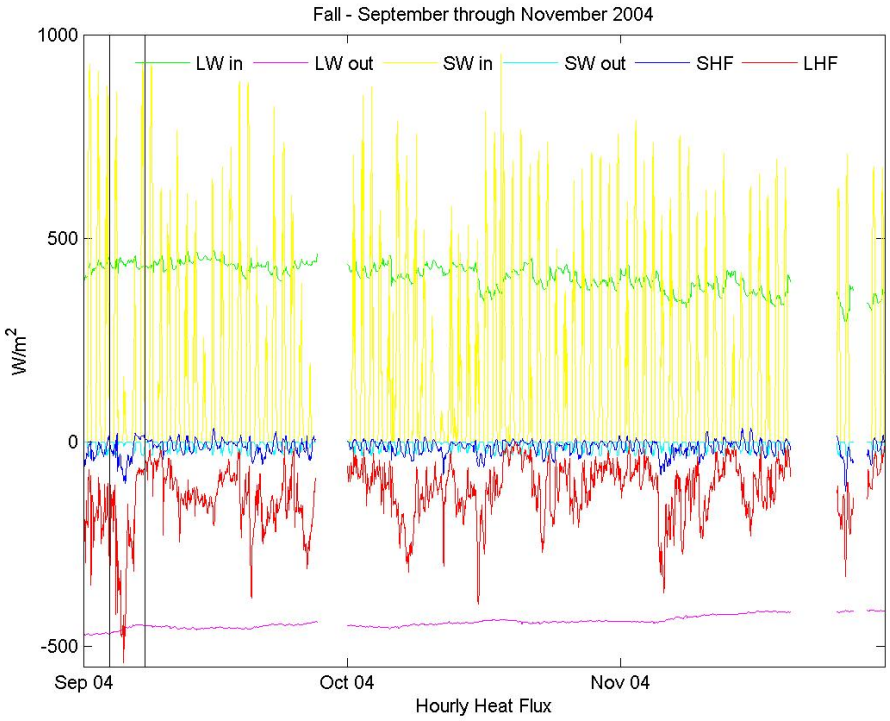

Figure 4-7b: Fall 2004 surface fluxes.

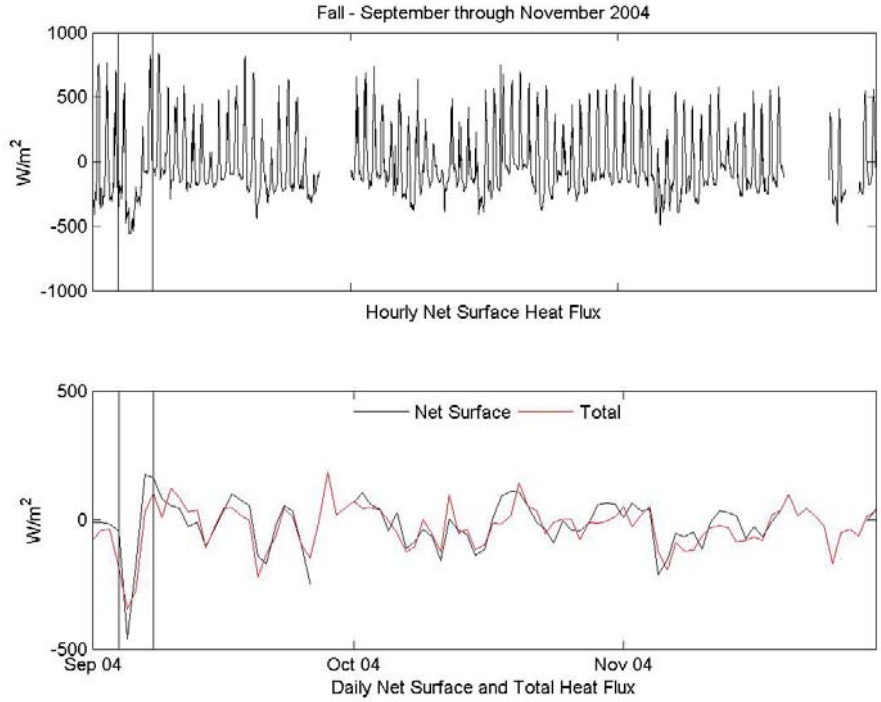

Figure 4-7c: Fall 2004 net surface and advective flux.

Winter – December through February

Surface heat flux variability remains high as water temperatures sink towards the annual minimum. Fronts continue to intermittently impact the region, spiking turbulent heat exchange rates and temporarily reducing sea temperature (Figures 4-8 and 4-9). These events are interspersed with periods of minimal winds when turbulent heat exchange dips to near-zero, and bay temperatures recover. Averaged over the season, insolation and latent heat exchange reach their minimum, counterbalancing each other and resulting in only slight wintertime cooling.

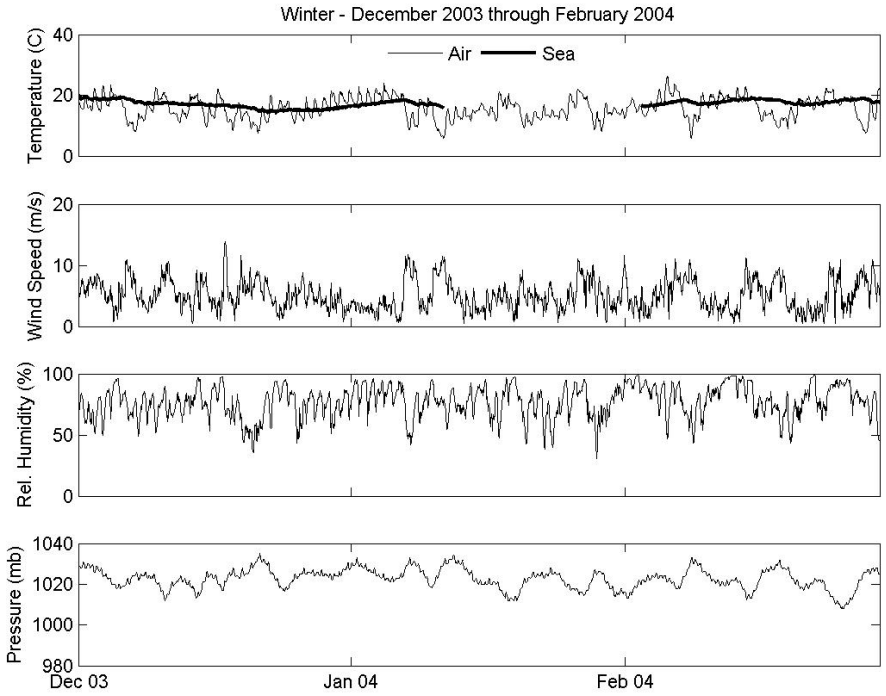

Figure 4-8a: Winter 2003/4 meteorological data.

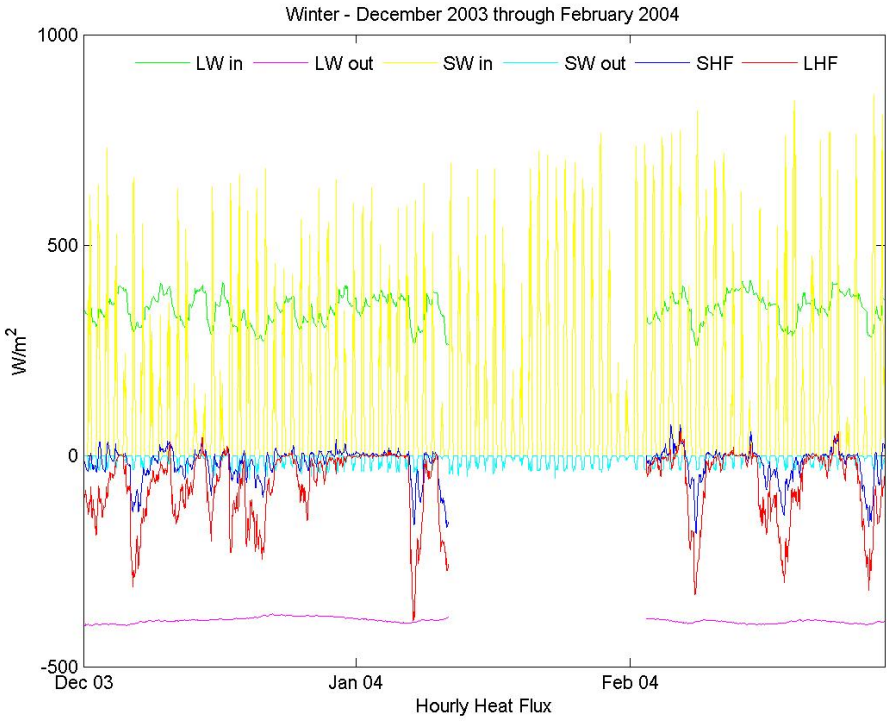

Figure 4-8b: Winter 2003/4 surface fluxes.

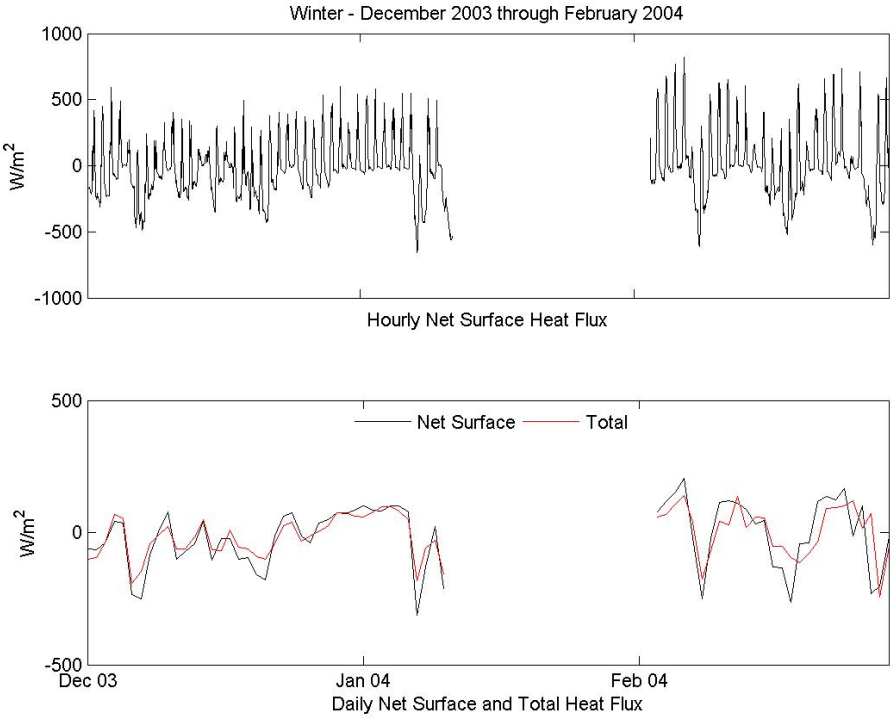

Figure 4-8c: Winter 2003/4 net surface and advective flux.

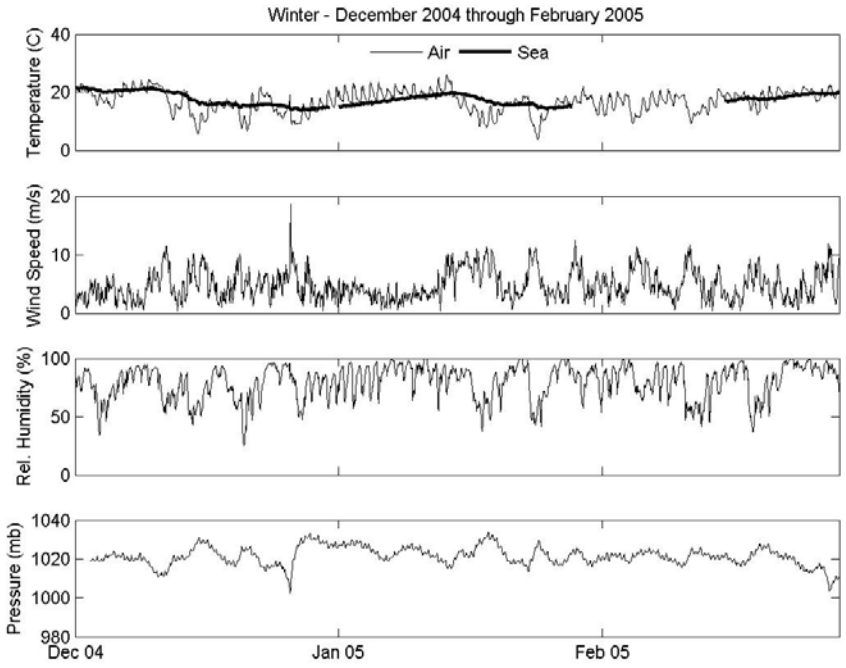

Figure 4-9a: Winter 2004/5 meteorological data.

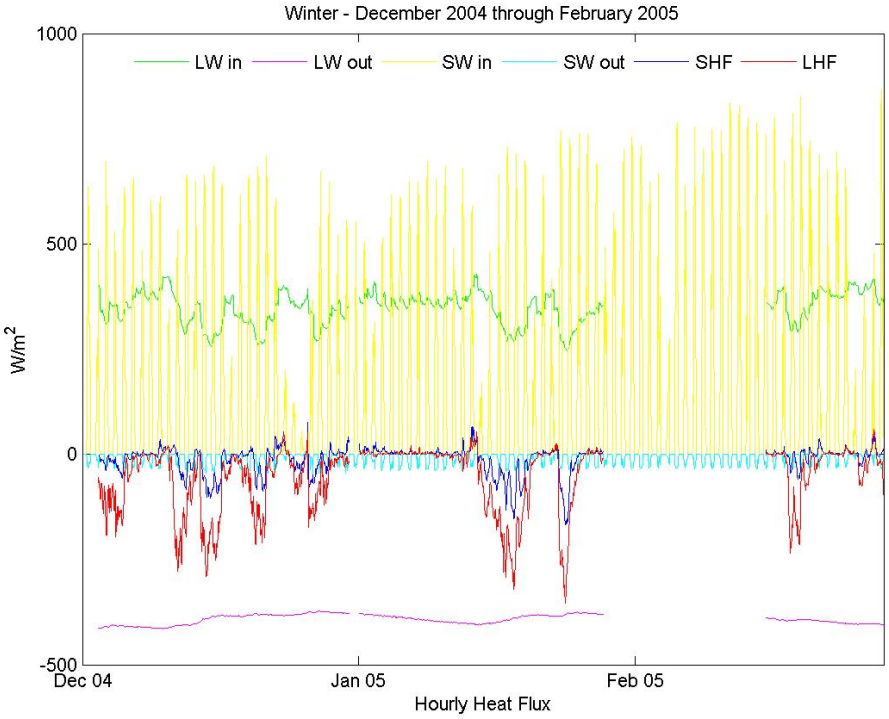

Figure 4-9b: Winter 2004/5 surface fluxes.

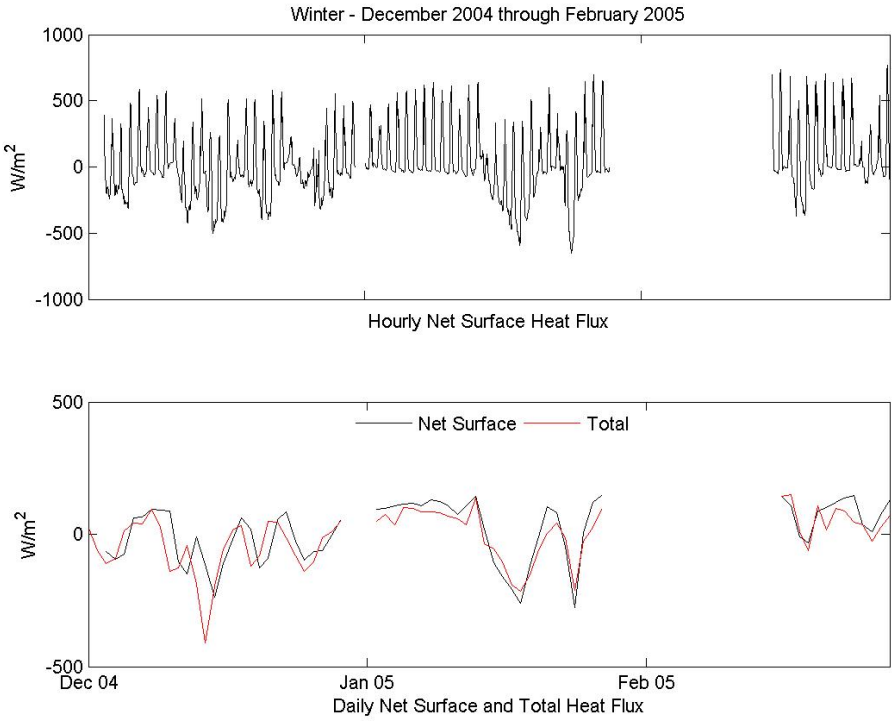

Figure 4-9c: Winter 2004/5 net surface and advective flux.

Spring – March through May

Early spring is characterized by intervals of increasing ocean temperature under the influence of heightened downwelling solar radiation and reduced windspeed. Episodic extratropical fronts disrupt the overall warming trend with decreasing frequency as the season progresses. By May, surface heat flux and meteorological parameters steady into a more summer-like pattern of reduced variability, essentially the converse of the fall transitional period. Bay temperature warmed by a total of 12.4 ºC in the spring of 2004, 8.7 ºC in 2005 (Figures 4-10 and 4-11, a and b). A break in the bay water temperature data record during the first half of the year prevents comparison with the 2003 spring season. In the following section, atmospheric conditions contributing to ocean warming are examined in a final case study.

Significant interannual variability is found, in addition to considerable differences in early and late springtime trends, in surface and advective (as residual) heat exchange. Rates of warming at the surface of the bay declined sharply from an average of 40.2 W/m^2 over March through April to 12.4 W/m^2 in May of 2004. Averaged net surface heat flux contributed to warming to a much lesser extent (22.5 W/m^2) in early spring, March – April, of 2005 and shifted to slightly favor cooling in May (-1.9 W/m^2). Combined, averaged rates of turbulent heat exchange opposed warming over all three months of spring: -120.3 W/m^2 in 2004 and –111.1 W/m^2 in 2005. Net longwave radiative heat flux is comparable year-to-year (-35.2 W/m^2 in 2004 and –29.4 W/m^2 in 2005). The disparity in combined, basin-averaged rainfall over the four major catchments feeding Tampa Bay

(the Tampa Bay Coastal Region Basin, the Hillsborough Basin, the Alafia River Basin, and the Little Manatee River Basin) during the spring seasons of 2004 and 2005 is noteworthy; a total of 49.26 inches of precipitation fell over these four regions in March – May of 2005 as compared to 31.74 inches over the same months in 2004 (SWFWMD; http://www.swfwmd.state.fl.us/data/wmdbweb/rnfpage.htm).

Similar shifts in magnitude and direction of advective heat exchange were found between early and late season. Bay hydrodynamics contradict surface warming over the early spring (March through April), cooling the bay waters at a rate of –13.5 W/m^2 in 2004 and –10.7 W/m^2 in 2005. The latter portion of spring each year brought about a change in favor of advective warming. Bay circulation acted to heat the bay at a rate of 29.7 W/m^2 in May of 2004 and 51.8 W/m^2 May of 2005.

Warming Trend –

Following the transition of a final, late extratropical frontal system in mid-April of 2004 is an extended period of steadily rising water temperature in the bay. Though the autumn-like front interrupted bay warming, reducing the daily mean sea temperature by more than 2 ºC over a four-day interval, the episode was succeeded by a period of light winds and strengthening insolation, from the 17th through the 25th of April (framed in black in Figure 4-10), which favored warming of estuarine waters. This prolonged interval of positive total heat flux into the bay drove a reversal of the frontal cooling and a continuation of the overall warming trend of the spring season; mean bay temperature is progressively higher each successive day with a total increase of 3.8 ºC over the nine-day period.

Wind speeds were slightly lower on average during this warming phase (4.4 m/s) in comparison to both the spring months of 2004 overall and the preceeding winter season (each with a mean windspeed of 5.1 m/s). Observed insolation, averaging 211.8 W/m^2, is significantly increased over the wintertime mean downwelling solar radiation (124.6 W/m^2). This period is characterized by strong surface heat flux into the bay (nine-day mean: 95.4 W/m^2) while bay circulation contributes only marginally to warming (5.9 W/m^2).

Several days into the highlighted interval of warming, winds shifted from blowing steadily out of the E-NE to blowing out of the E at night and out of the W over-water by day as a land/sea breeze pattern developed. Cooler sea breezes limited maximum daily air temperature over the bay on succeeding days. Measured incoming solar radiation was also somewhat reduced (min. daily mean of 175.5 W/m^2). However, wind speeds fell to less than 4.0 m/s, turbulent heat exchange at the surface weakened, and conditions remained favorable for warming. On April 23rd, winds shifted once more to blow easterly at night and northerly during the day, disrupting the land/sea breeze pattern. Peak air temperatures and daily mean insolation increased over the following days, extending the warming trend.

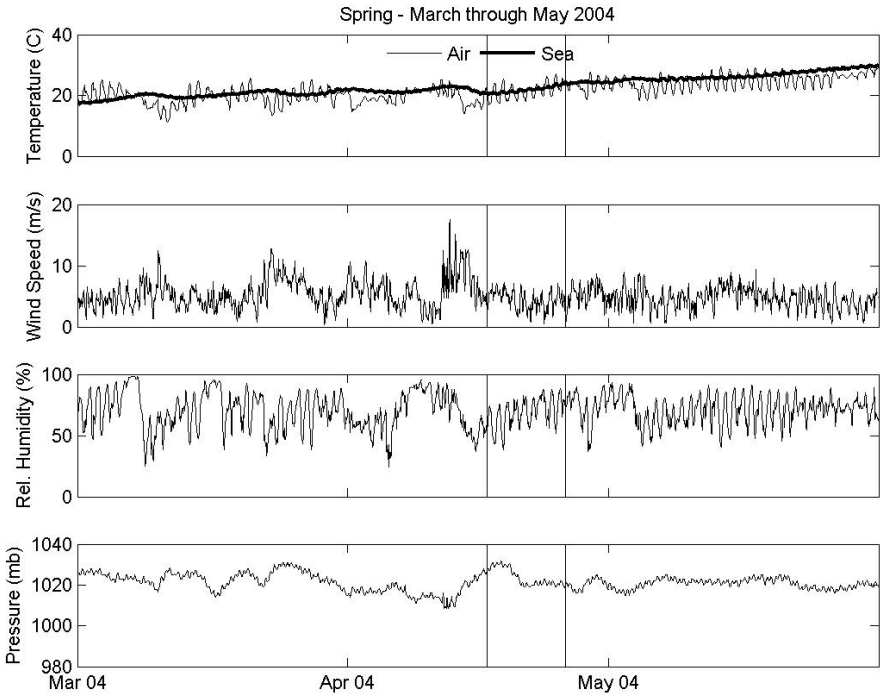

Figure 4-10a: Spring 2004 meteorological data.

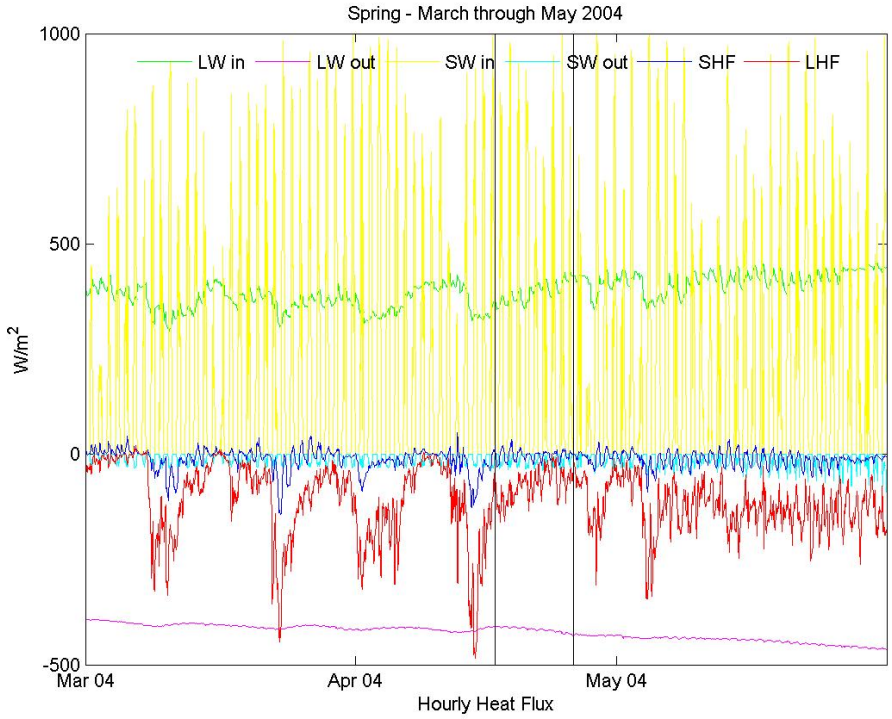

Figure 4-10b: Spring 2004 surface fluxes.

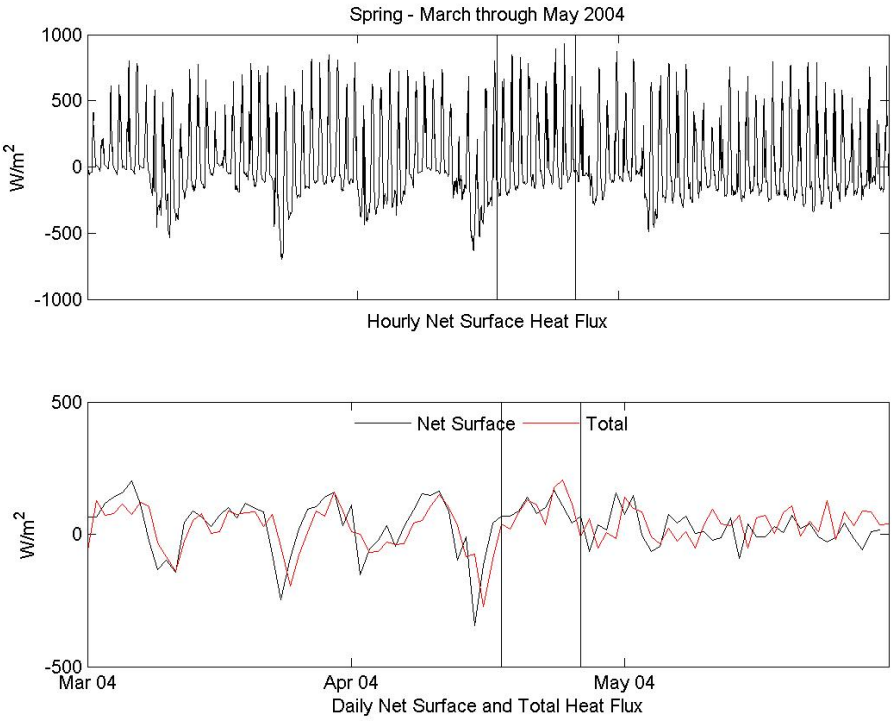

Figure 4-10c: Spring 2004 net surface and advective flux.

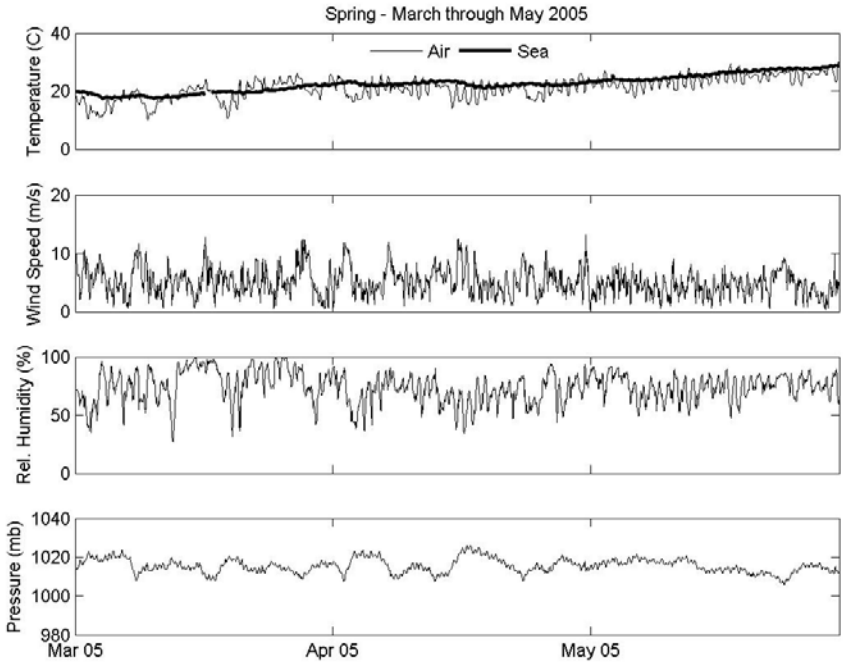

Figure 4-11a: Spring 2005 meteorological data.

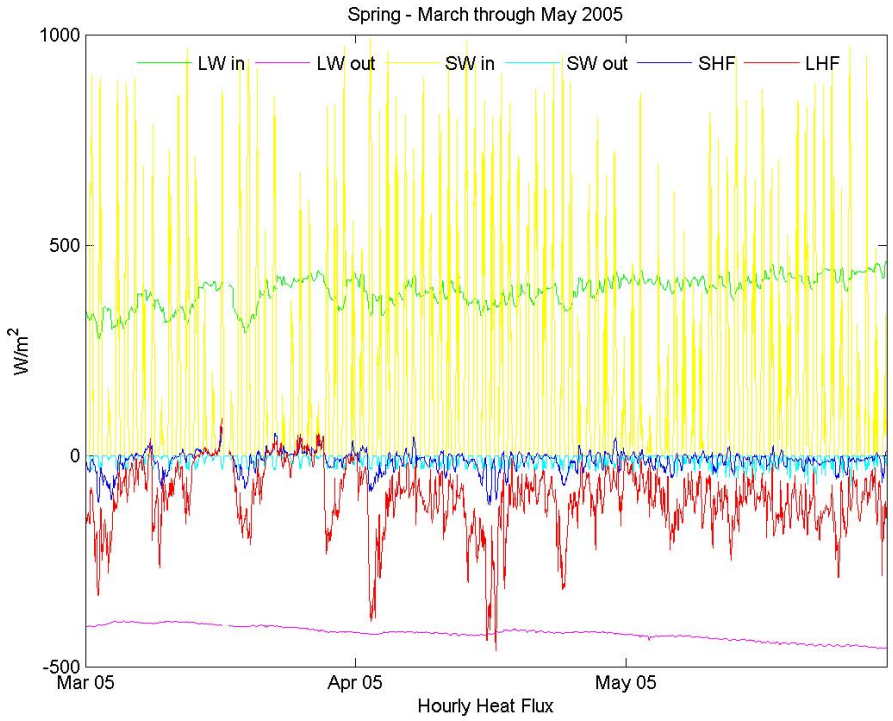

Figure 4-11b: Spring 2005 surface fluxes.

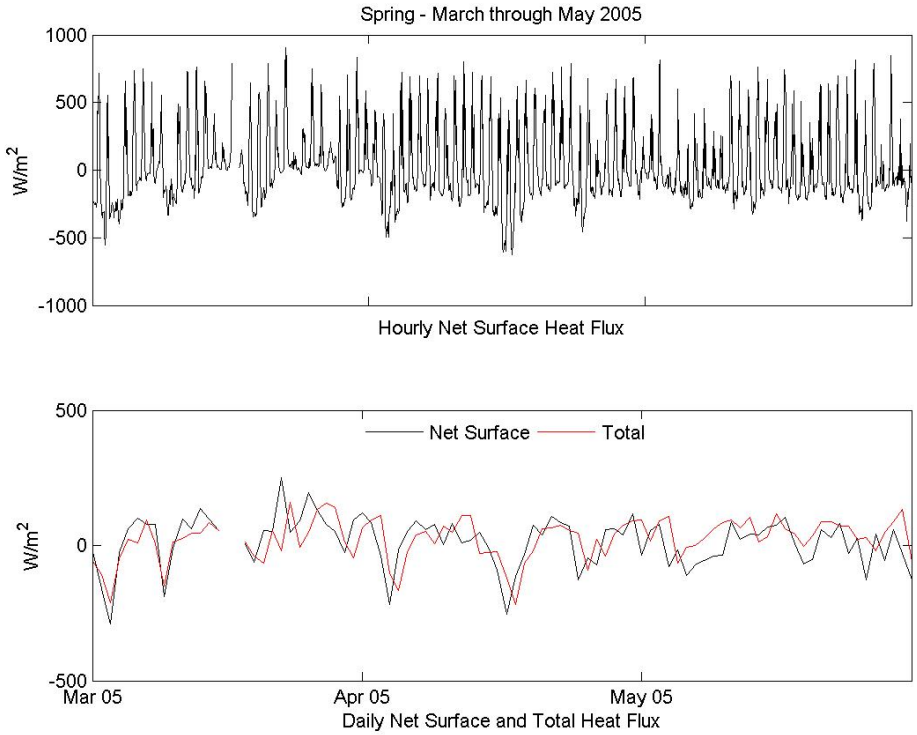

Figure 4-11c: Spring 2005 net surface and advective flux.

Summary and Conclusions

A three-year examination of the patterns of heat exchange at the surface and mouth of Tampa Bay revealed significant interannual and seasonal variability. Short time-scale atmospheric forcing due to tropical cyclones and extratropical frontal systems dramatically impacts net surface and advective heat exchange, driving rapid cooling of bay waters. During such events, the surface fluxes are inadequately described by climatological means and active thermodynamics potentially become important to overall accuracy in the Meyers et al. Tampa Bay hydrodynamic model computations. Somewhat counterintuitively, the extratropical fronts that sweep through the region frequently each year often individually force greater change in estuarine heat content than hurricanes or tropical storms. Those components of the heat budget that are negligible on long-term average, such as sensible heat flux due to precipitation, can become temporarily significant. For example, heat flux due to rainfall over Tampa Bay briefly reaches a maximum hourly contribution to warming of 28.8 W/m^2 in winter 2003/4, but acts to cool the bay at an hourly mean rate of 68.3 W/m^2 out of the bay in the fall of 2003.

As is the case for the coastal WFS (Virmani and Weisberg 2003, He and Weisberg 2002, 2003), surface heat fluxes dominate total cooling in the fall and warming in spring in Tampa Bay. Advective heat exchange was determined to variously enhance and oppose the direction of surface flux. On average over the spring season, advection acts to warm bay waters. However, over March and April of 2004 and 2005, advective heat flux counters surface warming before reversing sign, contributing to warming, late in the spring season. In contrast, advective heat exchange cools the bay throughout the autumn season. Averaged surface heat exchange into and out of the bay over 2004, the most complete year of the three-year period of this study, demonstrate that the surface heat fluxes nearly balance, as is expected over the annual cycle, with a mean flux into the bay of 572.4 W/m^2 and an annual average heat flux out of the bay of 570.1 W/m^2 at the surface.

This study presents bulk methods requiring commonly measured meteorological variables to determine model surface heat flux boundary condition. The methods chosen to estimate net surface heat exchange rates during this study are amenable to application in real-time model computations. Directions for future research include running parallel modeling studies with and without active thermodynamics in order to assess the importance of thermodynamic calculations to overall model accuracy.

Chapter Five

Freshwater Balance Study

Introduction

Tampa Bay, situated on the west central Florida coast, is the state's largest open water estuary (see Figure 1-1). Within the Tampa Bay estuary freshwater from terrestrial sources meets and mixes with the saline oceanic waters of the Gulf of Mexico. This interaction between fresh and salt water results in a horizontal salinity gradient ranging from an average of 26 ppt for the fresher, buoyant waters of the northernmost portions of the bay, where the majority of terrestrial runoff is received, to the Gulf waters (33 ppt mean salinity) at the southern mouth of the bay (Meyers et al. 2007). The existence of this horizontal salinity gradient is the dominant factor controlling Tampa Bay hydrodynamics. In a hindcast study of the residual circulation of Tampa Bay, Meyers et al. (2007) demonstrated that bay-wide salinity and circulation patterns are sensitive to alterations in the fresh water balance of the estuary. The long-term averaged horizontal salinity gradient is greatly reduced during dry periods and amplified during wetter periods. The 2007 examination of the time-averaged circulation of the bay illustrated the impacts of highly variable freshwater influx volumes on bay-wide circulation. During conditions of reduced freshwater inflow the residual circulation in Tampa Bay is weakened, while increased freshwater input greatly enhances surface current velocities.

The freshwater balance of the bay is comprised of several source and sink components, including precipitation, surface discharge and groundwater seepage into the bay, and evaporation. However, Meyers et al. (2007) note that evaporative freshwater outflow values are small as compared to the combined freshwater sources so that a numerical model of Tampa Bay hydrodynamics is likely responsive to some longer term mean evaporation rate rather than daily values.

Maximal rainfall and river discharge usually occur in the Tampa Bay region during the summer months, largely due to convective thunderstorms. Winter precipitation totals are typically significantly lower: 25-50% of summer rainfall levels. In addition to this predictable seasonal variability, Schmidt et al. (2001) demonstrated a significant response to El Niño/ La Niña events in both precipitation and streamflow for the Tampa Bay catchment area. The authors found that neutral winter (defined by the authors as January, February, and March) precipitation may be increased by as much as 50-150% under the influence of an El Niño event, while the region may experience a winter deficit of 50-100% during La Niña episodes. Likewise, surface water discharge is greatly enhanced during El Niño winters; mean river runoff is increased by over 200%. During La Niña winters, discharge levels were typically depressed by 70% compared to surface flow during neutral winters. Additionally, during both El Niño and La Niña events,

summer (defined as July through September) mean discharge levels were reduced as compared to neutral values at most stations.

Schmidt and Luther (2002) analyzed monthly measures of salinity gathered from sixty-three stations located throughout Tampa Bay, for the years 1974 – 1999, and discovered that bay salinities are generally negatively correlated with both El Niño and La Niña sea surface temperature anomalies (SSTAs; positive SSTAs indicate an El Niño episode while negative SSTAs identify La Niña events and the greater the magnitude of the SSTA, the stronger the event). The greatest correlation between El Niño conditions (indicated by positive SSTA) and reduced salinities occurred during the winter (JFM) and spring (April, May and June) months, with significant associations between these two parameters occurring during fall (October - December) as well. Additionally, the authors determined that closest correlations between El Niño SSTAs and depressed salinity measurements are found in the northern regions (near the head) of the bay where the majority of surface runoff is received.

Specification of surface evaporation rate is required as a boundary condition within the Meyers et al. Tampa Bay numerical model. During the recent 2001 – 2003 hindcast study (Meyers et al. 2007), evaporative water loss over Tampa Bay was approximated by measurements from a nearby pan evaporimeter. Availability of results from a three-year (June 2002 through May 2005) study of heat exchange over Tampa Bay permitted comparison of evaporation rates produced in latent heat flux computations over the bay to the evaporative loss rates utilized during the hindcast study for the interval of study overlap, from June 2002 to December 2003. The first half of this study period, June of 2002 through April of 2003, is classified as a moderate El Niño event based upon a threshold Oceanic Niño Index of ± 0.5 °C (NOAA Climate Prediction Center; http://www.cpc.noaa.gov/) while the remainder of the research time frame (May through December 2003) is categorized as neutral. This affords the opportunity to examine the impacts of an El Niño episode on the freshwater balance of Tampa Bay in comparison to neutral seasons.

The objectives of this research were twofold: 1) to infer the magnitude of fresh water loss at the surface of Tampa Bay from estimates of daily averaged evaporative heat loss over the bay produced by the TOGA COARE 3.0 bulk algorithm and compare estimates of evaporative water loss over the bay to evaporation rates acquired by pan evaporation technique as provided to the Meyers et al. Tampa Bay numerical model during the 2001-2003 hindcast residual circulation study and 2) to consider the variable importance of evaporation as a fresh water sink in the context of fresh water balance components supplied as boundary conditions to the numerical model during June 2002 through December 2003 of the 2001-2003 hindcast study. While fresh water loss through evaporation is typically small in comparison to the collective inputs of precipitation and land surface runoff into the bay, interannual and seasonal variability of fresh water sources and sinks affect the comparative importance of evaporative water loss as a control on bay-wide salinity.

Experimental Methods

Freshwater Budget Components

Freshwater is delivered to Tampa Bay through several sources: surface runoff from rivers and smaller tributaries, injection of waste water from water treatment plants and other industrial point sources, precipitation over the bay, and groundwater seepage. Rainfall over the bay is supplied to the Meyers et al. Tampa Bay model as a daily composite of cumulative rainfall measured at four sites around the bay: the Sarasota/Bradenton Airport (SRQ), the St. Petersburg Albert Whitted Airport (SPG), the St. Petersburg/Clearwater International Airport (PIE), and Tampa International Airport (TPA). Available measurements of waste water released from four waste water treatment plants situated around the bay area, process water discharge rates from the Piney Point phosphate mine operation, and freshwater contributed via the Tampa Bypass Canal are combined with USGS daily averaged streamflow measurements, and credible estimates of streamflow rates where point source measurements are unavailable, to produce a daily average surface water contribution. Groundwater is discharged to Tampa Bay from the surficial, intermediate and Floridan aquifers at an amount approximately equal to 0.081 times the total streamflow of each river and tributary (Brooks et al. 1993). This additional freshwater flux is added to the daily mean base flow rate of each point source specified within the model domain.

Pan Evaporation Rate –

The daily rate of evaporative freshwater loss from the surface of the estuary is assumed from a SWFWMD maintained evaporation pan located near McKay Bay. Gaps in the pan evaporation record occur spanning the end of July through September 2002 and mid-August through the middle of October of 2003. The daily rate is interpolated from monthly climatological averages where pan evaporation data is unavailable. Water loss from a pan evaporimeter responds to similar environmental forcing as does loss from a large water body (atmospheric humidity, net radiation, winds) and is therefore expected to represent an improvement to the previous practice of assigning a simple, static evaporation rate value (0.25 cm/day or 27.6 m^3/s) over Tampa Bay in model computations. Linacre (2005) notes, however, that the pan evaporation technique cannot capture characteristics unique to large bodies of water such as a high thermal inertia, heat transport via currents, increased near surface humidity present over wide water surface areas, and the occurrence of waves. Pan evaporimeters are also sensitive to pan placement. Shading from nearby plants, shielding from winds, and surface properties, such as aerodynamic roughness of the nearby area and the low heat capacity of surrounding land, may all skew evaporation measurements (Hillel 1997). Unlike natural surfaces, pan evaporimeters are exposed to more energy per unit surface area, as the sides and bottom of the pan remain open to additional radiative and conductive heat transfer from surroundings (Kahler and Brutsaert 2006). Rates of freshwater loss produced by pan evaporimeter, similar to evaporation rates derived from bulk formulae, do not represent a direct measurement of evaporation rate. Evaporative losses from a pan are instead related to actual evaporation from surrounding surfaces through the application of a correction

coefficient. This correction factor may vary from 0.5 to 0.85 (Hillel 1997) according to season and the environmental characteristics specific to pan location.

The reader is referred to Meyers et al. 2007 for a complete description of 2001-2003 model boundary condition parameterizations of freshwater sources and sinks applied during the Tampa Bay residual circulation study.

Evaporation Rate Produced in Latent Heat Flux Calculations –

The turbulent flux of latent heat at the surface typically represents a loss of energy from the bay in response to a gradient in specific humidity between the saturated air at the sea surface and drier air aloft. Molecules of water evaporating at the surface carry heat away from the surface, releasing this energy to the atmosphere and cooling estuarine waters. Latent heat transport is enhanced by high wind speeds generating increased near-surface turbulence, low atmospheric humidity strengthening the ocean/atmosphere moisture gradient, and elevated sea surface temperatures reducing the latent heat of vaporization. Bulk aerodynamic representation of the latent heat flux is given by:

$$Q_L=\rho L_e U C_E(q_s-q_a) \qquad (28)$$

where U is the wind speed , q_s-q_a is the difference between saturated sea surface and atmospheric specific humidity, L_e is the latent heat of vaporization, C_E is the dimensionless moisture transfer coefficient, and the density of air is given by ρ.

As one component of a three-year investigation into the heat budget of Tampa Bay, daily averaged latent heat exchange estimates were computed via the TOGA COARE 3.0 bulk algorithm (Fairall et al. 2003) for the period spanning June of 2002 through May of 2005. Inputs to the algorithm included measurements of water temperature and over-water winds, air temperature and humidity gathered at the BRACE meteorological tower located in Middle Tampa Bay (see Figure 1-1 for the location of the BRACE observational tower within Tampa Bay). Latent heat flux data availability overlaps with the latter half of the Tampa Bay residual circulation study: June 2002 through Dec 2003. However, for the December of 2002 through June of 2003 portion of the study, measurements of bulk water temp were unavailable, resulting in missing latent heat exchange data.

The evaporative freshwater loss, E, was inferred from the estimated energy lost due to evaporation (the latent heat flux, Q_L) and the amount of energy contained within each kilogram of water vapor formed (the latent heat of vaporization, L_e):

$$E = Q_L / L_e \qquad (29).$$

Results

Freshwater Balance in Tampa Bay for June 2002 – December 2003

On long term average, evaporative freshwater loss according to pan evaporimeter plays a secondary role in the freshwater balance: for June 2002 – December 2003 (n = 579 data points), the 1.5 yr mean daily pan evaporation rate is 31.7 m^3/s, removing approximately 22% of the total freshwater inflow rate (surface runoff, precipitation, and groundwater input) of 145.0 m^3/s. The time frame of this study includes two summers, the season of peak evaporation, but only one winter and spring, where evaporative water

loss is typically at a minimum according to pan evaporimeter, largely in response to reduced insolation during these seasons (see Fig 5-1). In addition, evaporation occurs evenly across the bay whereas the surface runoff and ground water seepage, which together account for nearly 61% of freshwater inflow over this study period (at a daily mean rate of 88.1 m^3/s), are confined to select regions of input that are mostly concentrated in the northern head of the bay. This heterogeneity of freshwater input results in surface waters becoming progressively fresher moving up the bay and is the force driving the overturning circulation of Tampa Bay. Precipitation, averaged over the entire bay, makes up the remaining 56.9 m^3/s of freshwater inflow. These observations support the assumption that evaporative water loss does not represent a dominant controlling factor on bay hydrodynamics and therefore a numerical model of Tampa Bay is likely not typically sensitive to daily variations in evaporation rate.

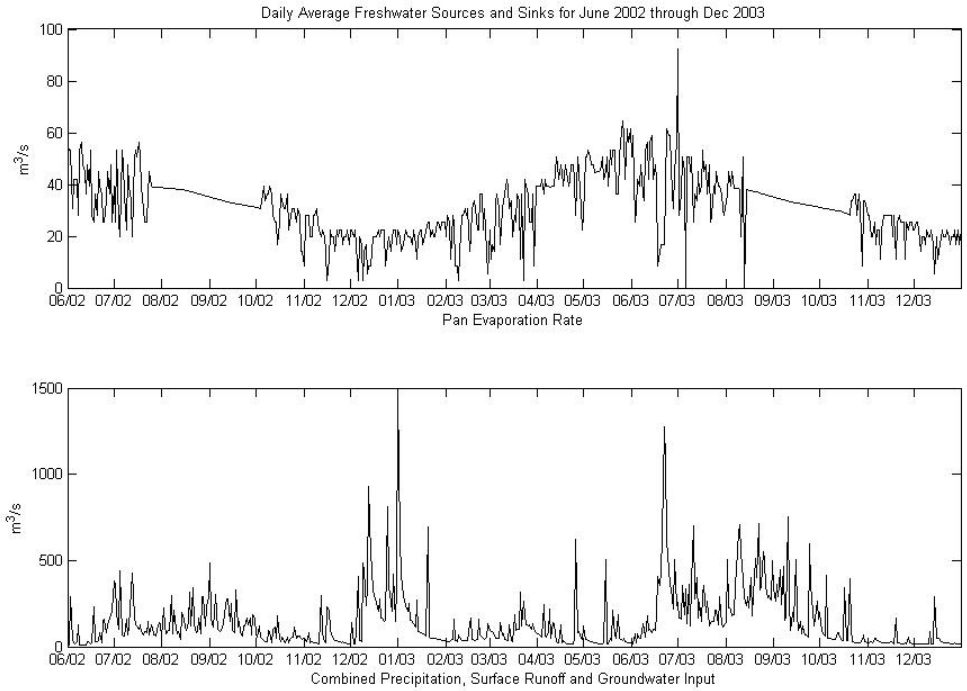

Figure 5-1: Daily mean rates of evaporative loss (pan evaporimeter) out of and total freshwater inflow into Tampa Bay in cubic meters per second.

Daily average evaporation rates produced in bulk latent heat flux (LHF) estimation over Tampa Bay were available for the periods spanning June 2002 through November 2002 and July 2003 through December of 2003 of the June 2002 – December 2003 study timeframe (n = 389; see Figure 5-2). For these combined intervals, over-water evaporative water loss (daily mean rate = 47.2 m^3/s) offsets a little over a third of the surface and rainfall freshwater contributions to the bay while the pan evaporimeter gives a mean evaporative loss, 31.5 m^3/s, a magnitude remaining approximately 22% of the

freshwater inflow. Bulk formula-derived evaporation rates support Vincent's (2001) preliminary findings that evaporative freshwater volume loss from Tampa Bay is of similar magnitude and opposite sign as volume inflow due to precipitation; the mean rainfall over the estuary for these two periods combined is 59.2 m^3/s.

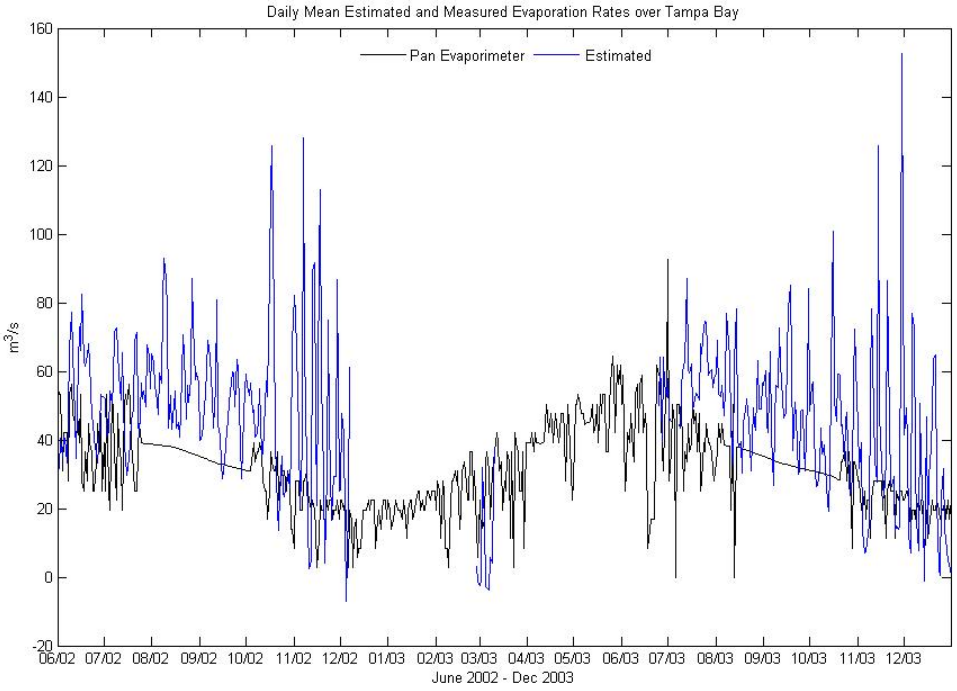

Figure 5-2: Daily mean estimated (bulk formula) and measured (pan evaporimeter) evaporation rates over Tampa Bay (m^3/s).

In keeping with Linacre's (2005) statement that pan evaporimeter measurements are largely governed by radiation, McKay Bay pan evaporation rates exhibit a clear tendency toward reduced magnitude and variability in the fall and winter months in response to diminished insolation as compared to the summer months (Figure 5-3). The mean evaporation rates over June and July of 2002 (n = 54; climatological mean evaporation data excluded) and June through July of 2003 (n = 61) are 39.4 m^3/s (std. deviation from the mean = 11.0 m^3/s) and 40.4 m^3/s (std. deviation of 14.8 m^3/s), respectively. In contrast, average evaporative water loss rate, as measured at McKay Bay, is decreased during November and December of 2002 to 18.6 m^3/s (std. deviation = 6.3 m^3/s). Evaporation rates for the same time span in 2003 are similarly reduced in magnitude (mean of 61 time steps: 21.3 m^3/s) and variability (std. deviation of 5.1 m^3/s).

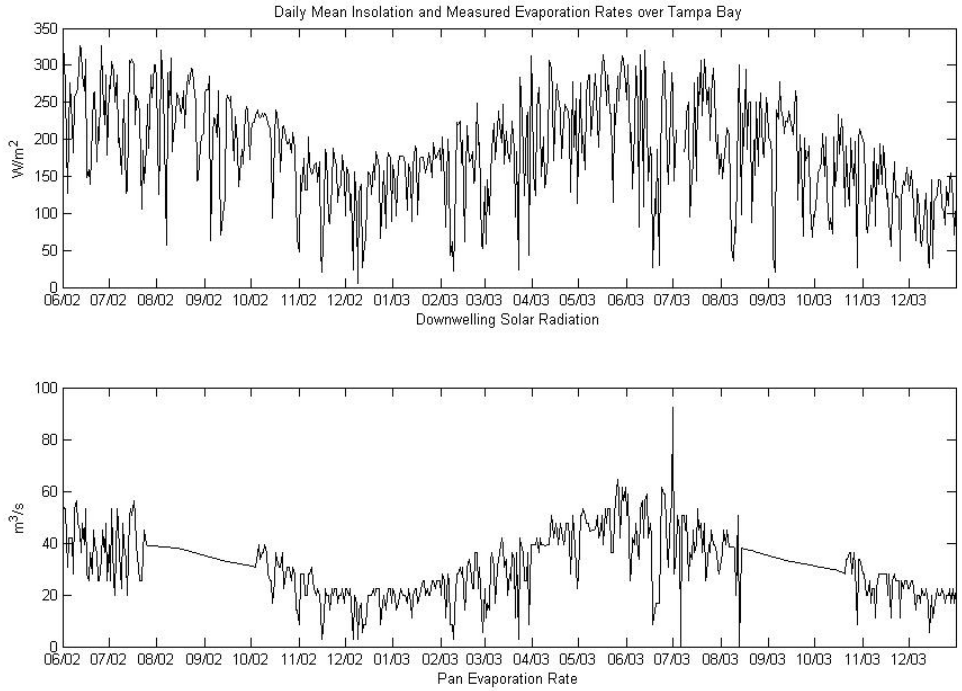

Figure 5-3: Daily mean insolation rates (acquired from the BRACE observational tower) and pan evaporation rates over Tampa Bay.

Conversely, over-water evaporation rates display the increased variability in the latter part of each year, as compared to summertime evaporative loss rates, that is expected in response to the episodic high winds and reduced humidity associated with the wintertime passage of extratropical fronts (see Figure 5-2). On November 16th of 2002, an approaching cold front precipitated an upsurge in rainfall over Tampa Bay to a daily average of 193.2 m^3/s from a mean of only 0.4 m^3/s for the prior day. Relative humidity increased by nearly 20 percent to 88.2%. By November 18th, the rains had passed from the region and daily averaged air temperature, as measured at standard anemometric height at the BRACE tower, fell to 14.3 ºC from a mean of 21.2 ºC on November the 16th. The 10m relative humidity reading descended to 50.2%. Winds that peaked on the 17th at a mean of 9.2 m/s remained high on the 18th at 7.8 m/s, as compared to wind speeds averaged over the entire study period (4.8 m/s). In response to this strong atmospheric forcing, evaporation rates produced in over-water LHF estimation fell from 45.0 m^3/s on November 15th to 20.9 m^3/s as the rains swept through the area on the 16th, spiking to a daily mean of 112.8 m^3/s on November 18th. Evaporation rates determined from pan evaporimeter exhibited a similar pattern of response to the passage of the front, but to a much lesser degree in magnitude: evaporative water loss rates were at a minimum of 2.8 m^3/s on the 16th and reached a maximum daily average of no more than 22.4 m^3/s on November the 18th.

Both methods of parameterizing evaporative freshwater loss from the surface of the bay are disadvantaged in being point estimates; pan evaporimeter measurements are

acquired from a single pan located near McKay Bay while over-water estimates are inferred from heat exchange rates computed at the BRACE tower in Middle Tampa Bay. In addition, pan evaporimeter observations necessitate the inclusion of a correction coefficient and thus, like over-water evaporative volume loss rates, do not represent a direct measurement of evaporation. Evaporation rates obtained from a pan evaporimeter reflect the immediate environment of the instrument and cannot adequately capture over-water conditions. However, evaporation rate estimates inferred from latent heat transfer rates incorporate over-water measurements of relative humidity, wind speed, bulk water and air temperatures and insolation gathered at the BRACE tower located within Tampa Bay and capture the variability expected during seasonal transition periods. As such, these over-water estimates of evaporation represent an improvement over rates determined via nearby pan evaporimeter and are utilized for the remainder of the Tampa Bay freshwater budget study.

Inter-Annual Variability in Freshwater Inflow/ ENSO Impacts

Signatures of the El Niño episode that spans the latter half of 2002 through the spring of 2003 may be clearly seen in the sharp contrast in combined freshwater inflow to Tampa Bay between June and December of 2002 and the corresponding months in 2003 (a neutral season; see Figure 5-1). In agreement with Schmidt et al. (2001), bay-wide daily average winter precipitation levels are found to be greatly enhanced under the influence of this El Niño event. Mean daily rainfall for December of 2002 is 87.1 m^3/s, an amount nearly 8 times the average daily rainfall rate during the neutral month of December 2003 (11.1 m^3/s). Accordingly, surface and ground water inflow to the estuary diminishes from an average daily rate of 194.4 m^3/s during December 2002 to a mean daily flow of 21.1 m^3/s for the neutral December of 2003. In contrast, while Schmidt et al. (2001) did not find a significant relationship between the presence of either La Niña or El Niño conditions and discharge levels, the authors found summer river and stream discharge rates were depressed relative to rates during neutral summer seasons. Again the moderate El Niño event is evident in the disparity between mean daily combined surface and groundwater inflow rates for June 2002 (31.0 m^3/s) and the neutral June of 2003 (195.5 m^3/s). While the influence of evaporative freshwater loss on estuarine salinity is negligible during an extremely wet El Niño winter, the relative importance of evaporation to the freshwater balance of the bay is amplified through El Niño/ La Niña summers.

The contrast between freshwater input rates for the summer months when El Niño conditions were prevalent (July, August and September of 2002), and the same months in the neutral latter half of 2003, illustrates the impact even moderate events can exert on the freshwater balance (Figure 5-1). During the El Niño summer of 2002, rain fell over Tampa Bay at the mean rate of 73.4 m^3/s per day while the combined surface runoff and groundwater seepage contributed at the rate of 85.4 m^3/s. The neutral summer of 2003 brought an average precipitation rate of 115.7 m^3/s, while ground and surface water input to the bay swelled to a mean rate of 285.6 m^3/s. Other mean meteorological parameters, such as 10-meter air temperature, relative humidity and wind speed, were remarkably similar between the summers of 2002 and 2003. Interestingly, the average rate of evaporation is identical for these time frames: 53.9 m^3/s. While evaporative water loss counterbalances 34.0% of freshwater inflow during the moderate El Niño summer of

2002, it offsets only 18.9% of freshwater influx throughout the summer of 2003. Under unusually dry conditions, knowledge of the variable rate of freshwater volume loss from the bay surface becomes important.

Bulk sea temperature measurements are unavailable from the BRACE tower array for the period of December of 2002 through June of 2003, preventing a similar comparison between El Niño and neutral winters. However, based upon the work of Schmidt et al. (2001), it is expected that the disparity in the relative impacts of evaporative water loss during neutral and El Niño winter times to the overall freshwater budget of Tampa Bay would be even more pronounced.

Seasonal Variability in Freshwater Balance

Overlap of the three-year Tampa Bay heat budget study data records with the data set of model boundary conditions from the Meyers et al. (2007) residual circulation hindcast study permitted intra-annual comparisons of freshwater budget components in Tampa Bay for the summer and fall 2003, a neutral year according to ONI index. Passing extratropical fronts sweep across the bay during the autumn and winter months bringing higher winds and drier air to the bay region coupled with periodic sharp declines in air and water temperatures. Over-water evaporation rates spike in response to these intense meteorological events. Standard deviation from the mean, as a measure of variability, points to significantly increased variance in evaporative volume loss from the bay during the late year months of November and December of 2003 (std. deviation = 29.7 m^3/s) as compared to the mid summer months of August – September of the same year (std. deviation of 13.8 m^3/s).

Mean evaporation rates during these periods are not vastly different. The average rate of evaporative freshwater loss from Tampa Bay through August and September (51.6 m^3/s) lowered to 34.3 m^3/s for November and December, likely in response to reduced mean sea temperature (down to 20.0 ºC from a summer mean of 29.3 ºC) combined with weakened insolation (an average of 119.7 W/m^2 in the winter versus a mean of 184.2 W/m^2 for these summertime months). Wintertime rainfall, surface inflow and groundwater seepage rates, however, are dramatically diminished from summertime values. Emphasizing the potential importance of evaporation in the total freshwater budget of Tampa Bay, mean total freshwater inflow for the November – December interval is 31.4 m^3/s, an amount roughly equal to evaporative freshwater loss. In contrast, the average inflow rate from all freshwater sources for the summer months (August through September) is 311.0 m^3/s. Freshwater loss from the surface of the bay plays a much greater role in the estuarine salinity balance in the course of the transitional autumn season and the error incurred by assigning a constant value to the evaporative volume loss model surface boundary condition is expected to be compounded.

Summary and Conclusions

The present research confirms that, on long-term average, freshwater volume loss at the bay surface is a minor component of the freshwater balance of Tampa Bay. However, it is demonstrated that the relative importance of evaporative volume loss varies considerably on seasonal scales. Summer is typically the peak rainy season over

south central Florida while wintertime precipitation is usually low: 25 – 50% of summertime values. Combined freshwater input to the bay (surface and groundwater inflow and precipitation) clearly dominates the balance during the summer of 2003. Conversely, rates of evaporation over the bay completely counterbalance depressed freshwater influx rates in the latter months of 2003.

Rainfall and runoff patterns in the Tampa Bay catchment are drastically altered under El Niño conditions. Comparisons of total freshwater inflow to the bay under the influence of a moderate El Niño event and during the neutral summer and winter of 2003 caution against the application of climatological seasonal mean evaporation rates as surface boundary conditions within the numerical model. Additionally, autumn and winter extratropical fronts, bringing cold, dry air and high winds to the region, dramatically accelerate over-water evaporation in the short term. During such events, evaporative volume loss rates, as computed in surface heat flux computations, are significantly greater than both the pan evaporimeter-derived freshwater flux rates and the constant evaporation rate applied previously in Meyers et al. numerical model studies. Bulk formula estimates of evaporation rates over Tampa Bay are readily computed real-time from over-water meteorological parameters.

Chapter Six

Summary and Recommendations

Integration of a water quality model with the Meyers et al. Tampa Bay hydrodynamic model, the next stage in development of the Tampa Bay Integrated Model, motivated the present research into bay-atmosphere heat exchange. Definition of a heat transfer boundary condition at the bay surface is required as a precursor to computations of three-dimensional temperature fields within the bay and estuarine water quality modeling. Toward that end, quantification of heat exchange at the air-water interface was the primary objective of this research.

An initial six-month examination of over-water turbulent heat exchange, the portion of total surface heat flux occurring in response to bay-atmosphere gradients in temperature and moisture and driven by the passage of turbulent eddies, demonstrated the skill of two algorithms, the TOGA COARE v. 3.0 (TC3) algorithm and the NOAA Buoy model (NBM), in predicting directly measured sensible heat flux over Tampa Bay. At the core of each algorithm, the bulk aerodynamic method of computing sensible (latent) heat exchange rates relies on the product of horizontal wind speed and the temperature (moisture content) differential between near surface and the standard anemometric measurement height of 10 m to approximate the eddy covariance of vertical wind velocity and air temperature (relative humidity). This eddy covariance of vertical wind and air temperature is also directly measured by sonic anemometer and used to produce sensible heat exchange at the surface. However, sensible heat flux measured by sonic anemometer is vulnerable to bias during rainfall events. Direct measurements of the turbulent fluctuations of vertical wind and relative humidity are unavailable and therefore latent heat flux over Tampa Bay must be approximated by the bulk aerodynamic approach described above or the gradient method, a technique that assumes the shape of the near-surface temperature (humidity) profile based upon measurements of air temperature (moisture content) gathered at two heights over water to predict sensible (latent) heat exchange. The gradient method of computing sensible and latent heat flux is restricted in relevance to near-neutral atmospheric stability regimes and was determined to be too limited for applicability to the present research. For the remainder of this study, the bulk aerodynamic method of turbulent heat exchange estimation was utilized due to a lack of direct measurements of latent heat transfer at the bay surface and susceptibility of the sonic anemometer to bias during frequent rainfall events over Tampa Bay.

Inter-model comparisons showed close agreement in modeled sensible heat exchange rates between the NBM and the TC3 algorithm. Modeled latent heat exchange rates agreed less satisfactorily. A minor adjustment to specific humidity computation within the NOAA Buoy model dramatically improved model agreement. Though the NBM was specifically designed for coastal application, development of the TC3 algorithm incorporated model verification studies from the equator to high latitudes and

previous model application ranges from deep ocean to near-shore regions. In addition, the TC3 algorithm is applicable in a wider range of stability regimes. For the remainder of this study, the TOGA COARE v. 3.0 algorithm provided estimates of turbulent heat exchange for the analysis of surface heat fluxes over Tampa Bay.

Net heat exchange at the surface of Tampa Bay has been computed for a three-year interval spanning June 2002 to May 2005. This total heat energy gained or lost at the bay-atmosphere interface represents the summation of the turbulent and radiative heat fluxes. Changes in the total heat content of the bay encompass the net surface heat exchange and advective heat flux at the mouth of Tampa Bay with the Gulf of Mexico. Analogously to the coastal WFS region (Virmani and Weisberg 2003, He and Weisberg 2002, 2003), surface heat fluxes dominate total cooling in the fall and warming in spring in Tampa Bay while advective heat exchange becomes relatively more important during the summer season.

Short time-scale events such as tropical cyclones and extratropical frontal systems dramatically impact net surface heat exchange, driving rapid cooling of bay waters. Heat budget components that are typically small in magnitude, for example, sensible heat flux due to precipitation, may become temporarily important under the influence of these events. Interestingly, the frontal systems that regularly sweep over the bay area each year frequently exert greater influence over surface heat exchange rates and change in total heat content than the near approach of a tropical cyclone (Hurricane Frances). These findings recommend against the application of climatological means in Meyers et al. Tampa Bay hydrodynamic model computations and emphasize the need for frequent over-water observations in order to define model boundary conditions.

Rates of evaporation over the bay fall naturally out of calculations of turbulent heat exchange at the surface. Estimates of evaporation rates produced in over-water flux computations are preferred to either incorporation of measurements from a nearby pan evaporimeter or assignment of a constant evaporative volume loss in modeling of bay hydrodynamics. A secondary objective of this project was therefore improvement on the present evaporation surface boundary condition specification. While freshwater loss from the surface of the bay is typically small relative to the combined contributions of precipitation, groundwater seepage and surface runoff, this study demonstrates that the rate of evaporation over Tampa Bay is highly variable and intermittently important to the overall freshwater balance of the bay.

The methods applied in computation of heat flux components and evaporation rates in this research are amenable to incorporation in real-time modeling exercises. Recommended future research includes the creation of parallel runs of the Meyers et al. Tampa Bay Model, with and without active thermodynamics and real-time evaporation rate computations, in order to evaluate the importance of surface heat exchange and evaporation rate information to overall model accuracy.

List of References

Ahuja, S. and A. Kumar. (1996). Evaluation of MESOPUFF-II SOx Transport and Deposition in the Great Lakes Region. *AWMA Speciality Conference on Atmospheric Deposition to the Great Lakes*. VIP-72: 283-299. Oct. 28-30.

Anderson, S. P., A. Hinton and R. A. Weller (1998). Moored observations of Precipitation Temperature. *Journal of Atmospheric and Oceanic Technology*. 15(4): 979–986.

Arya, S. P. (1988). *Introduction to Micrometeorology*. New York, Academic Press, Inc.

Arya, S. P. (1991). Finite difference errors in estimation of gradients in the atmospheric surface layer. *Journal of Applied Meteorology*. 30:251-253.

Arya, S. P. (2001). *Introduction to Micrometeorology*. San Diego, Academic Press, Inc. 415 pp.

Beardsley, R. C., E. P. Dever, S. J. Lentz, and J. P. Dean (1998). Surface heat flux variability over the northern California shelf. *Journal of Geophysical Research*. 103(C10): 21,553-21,586.

Beljaars, A. C. M. and A. A. M. Holtslag (1991). Flux Parameterization over Land Surfaces for Atmospheric Models. *Journal of Applied Meteorology.* 30: 327-341.

Berliand, M. E. and T. G. Berliand (1952). Measurement of the effective radiation of the earth with varying cloud amounts (in Russian), *Izv. Akad. Nauk SSSR Ser. Geofiz.* No. 1.

Bhethanabotla, V.R. (2002). NOAA Buoy-Williams Model. Web address: http://www.eng.usf.edu/~bhethana.

Bögel, W. (1979). *New approximate equations for the saturation vapor pressure of water vapor and for humidity parameters used in meteorology.* European Space Agency, ESA-TT-509 (revised), 150 pp.

Brooks, G., T. Dix and L. Doyle (1993). Groundwater surface interactions in Tampa Bay, implications for nutrient fluxes. *The Center for Nearshore Marine Science, College of Marine Science, University of South Florida, St. Petersburg, FL.*

Buck, A. L. (1981). New Equations for Computing Vapor Pressure and Enhancement Factor. *Journal of Applied Meteorology*. 20: 1527-1532.

Chang, J.C. and S.R. Hanna. (2004). Air quality model performance evaluation. *Meteorology and Atmospheric Physics.* 87: 167-196.

Charnock, H. (1955). Wind stress on a water surface. *Quarterly Journal of the Royal Meteorological Society.* 81:639-640.

Clark, N. E., L. Eber, R. M. Laurs, J. A. Renner and J. F. T. Saur (1974). Heat exchange between ocean and atmosphere in the eastern North Pacific for 1961-71, *NOAA Tech. Rep. NMFS SSRF-682*, U. S. Dept. of Commer., Washington, D. C.

Dyer, A. J. and B. B. Hicks (1970). Flux-gradient relationships in the constant flux layer. *Quarterly Journal of the Royal Meteorological Society*. 96: 715-721.

Edson, J., C. Fairall, and P. Sullivan (2006). Evaluation and continued improvements to the TOGA COARE 3.0 algorithm using CBLAST data. *27th Conference on Hurricanes and Tropical Meteorology. CBLAST LOW Special Session. Monterey, CA. 26, April 2006.*

Evans, M.C., S.W. Campbell, V. Bhethanabotla, and N.D. Poor (2004). Effect of sea salt and calcium carbonate interactions with nitric acid on the direct dry deposition of nitrogen to Tampa Bay, Florida. *Atmospheric Environment* 38: 4847-4858.

Fairall, C. W., E. F. Bradley, D.P. Rogers, J.B. Edson, and G.S. Young (1996). Bulk parameterization of air-sea fluxes for the Tropical Ocean-Global Atmosphere Coupled-Ocean Atmosphere Response Experiment. *Journal of Geophysical Research.* 101(C2): 3747-3764.

Fairall, C. W., E. F. Bradley, J. S. Godfrey, G. A. Wick, J. B. Edson, and G. S. Young (1996). Cool-skin and warm-layer effects on sea surface temperature. *Journal of Geophysical Research*. 101(C1): 1295-1308.

Fairall, C. W., E. F. Bradley, J. E. Hare, A. A. Grachev, J. B. Edson (2003). Bulk Parameterization of Air-Sea Fluxes: Updates and Verification for the COARE Algorithm. *Journal of Climate*,.16: 571-591.

Fleagle, R. G. and J. A. Businger (1980). *An Introduction to Atmospheric Physics*. New York, Academic Press. 432 pp.

Fung, I. Y., D. E. Harrison, and A. A. Lacis (1984). On the Variability of the Net Longwave Radiation at the Ocean Surface. *Reviews of Geophysics and Space Physics*. 22(2): 177-193.

Galperin, B., A. F. Blumberg and R. H. Weisberg (1991). The importance of density driven circulation in well mixed estuaries: the Tampa Bay experience, pp. 332-343. In: *M. L. Spaulding (ed.), Proceedings of the 2nd International Conference on Estuarine and Coastal Modeling, American Society of Civil Engineers, Tampa, Florida.*

Gill, A. (1982). *Atmosphere-Ocean Dynamics*. Academic Press. 662 pp.

Godfrey, J. S. and A. C. M. Beljaars (1991). On the Turbulent Fluxes of Buoyancy, Heat and Moisture at the Air-Sea Interface at Low Wind Speeds. *Journal of Geophysical Research.* 96(C12): 22,043-22,048.

Goodwin, C. R. (1980). Preliminary simulated tidal flow and circulation patterns in Hillsborough Bay, Florida. *U. S. Geological Survey Open-File Report 80-1021.* 25 pp.

Goodwin, C. R. (1987). Tidal-flow, circulation, and flushing changes caused by dredge and fill in Tampa Bay, Florida. *U. S. Geological Survey Water Supply Paper 2282.* 88 pp.

Gosnell, R., C. W. Fairall and P. J. Webster (1995). The surface sensible heat flux due to rain in the tropical Pacific Ocean. *Journal of Geophysical Research*. 100(18) 437 – 18 442.

Gudivaka, V. and A. Kumar. (1990). An Evaluation of Four Box Models for Instantaneous Dense-Gas Releases. *Journal of Hazardous Material.* 25: 237-255.

He, R. and R. H. Weisberg (2002). West Florida shelf circulation and temperature budget for the 1999 spring transition. *Continental Shelf Research.* 22: 719-748.

He, R. and R. H. Weisberg (2003). West Florida shelf circulation and temperature budget for the 1998 fall transition. *Continental Shelf Research.* 23: 777-800.

Hicks, B. B. (1975). A procedure for the formulation of bulk transfer coefficients over water. *Boundary Layer Meteorology* 8: 515-524.

Hicks, B. B., R. A. Valigura and F. B. Courtright (2000). The role of the atmosphere in coastal ecosystem decline - Future research directions. *Estuaries* 23(6): 854-863.

Hicks, B. B. and P. S. Liss (1976). Transfer of SO2 and other reactive gases across air-sea interface. *Tellus* 28(4): 348-354.

Hillel, D. (1997). *Small-scale irrigation for arid zones.* Report to the Food and Agriculture Organization of the United Nations.

Jerlov, N. G. (1968). *Optical Oceanography*. New York, Elsevier Pub. Co. 199 pp.

Jerlov, N. G. (1976). *Marine Optics.* NewYork, Elsevier Scientific Pub. Co. 231 pp.

Josey, S. A., R. W. Pascal, P. K. Taylor, and M. J. Yelland (2003). A new formula for determining the atmospheric longwave flux at the ocean surface at mid-high latitudes. *Journal of Geophysical Research.* 108(C4): doi:10.1029/2002JC001418.

Kahler, D. M. and W. Brutsaert (2006). Complementary relationship between daily evaporation in the environment and pan evaporation. *Water Resources Research* 42.

Kantha, L. H. and C. A. Clayson (2000). *Numerical Models of Oceans and Oceanic Processes.* San Diego, Academic Press.

Kara, A., H. Hurlburt and A. Wallcraft (2005). Stability-dependent exchange coefficients for air-sea fluxes. *Journal of Atmospheric and Oceanic Technology* 22(7): 1080-1094.

Kumar, A., J. Luo and G. Bennett. (1993). Statistical Evaluation of Lower Flammability Distance (LFD) using Four Hazardous Release Models. *Process Safety Progress.* 12(1): 1-11.

Kumar, A., N. Bellam, and A. Sud. (1999). Performance of Industrial Source Complex model in predicting long-term concentrations in an urban area. *Environmental Progress.* 18(2): 93-100.

Lange, B. and J. Højstrup (2000). The influence of waves on the offshore wind resource. *Proceedings of the European Seminar OWEMES Offshore Wind Energy in Mediterranean and other European Seas,* Siracusa, Italy, 13.-15.04.2000: 491-503.

Linacre, E. (2005). Lake Eo, pan Ep, actual (terrestrial) Ea, potential Et and ocean evaporation rates. *Proceedings of a workshop held at the Shine Dome,* Australia Academy of Science, Canberra, 22 – 23.11.2004: 32-35.

Liu, P. C. and D. J. Schwab (1987). A comparison of methods for estimating u^* from given u_z and air-sea temperature differences. *Journal of Geophysical Research-Oceans*. 92(C6): 6488-6494.

Lukas R, and P.J. Webster (1992). *TOGA-COARE - TROPICAL OCEAN GLOBAL ATMOSPHERE PROGRAM AND COUPLED OCEAN-ATMOSPHERE RESPONSE EXPERIMENT*. *Oceanus* 35 (2): 62-65.

Meyers, S. D., M. E. Luther, M. Wilson, H. Havens, A. Linville and K. Sopkin (2007). A numerical simulation of residual circulation in Tampa Bay. Part I: Low-frequency temporal variations. *Estuaries and Coasts.* 30(4):679-697.

Mizak, C., S. Campbell, K. Sopkin, S. Gilbert, M. E. Luther and N. Poor (2007). Effect of shoreline meteorological measurements on NOAA Buoy model prediction of coastal air-sea gas transfer. *Atmospheric Environment.* 41(20): 4304-4309.

Morey, S. L. and J. J. O'Brien (2002). The spring transition from horizontal to vertical thermal stratification on a midlatitude continental shelf. *Journal of Geophysical Research.* 107(C8): 3097

National Research Council (2000). *Clean Coastal Waters: Understanding and Reducing the Effects of Nutrient Pollution*. Washington, National Academy Press.

Oost, W.A, C.M.J. Jacobs, and C. Van Oort (2000). Stability effects on heat and moisture fluxes at sea. *Boundary-Layer Meteorology*. 95: 271-302.

Panofsky, H. A. (1963). Determination of stress from wind and temperature measurements. *Quarterly Journal of the Royal Meteorological Society.* 89: 85-94.

Patel, V.C. and A. Kumar. (1998). Evaluation of Three Air Dispersion Models: ISCST2, ISCLT2, and SCREEN2 For Mercury Emissions in an Urban Area. *Environmental Monitoring and Assessment.* 53: 259-277.

Paulson, C. A. and J. J. Simpson (1977). Irradiance measurements in the upper ocean. *Journal of Physical Oceanography*. 7:952-956.

Paulson, C. A. and J. J. Simpson (1981). The Temperature Difference Across the Cool Skin of the Ocean. *Journal of Geophysical Research*. 86(C11): 11,044-11,054.

Payne, R. E. (1972). Albedo of the Sea Surface. *Journal of the Atmospheric Sciences.* 29: 959-970.

Poor, N. (2000). *Tampa Bay Atmospheric Deposition Study (TBADS) Final Interim Report: June 2000.* 102 pp.

Poor, N., R. Pribble, H. Greening (2001). Direct wet and dry deposition of ammonia, nitric acid, ammonium and nitrate to the Tampa Bay Estuary, FL, USA. *Atmospheric Environment* 35(23): 3947-3955.

Poor, N., R. Tremblay, H. Kay, V. Bhethanabotla, E. Swartz, M. E. Luther and S. Campbell (2004). Atmospheric concentrations and dry deposition rates of polycyclic aromatic hydrocarbons (PAHs) for Tampa Bay, Florida, USA. *Atmospheric Environment* 38(35): 6005-6015.

Reed, R. K. (1977). On Estimating Insolation Over the Ocean. *Journal of Physical Oceanography.* 7:482-485.

Riswadkar, R.M. and A. Kumar. (1994) Evaluation of the ISC Short Term Model in a Large-Scale Multiple Source Region for Different Stability Classes. *Environmental Monitoring and Assessment.*1-14.

Rutgersson, A., A. S. Smedman, and A. Omstedt, (2001). Measured and Simulated Latent and Sensible Heat Fluxes at Two Marine Sites in the Baltic Sea. *Boundary Layer Meteorology*. 99, 53-84.

Schmidt, N., E. K. Lipp, J. B. Rose and M. E. Luther (2001). ENSO influences on seasonal rainfall and river discharge in Florida. *Journal of Climate.* 14: 615-628.

Schmidt N. and M. E. Luther (2002). ENSO impacts on salinity in Tampa Bay, Florida. *Estuaries.* 25(5):976-986.

Sheng, Y. P., J. R. Davis, V. Paramygin, K. Park, T. Kim and V. Alymov (2003). Integrated-process and integrated-scale modeling of large coastal and estuarine areas, pp. 407-422. In: *M. L. Spaulding (ed.), Proceedings of the 8th International Conference on Estuarine and Coastal Modeling, American Society of Civil Engineers, Monterey, California.*

Sopkin, K., C. Mizak, S. Gilbert, V. Subramanian, M. E. Luther and N. Poor (2007). Modeling air/sea flux parameters in a coastal area: a comparative study of results from the TOGA COARE model and the NOAA Buoy model. *Atmospheric Environment.* 41(20): 4291-4303.

Stull, R. B. (1984). *An introduction to boundary layer meteorology.* Boston, Kluwer Academic Publishers. 666 pp.

Sun, B., L. Yu, and R. A. Weller (2003). Comparisons of Surface Meteorology and Turbulent Heat Fluxes over the Atlantic: NWP Model Analyses versus Moored Buoy Observations. *Journal of Climate*. 16: 679-695.

Tampa Bay Soundings (2003). Tampa Bay After Dark. *Winter 2003 3(1). Pinellas Park, FL.*

Tampa Port Authority (2005). *The 2005 State of the Port Address.* http://www.tampaport.com/

TBEP. (1996). *Charting the Course for Tampa Bay*. Tampa Bay National Estuary Program. http://www.tbep.org.

Tetens, O. (1930). Über einige meteorologische Begriffe. *Z. Geophys.* 6: 297-309.

Valigura, R. A. (1995). Iterative bulk exchange model for estimating air-water transfer of HNO3. *Journal of Geophysical Research-Atmospheres* 100(D12): 26045-26050.

Vincent, M. S. (2001). *Development, Implementation and Analysis of the Tampa Bay Coastal Prediction System.* Dissertation. College of Engineering. Tampa, FL, University of South Florida.

Vincent, M., D. Burwell, and M. Luther (2000). The Tampa Bay Nowcast-Forecast System. In: Estuarine and Coastal Modeling, M. L. Spaulding and H. L. Butler, eds., ASCE, Reston, VA, pp 765-780.

Virmani, J. I. (2005). *Ocean-Atmosphere Interactions on the West Florida Shelf.* Dissertation. College of Marine Science. St. Petersburg, FL, University of South Florida.

Virmani, J. I. and R. H. Weisberg (2003). Features of the observed annual ocean-atmosphere flux variability on the West Florida Shelf. *Journal of Climate.* 16: 734-745.

Webb, E.K. (1970). Profile relationships, log-linear range, and extension to strong stability. *Quarterly Journal of the Royal Meteorological Society* 96 (407): 67.

Weisberg, R. H., and L. Zheng (2006a). Circulation of Tampa Bay driven by buoyancy, tides, and winds, as simulated using a finite volume coastal ocean model. J. Geophys. Res. 111, C01005, doi:10.1029/2005JC003067.

Weisberg, R. H. and L. Zheng (2006b). Hurricane storm surge simulations for Tampa Bay. *Estuaries and Coasts*. 29: 899-913.

Wilson, M., S. D. Meyers and M. Luther (2006). Changes in the circulation of Tampa Day due to Hurricane Frances as recorded by ADCP measurements and reproduced with a numerical ocean model. *Estuaries and Coasts*. 29(6A): 914-918.